FINITE ELEMENT METHOD SOLUTION FOR STEADY MAGNETOHYDRODYNAMIC FLOW IN A STRAIGHT HORIZONTAL PIPE OF ELLIPTICAL CROSS SECTION

BY

DAVID KWEYU

A THESIS SUBMITTED IN FULFILLMENT OF THE REQUIREMENTS FOR THE DEGREE OF DOCTOR OF PHILOSOPHY IN APPLIED MATHEMATICS

SCHOOL OF MATHEMATICS, STATISTICS AND ACTUARIAL SCIENCE

MASENO UNIVERSITY

DECLARATION

DECLARATION BY CANDIDATE:

This research thesis is my original work and has not been presented for award of a degree in any other University. No part of this thesis may be reproduced without prior written permission of the author and/or Maseno University.

Signature_____ **Date**_____

DAVID KWEYU

PHD/MAT/00044/2014

DECLARATION BY THE SUPERVISORS

This research thesis has been submitted with our approval as University Supervisors.

Signature_____ **Date**_____

Professor. Alfred Manyonge Wanyama

Department of Pure and Applied Mathematics,

Maseno University.

Signature_____ **Date**_____

Professor. Jacob K. Bitok

Department of Mathematics and Computer Science,

University of Eldoret.

ACKNOWLEDGEMENT

From the bottom of my heart, I would like to say big thank you to my supervisors Professor Manyonge Alfred Wanyama and Professor Bitok K. Jacob for their dedicated support and guidance. They continuously provided encouragement and were always willing and enthusiastic to assist in any way they could throughout the research. I would like to also thank: Dr. Isaac Owino, Chair, Department of Pure and Applied Mathematics. Dr. Edgar Otumba, Chair, School of Post Graduate Committee (School of Mathematics, Statistics and Actuarial Science). The entire fraternity of the Department of Pure and Applied Mathematics at Maseno University. Thank you very much for your energy, understanding and help throughout my study. Finally, I cannot forget to thank my wife, children, family members, friends and Mukhuyu Friends Church-Webuye members for their patience and encouragement. Thank you for all the unconditional support in this very intense academic work.

DEDICATION

First of all, I dedicate this dissertation to God Almighty my creator, my strong pillar, my source of inspiration, wisdom, knowledge and understanding. He has been the source of my strength throughout this program and on His wings only have I soared. I also dedicate this work to my dear wife, Gaudencia Khalayi, who has encouraged me all the way and whose encouragement has made sure that I give it all it takes to finish that which I have started. Finally to my beloved daughters: Lindsay Khwaka Kweyu, Melinda Lukelesia Kweyu and Diana Namwali Kweyu who have been affected in every way possible by this quest. Thank you. My love for you all can never be quantified. God bless you.

ABSTRACT

Velocity profile and temperature distribution for Magnetohydrodynamic (MHD) flow in a straight horizontal pipe of elliptical cross section has been investigated. Many researchers have carried out research on pipes of circular, square, rectangular, annular and elliptical cross sections in magnetohydrodynamics because there are many applications. Their studies concentrated on a given cross section as a different entity with fluid being driven by pumps. In this study, investigation is done on a circular pipe as it changes into an elliptical pipe when fluid is propelled by gravitational force. The main purpose of the study is to find out which pipe between one which has a circular cross section and another of elliptical cross section is more beneficial. Effects of velocity profile and temperature distribution on the pipe as it changes cross section from circular to elliptical are investigated. Governing equations, partial differential equations (pdes), are formulated, non dimensionalised, expressed in terms of stream function and transformed into ordinary differential equations (odes) using similarity transformation. The odes are solved by Finite Element Method in conjunction with Mathematica version 12.0. The objectives of the study are: To model Finite Element Method solution for steady Magnetohydrodynamic flow in a straight horizontal pipe of elliptical cross section. To formulate governing equations (pdes) in cylindrical coordinates $(\mathrm{r}, \theta, \mathrm{z})$ comprising Navier-Stokes equations, Ohm's law of electromagnetism, equation of continuity, cross section of elliptical pipe and heat energy equation. To solve by Finite Element Method the ordinary differential equations (odes) formed when non dimensionalisation and similarity transformation are carried out on the governing equations. To determine the effects of dimensionless numbers of Hartmann number, Reynolds number, Eckert number and Prandtl number as well as other physical quantities of gravitational force and aspect ratio on fluid velocity and temperature. To find out the repercussions of velocity and temperature on a pipe as it transits from circular to elliptical cross section. Finite Element Method (FEM) is embraced instead of other methods like Finite Difference Method (FDM) because FEM is able to handle complicated geometries and boundaries with relative ease while other methods are restricted to handle rectangular shapes. Also many of the real life medical, engineering, astrophysics, etc problems can be solved in weak form, which FEM encompasses compared to strong form, which other methods employ. Results are displayed as tables and graphs and reveal that: Increase in Hartmann number, $1.0 \leq \mathrm{Ha} \leq 40.0$, increases temperature but retards velocity. Rise in Reynolds number, $0.5 \leq \mathrm{Re} \leq 8.0$ and aspect ratio, $1 \leq \alpha \leq 1.6$, leads to rise in both velocity and temperature. An upsurge in gravitational force, $0.00002 \leq \lambda_\theta \leq 0.00008$, results in an upsurge in velocity. Temperature increases when Eckert number, $1 \leq \mathrm{Ec} \leq 40$, increases but decreases when Prandtl number, $0.5 \leq \mathrm{Pr} \leq 2.0$, is raised. In all scenarios, velocity and temperature are maximum at the centre of pipe but diminish to zero at the periphery. Spike in aspect ratio leads to rise in velocity which results in increase in temperature. A pipe of elliptical cross section will be more convenient where there is limited space in the vertical direction due to existing structures yet there is demand in increase in productivity. This is in comparison to circular shape. A pipe of elliptical cross section has greater capacity for the same depth of flow. It is envisaged that the conducting fluid is flowing as a coolant at a nuclear power plant or as molten metal at a metallurgical process. A pipe of elliptical cross section would therefore be more productive in industrial processes than one which is circular according to the findings of this dissertation.

TABLE OF CONTENTS

Page

NOMENCLATURE

Alphabet letter symbols

a : half of the ellipse's major axis (metre)

B : magnetic flux density (Weber per square metre)

B : component of magnetic flux density (Weber per square metre)

b : half of the ellipse's minor axis (metre)

$\mathrm{c_p}$: specific heat capacity of fluid (Joule per kilogram per Kelvin)

E : electric field (Volt per metre)

E : number of elements

Ec : Eckert number (unitless)

e : element

f : function representing stream function (kilogram per metre per second)

$\mathrm{f_r}$: Lorentz force in r-direction (Newton)

f_θ : Lorentz force in θ-direction (Newton)

$\mathrm{f_0}$: velocity profile essential boundary condition

GP : Gauss quadrature points

g : gravitational field strength (metre per square second)

$\mathrm{g_r}$: gravitational field strength in r-direction (metre per square second)

g_θ : gravitational field strength in θ-direction (metre per square second)

Ha : Hartmann number (unitless)

h : function representing thermodynamic temperature (Kelvin)

$\mathrm{h_0}$: temperature distribution essential boundary condition

$\mathrm{h^e}$: length of element (metre)

I : temperature square stiffness matrix

J : temperature vector of unknowns

J^{e} : Finite Element Jacobian

K : temperature global force vector

L : temperature boundary integral vector

N : Stuart number (unitless)

n_{η} : η- component of unit outward normal of boundary

n_{τ} : τ- component of unit outward normal of boundary

Pr : Prandtl number (unitless)

p : pressure (Pascal)

p_0 : temperature distribution natural boundary condition

q_0 : velocity profile natural boundary condition

R : characteristic length (metre)

Re : Reynolds number (unitless)

r : length measured from the ellipse's centre (metre)

SV : secondary variable

s_{i} : Galerkin shape function

s_{j} : shape basis function

T : thermodynamic temperature (Kelvin)

T_0 : thermodynamic temperature at the centre of pipe (Kelvin)

T_1 : thermodynamic temperature at pipe boundary (Kelvin)

T_{r} : thermodynamic temperature in r-direction (Kelvin)

T_{θ} : thermodynamic temperature in θ-direction (Kelvin)

U_0 : Characteristic velocity

$\mathbf{u}$: fluid velocity (metre per second)

$\mathrm{u_r}$: fluid velocity in r-direction (metre per second)

u_θ : fluid velocity in θ-direction (metre per second)

$\mathrm{V_c}$: core velocity (metre per second)

W : velocity stiffness matrix

w : weight function

$\mathrm{w_k}$: Gauss quadrature weight

X : velocity vector of nodal unknowns

Y : velocity global force vector

Z : velocity boundary integral vector

z : component of cylindrical coordinates

Alphabet letter-like symbols

$\mathscr{J}_\mathrm{v}$: electric current density for velocity (Ampere per square metre)

$\mathscr{J}_\mathrm{t}$: electric current density for temperature (Ampere per square metre)

$\mathscr{P}$: length of half major axis measured from centre of ellipse (metre)

Greek letter symbols

α : aspect ratio

Γ : boundary of cross section of elliptical pipe

ε : base of natural logarithm

η : independent function of f, velocity

η_1^{e} : coordinate of origin of pipe for velocity

η_2^{e} : coordinate of first point from origin of pipe for velocity

θ : the central angle in the cross section of elliptical pipe (radians). Also a component of cylindrical coordinates

λ_{r} : gravitational force in the r- direction (Newton)

λ_θ : gravitational force in the θ- direction (Newton)

μ : dynamic viscosity (Newton-second per square metre)

ν : kinematic viscosity (square metre per second)

ξ : master element

ρ : fluid density (kilogram per cubic metre)

σ : electrical conductivity (per omega per metre)

τ : independent variable for temperature

τ_1^{e} : coordinate of origin of pipe for temperature

τ_2^{e} : coordinate of first point from origin of pipe for temperature

ψ : stream function (kilogram per metre per second)

Ω : domain of elliptical cross section of pipe

LIST OF TABLES

LIST OF FIGURES

LIST OF APPENDICES

CHAPTER ONE

INTRODUCTION

1.1 Background information

The word Magnetohydrodynamics comprises three words: Magneto- meaning magnetic, hydro- meaning liquid and dynamics-referring to movement of an object by forces. MHD is therefore a union of three widely separated disciplines namely electrodynamics, fluid dynamics and thermodynamics. MHD is concerned with the phenomena that arise in fluid dynamics from the interaction of an electrically conducting fluid with the magnetic field. The conducting fluids include plasmas (ionized gases), liquid metals (mercury, gallium, sodium, molten iron) and electrolytes. Practical MHD devices have been in use since the early part of the 20th century, Alam and Khan [1]. MHD generators are used in power plants. The basic concept of the MHD generator is to generate electrical energy from the motion of conductive fluid that is crossing a perpendicular magnetic field. When the conducting fluid moves through the magnetic field, it creates an electric current perpendicular to the magnetic field and direction of movement of conducting fluid. Another application of MHD is in MHD pumps and flow meters. In these type of pumps, the electrical energy is converted directly to a force which is applied on the conducting fluid. In MHD flowmeters, the potential induced by fluid motion is measured and used to infer (accurately predict) the average flow rate. The MHD pumps use this force to control liquid metal flows where high temperatures and corrosive tendencies prohibit the use of seals in standard mechanical pumps. Electromagnetic forces are used to pump liquid metals (eg. in cooling systems of nuclear power stations) without the need for any moving parts. They can shape the flow of a molten metal and so aid controlling its shape once solidified and can even levitate (to rise or float as if in the air especially in seeming defiance of gravitation) and heat a sample of metal to prevent

any contact with a container.

Many researchers are interested in Magnetohydrodynamics (MHD) due to the fact that magnetism is found throughout the universe and has many applications. Studies on MHD range from research on generation of both solar and earth's magnetic fields to medical and industrial use. Investigations are on-going to copy the sun. In copying the sun, researchers are trying to fuse hydrogen into helium, Kramer [2]. This will result in release of huge quantities of energy for both domestic and industrial use. In cancer treatment, research is going on to develop more precise methods of delivery of medicine to affected areas. One such method involves the binding of medicine to biologically compatible magnetic particles (e.g ferrofluids). These particles are guided to the target via careful placements of permanent magnets on the external body. MHD equations and Finite Element Method are used to study interaction between the magnetic fluid particles in the blood stream and the external magnetic field, Saman *et. al* [3].

Many researchers have investigated on MHD flows in pipes and ducts of circular, square, sector, ellipse etc as different entities. In this study, research is carried out on a circular pipe as it changes into an elliptical pipe. The fluid is moved by gravitational force which is economically cheaper in comparison to the work done by other researchers where they used pumps to provide suction or injection force. The similarity transformations used are also unique from those of other investigators and convert the non-linear pdes directly to linear odes which are easier to solve. The main aspiration of the research is to find out the impact of change in cross section from circular to elliptical and increase in gravitational force on velocity and temperature of fluid.

1.2 Statement of the problem

Analytical and/or numerical solutions have been obtained for MHD flow between two parallel plates, a pipe whose cross section is a sector and through pipes or ducts whose cross section are: circular, square, triangular, rectangular and annular. Many industries use circular pipes to obtain MHD products. With human population increasing, there is need to increase these products. One way being use of a pipe of elliptical cross section instead of a circular one. A pipe of elliptical cross section has greater volume and torque in comparison with a circular one of the same depth. Furthermore, in this investigation, the fluid is driven by gravitational force only instead of pumps . This reduces costs further.

The main aspiration of this research is to find out which one between the two cross sections is more effective. Modeling for velocity profile and temperature distribution is done for a circular pipe as it changes to an elliptical pipe when fluid is propelled by gravitational force. This is executed by formulating governing equations (pdes), converting them into ordinary differential equations (odes), solving odes by FEM and Mathematica version 12.0 to obtain results in form of tables and graphs. The results are analysed to find out which cross section is more beneficial.

1.3 Objectives of the study

1.3.1 General objective

To model Finite Element Method solution for steady Magnetohydrodynamic flow in a straight horizontal pipe of elliptical cross section.

1.3.2 Specific objectives

i. To formulate governing equations (pdes) in cylindrical coordinates $(\mathrm{r}, \theta, \mathrm{z})$ comprising Navier-Stokes equations, Ohm's law of electromagnetism, equation of continuity, cross section of elliptical pipe and heat energy equation.

ii. To solve by Finite Element Method the ordinary differential equations (odes) formed when non dimensionalisation and similarity transformation are carried out on the governing equations.

iii. To determine the effects of dimensionless numbers of Hartmann number, Reynolds number, Eckert number and Prandtl number as well as other physical quantities of gravitational force and aspect ratio on fluid velocity and temperature.

iv. To find out the repercussions of velocity and temperature on a pipe as it transits from circular to elliptical cross section.

1.4 Significance of the study

Magnetohydrodynamics has many applications ranging from technological applications like medicine, energy generation, processing of materials, energy storage and flow measure to natural phenomena like astrophysics, planetary physics and geophysics, Cuevas [4]. Many establishments use circular pipes to obtain MHD products. With the ever increasing demand for these products due to population growth, there is need to replace the circular pipe with a pipe of elliptical cross section. A pipe of elliptical cross section will be very appropriate in MHD processes where vertical clearance is limited by existing structures yet there is demand in increase in productivity. A horizontal pipe of this type is particularly suitable since the vertical height is less than the

height of hydraulically equivalent circular pipe. A pipe of elliptical cross section also offers the hydraulic advantage of greater capacity for the same depth of flow than circular pipe. The velocity profile and temperature distribution will be higher in elliptical pipe than circular one. Again in this model, the fluid is driven by gravitational force which is cheaper economically in comparison to other models being used which require pumps to provide injection or suction force. All these will in turn result in increase in productivity in MHD products.

1.5 Research methodology

MHD encompasses three disciplines namely: Electrodynamics, phenomena associated with electric charges and their interaction with magnetic and electric fields, Ohm's law of electromagnetism caters for this field. Secondly, fluid dynamics, which describes fluid flow, is represented by Navier-Stokes equations. Heat energy equation, act for thermodynamics, which is the relation between heat and other forms of energy. Navier-Stokes equation is non linear pde. Heat energy equation also becomes non linear pde when stream function is introduced. Non-linearity make it difficult or impossible to solve these pdes. This necessitates consideration of some assumptions.

Formulation of governing equations is done in terms of cylindrical coordinates rather than Cartesian coordinates. Cylindrical coordinates are useful, Graebel [5], for geometries that involve circular cylinders, ellipses, spheres, or ellipsoids. Cylindrical coordinates make satisfaction of boundary conditions easiest and are useful in connection with phenomena that have rotational symmetry about longitudinal axis such as fluid flow in a pipe of round cross section, heat distribution in a cylinder etc. However, mathematical functions formed, their length and complexity of equations become more complicated than in Cartesian coordinates. Cylindrical coordinates are utilized in this investigation because geometry involved is elliptical, boundary conditions are

easily satisfied and rotational symmetry is involved.

Similarity transformation approach is employed to transform non linear pdes to linear odes.

Non-dimensionalization is done to reduce the number of parameters involved in the equations and results in dimensionless numbers like Reynolds and Prandtl. These numbers enable the grouping of a large number of experiments so that results are provided conveniently using dimensionless numbers.

FEM is chosen to solve the odes numerically instead of other methods like Finite Difference Method (FDM) because of the following advantages, Darrell and Juon [6]:

i. FEM works with weak form of differential equations while other methods work with strong form of differential equations. Many of the real life medical, engineering, astrophysics, etc problems can be solved in weak form compared to strong form.

ii. Modeling of complex geometries and irregular shapes are easier as a variety of finite elements are available for discretization of the domain.

iii. Boundary conditions can be easily incorporated in FEM.

iv. Different types of material properties can be easily accommodated in modeling from element to element or even within an element.

However, FEM also has disadvantages which are:

a. Large amounts of data is required as input for the mesh used in terms of nodal connectivity and other parameters.

b. It requires large computer memory and computational time to get results.

c. It requires longer execution time.

d. Output result will vary considerably.

FEM is selected for this investigation because it is concerned with weak form of differential equations and boundary conditions are easily incorporated.

Mathematica version 12.0 is embraced for solution of numerous algebraic equations, integration, differentiation, simplification and construction of graphs.

CHAPTER TWO

LITERATURE REVIEW

The first theoretical and laboratory studies of MHD flow in pipes and ducts were carried out in the 1930s by Williams, Al-Khawaja and Selmi [7]. They published results of experiments with electrolytes flowing in insulated tubes. The tubes were placed between the poles of a magnet. The potential difference across the flow was measured using wires passed through the walls.

Moffatt [8] researched on a liquid metal placed in a closed container placed in a magnetic field. The field was caused to rotate by suitably phased external current circuits. A rotational Lorentz force was produced and drove the rotational flow. He found out that: In the weak field limit, the rotational part of Lorentz force was steady. In the high frequency limit, flow with circular streamlines was possible when the Hartmann number was not too large. For a pipe of elliptical cross section, of large aspect ratio $\frac{\mathrm{a}}{\mathrm{b}}$, the torque distribution associated with the Lorentz force was concentrated near the points of maximum curvature on the boundary. Where a and b were half lengths of major and minor axes of the ellipse respectively.

The transient MHD flow of a particulate suspension in an electrically conducting fluid in a circular pipe was studied considering the Hall effect by Attia [9]. The governing partial differential equations were solved numerically using Finite Difference Method. The effect of the magnetic field parameter, the Hall parameter and the particle-phase viscosity on the transient behavior of the velocity, volumetric flow rates and skin friction coefficients of both fluid and particle-phases were investigated. He observed that: increasing the magnetic field decreases the fluid and particle velocities, increasing the Hall parameter increases fluid-phase volumetric flow rate and fluid-phase skin friction coefficient for all values of magnetic field parameter and particle-phase viscosity. The effect of the Hall parameter on the quantities fluid-phase volumetric flow rate and fluid-phase skin friction coefficient becomes more pronounced for higher values of magnetic field parameter

or smaller values of particle-phase viscosity.

Gedik *et.al* [10] studied the steady, laminar, incompressible viscous flow of an electrically conducting liquid-metal fluid in a circular non-conducting pipe numerically. The galistan liquid-metal was subjected to constant pressure gradient a long the axial direction and uniform transverse magnetic field in the spanwise direction. Magnetic field induction took values between 0 and 1.5T with a 0.5T step size. They found that velocity decreased with an increase in the intensity of applied magnetic field.

İbrahim [11] applied Chebyshev polynomial method to solve magnetohydrodynamic flow equations in a rectangular duct in the presence of transverse external oblique magnetic field. Truncated Chebyshev series was considered the approximate solution. The MHD equations were decoupled first and then the Chebyshev polynomial method was used to solve for positive and negative Hartmann numbers. Numerical solutions of velocity and induced magnetic field were obtained for steady-state, fully developed, incompressible flow for a conducting fluid inside the duct. The results for velocity and induced magnetic field were visualized in terms of graphics for values of Hartmann numbers, $\mathrm{Ha} \leq 1000$. He observed that the method was capable of producing highly accurate solutions using small number of algebraic system of equations leading to less computational effort.

Altintas and Ozkol [12] analyzed Computational Fluid Dynamics (CFD) of external magnetic field effect on the steady, laminar, incompressible flow of an electrically conducting liquid metal fluid in a pipe. They used the MHD module of ANSYS fluent commercial programme to compute the flow and temperature fields. Sodium potassium alloy which is a liquid at room temperature was used as a conducting fluid. The simulations were performed for non-heated pipe flow and externally heated pipe flow. They observed that heating reduced magnetic effect on flow.

Verma [13] studied flow of viscous, incompressible, electrically conducting fluid with varying

viscocity through an annular pipe in the presence of a radial magnetic field. He obtained exact solutions for velocity, rate of volume flow and stress on the wall of the channel. In limiting case, the solutions reduced to the classical case flow when viscocity was constant and magnetic field was zero. Results obtained were exhibited graphically and revealed that: For a fixed integer of a hypergometric function, increase in non dimensional viscosity variation parameter causes increase in velocity. Velocity profiles are almost symmetrical when viscosity is constant and profiles get more and more asymmetric with position of maximum velocity shifting towards outer cylinder as non dimensional viscosity variation parameter increases. The effect of increase in magnetic parameter was to flatten the velocity profile. Stress on the outer cylinder decreases as non dimensional viscosity variation parameter increases. Stress on the inner cylinder increases with non dimensional viscosity variation parameter for a small fixed integer of a hypergometric function due to increase in viscosity.

The case of an analytical solution for convective heat transfer in straight elliptical pipes was presented by Shahmardan *et.al* [14]. The solution was obtained by using finite series expansion method for fully developed heat transfer under the constant heat flux at walls. The variations of Nusselt number as well as the temperature at the centre of cross section were expressed in terms of aspect ratio. The solution indicated that the Nusselt number increased when the geometry of cross section changed from circular to elliptical shape from 48/11 to 4356/833 for large enough aspect ratios.

Numerical solution for steady MHD flow of liquid metal through a square duct under the action of strong transverse magnetic field was investigated by Dipjyoti *et.al* [15]. The walls of the duct were considered to be electrically insulated as well as isothermal. The numerical solutions for velocity and temperature distributions were obtained by Finite Difference Method. The solutions for different values of Hartmann number and Prandtl were analyzed and presented

graphically. They found out that increase of Hartmann number leads to temperature increase. Increase in Prandtl numbers result in increase in temperature of the flow.

Usman *et.al* [16] investigated the analytical solution of the temperature profile distribution of a one-dimensional fluid under the influence of magnetic fluid strength of a reactive hydromagnetic fluid flow through porous media between permeable beds under optically thick limit radiation. The fluid considered was incompressible, electrically conducting and flowed steadily through porous media with the effect of magnetic strength. The analytical solutions of the non-linear dimensionless energy equations governing the fluid flow were obtained using integration and series solution of Adomian Decomposition Method (ADM) and the effects of flow properties on the fluid flow were presented graphically and discussed. Their results showed that an increase in the viscous dissipation increases the temperature profile of the fluid flow under optically thick limit radiation. An increase in the Reynold number also increases the temperature of the fluid. An increase in the internal heat generation increases the temperature of the fluid flow. As the thermal radiation and Hartmann number decreases, the temperature of the fluid flow increases due to the effect of the magnetic field strength.

A Finite Difference Method solution for coupled convection diffusion equations of magnetohydrodynamic flow was obtained by Prasanna and Ganesh [17]. They presented solutions for ducts of different cross sections namely square, rectangle, triangle, circle, ellipse, sector and annulus under steady state conditions. Walls of ducts were electrically insulated and Hartmann number fixed. It was observed from the graphs plotted that for all the cross sections, the velocity profile was flat in the core region.

A numerical study was carried out to examine the magnetohydrodynamic (MHD) flow of micropolar fluid on a shrinking surface in the presence of both Joule heating and viscous dissipation effects by Liaquat *et.al* [18]. The governing system of non-linear odes were obtained

from the system of pdes by employing exponential transformations. The resultant equations were transformed into initial value problems and solved by Runge-Kutta method. The effects of different parameters on velocity, angular velocity, temperature profiles, skin friction coefficient and Nusselt number were obtained and demonstrated by constructed graphs. They observed that the temperature of fluid rose at higher values of the Eckert number in all solutions.

In their study, Mohammad *et.al* [19] considered a laminar magnetohydrodynamics (MHD) developing flow of an incompressible electrically conducting fluid subjected to an external magnetic field . The aim of the study was to propose a correlation for computing the development length of the laminar MHD developing flow in a pipe. A numerical approach was considered to solve the problem. In the first step, the numerical Finite Volume Method (FVM) was conducted to analyze the problem. Later, the Artificial Neural Network (ANN) was used to develop the data sets and in the last step, the curve fitting was applied to find a correlation for the prediction of the development length as a function of the Reynolds and Hartmann numbers. They observed that the development length declines with the increase of the Hartmann number and grows with the rising of the Reynolds number.

The flow of an electrically conducting fluid through a curved channel with wavy boundaries was studied by Okechi *et.al* [20]. The waviness of the curved boundaries was sinusoidal and periodic. The analytical results for the velocity field and the volumetric flow rate were obtained using the boundary perturbation method. The effects of the wavy boundaries, the channel radius of curvature and the applied magnetic field on the flow field were analyzed. They observed that the impact of the wavy boundaries on the flow decreases with the increase in Hartmann number. However, the flow rate increases for any alignment of the wavy curved boundaries and for the wave numbers less than a threshold wavenumber (depending on the radius of curvature and the Hartmann number). Also, the flow rate decreases with the increasing wavenumber.

In the investigation done by Moffatt [8], the torque distribution associated with Lorentz force was concentrated near the points of maximum curvature on the boundary. When comparison is made between a circular and an elliptical pipe, the elliptical pipe provides higher torque. In the findings of Shahmardan *et.al* [14], Nusselt number increased when the geometry of the cross section changed from circular to elliptical. They did not research on velocity and temperature as the shape changed. Prasanna and Ganesh [17] observed that velocity profile was flat in the core region of pipes of various cross sections. However, they did not compare the velocities for the different shapes of cross section.

The main intention of this research is to examine the effects of change in cross section of pipe from circular to elliptical and change in gravitational force on velocity profile and temperature distribution. This will enable us to find out which cross section of pipe between circular and elliptical is more productive. Governing equations (pdes) are formulated, non-dimensionalised, converted into odes by use of similarity transformation technique. The odes are solved numerically by Finite Element Method. Results are obtained and presented in form of tables and graphs by manipulation of Mathematica version 12.0. Conclusions are drawn relating velocity profile and temperature distribution with Hartmann number, gravitational force, Reynolds number, Prandtl number, Eckert number and distance of major axis of cross section of elliptical pipe (aspect ratio).

CHAPTER THREE

FORMULATION AND NUMERICAL SOLUTION

The equations which describe MHD flow are a combination of: Ohm's law of electromagnetism. θ- component of Navier-Stokes equations of fluid mechanics. Equation of continuity. Heat energy equation. Elliptical cross section of pipe and boundary conditions. Where θ is the component of cylindrical coordinates.

3.1 The Physical Problem

Consideration is made for MHD flow in a straight horizontal pipe of sufficient length and of elliptical cross-section as shown in figure 3.1.1.

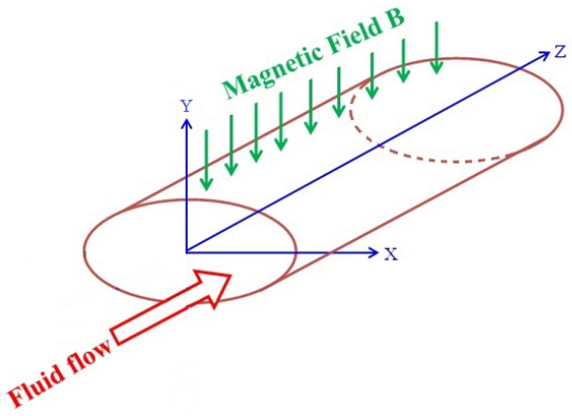

Figure 3.1.1: Flow of fluid in pipe of elliptical cross section

The fluid flows through the pipe due to an applied constant pressure gradient in the z direction. The pressure arises from Lorentz force and gravitational force. Lorentz force is the force exerted on the charged fluid particles moving with some velocity through an electric and magnetic field. The fluid is viscous, incompressible and electrically conducting. The electrical permittivity and magnetic permeability of the fluid are assumed to be close to those of the external space. Permitivity quantifies the extent to which a material concentrates electric flux. Electric flux will

be the same for the fluid, pipe and the surrounding. Otherwise, concentration of electric flux will be different in the three media. Magnetic permeability is the measure of magnetisation that a material obtains in responds to applied magnetic field. This measure is different for fluid, air and pipe. Different electrical permittivity and magnetic permeability in the three media calls for a different formulation. Externally applied magnetic field with an intensity **B** is parallel to the y-direction. In defining this investigation, the domain, Ω, is the elliptical cross section of the pipe. The boundary, Γ, is the inside of the cross section of the pipe.

3.2 Assumptions

The following assumptions are made :

i. The walls of the pipe and the outside media are also electrically conducting having the same electrical conductivity and magnetic permeability since the thickness of the pipe wall is assumed to be very small.

ii. Directed magnetic field is applied on the pipe parallel to the y-axis and perpendicular to the z-axis.

   For θ -component of velocity, magnetic field varies in the direction r but zero in θ and z, the directed magnetic field is :

$$\mathbf{B} = \{\mathrm{B_r}, 0, 0\} \tag{3.2.1}$$

   θ is the cylindrical coordinate.

   For r -component of velocity, directed magnetic field varies in θ direction but zero in r and

z directions, the directed magnetic field is

$$\mathbf{B} = \{0, \mathrm{B}_{\boldsymbol{\theta}}, 0\} \tag{3.2.2}$$

For temperature, it varies in the direction r and $\boldsymbol{\theta}$ but is zero in z direction, the magnetic field is :

$$\mathbf{B} = \{\mathrm{B}_{\mathrm{r}}, \mathrm{B}_{\boldsymbol{\theta}}, 0\} \tag{3.2.3}$$

where B_{r} and $\mathrm{B}_{\boldsymbol{\theta}}$ are the r and $\boldsymbol{\theta}$ components of incident magnetic field **B** respectively.

iii. Velocity of fluid, **u**, vary in the directions $\boldsymbol{\theta}$ and r but zero in z for Navier-Stokes equations. Velocity is then:

$$\mathbf{u} = \{\mathrm{u}_{\mathrm{r}}, \mathrm{u}_{\boldsymbol{\theta}}, 0\} \tag{3.2.4}$$

where u_{r} and $\mathrm{u}_{\boldsymbol{\theta}}$ are components of fluid velocity, **u**, in r and $\boldsymbol{\theta}$ directions respectively.

iv. Lorentz force in the $\boldsymbol{\theta}$ -component, $\mathrm{f}_{\boldsymbol{\theta}}$, is obtained from

$$\mathscr{J}_{\mathrm{v}} \times \mathbf{B}$$

where $\mathscr{J}_{\mathrm{v}}$ is electric current density for velocity profile. $\mathscr{J}_{\mathrm{v}}$ is worked out in cylindrical coordinates $(\hat{\boldsymbol{\rho}}_{\mathbf{r}}, \hat{\boldsymbol{\rho}}_{\boldsymbol{\theta}}, \hat{\boldsymbol{\rho}}_{\mathbf{z}})$ as follows: From Ohm's law of electromagnetism ($\mathscr{J}_{\mathrm{v}} = \boldsymbol{\sigma}(\mathbf{E} + \mathbf{u} \times \mathbf{B})$) when $\mathbf{E} = 0$ (when $\mathbf{E} \neq 0$, a different formulation is required) and using equation

(3.2.1) and equation (3.2.4)

$$\mathscr{J}_{\mathrm{v}} = \boldsymbol{\sigma}(\mathbf{u}\times\mathbf{B}) = \boldsymbol{\sigma}\begin{vmatrix} \hat{\boldsymbol{\rho}}_{\mathbf{r}} & \hat{\boldsymbol{\rho}}_{\boldsymbol{\theta}} & \hat{\boldsymbol{\rho}}_{\mathbf{z}} \\ \mathrm{u_r} & \mathrm{u}_{\boldsymbol{\theta}} & 0 \\ \mathrm{B_r} & 0 & 0 \end{vmatrix} = -\boldsymbol{\sigma}\mathrm{B_r u}_{\boldsymbol{\theta}}\hat{\boldsymbol{\rho}}_{\mathbf{z}}$$

so that

$$\mathscr{J}_{\mathrm{v}}\times\mathbf{B} = \begin{vmatrix} \hat{\boldsymbol{\rho}}_{\mathbf{r}} & \hat{\boldsymbol{\rho}}_{\boldsymbol{\theta}} & \hat{\boldsymbol{\rho}}_{\mathbf{z}} \\ 0 & 0 & -\boldsymbol{\sigma}\mathrm{B_r u}_{\boldsymbol{\theta}} \\ \mathrm{B_r} & 0 & 0 \end{vmatrix} = \boldsymbol{\sigma}\mathrm{B}_{\mathrm{r}}^{2}\mathrm{u}_{\boldsymbol{\theta}}\hat{\boldsymbol{\rho}}_{\boldsymbol{\theta}}$$

Lorentz force become

$$\mathrm{f}_{\boldsymbol{\theta}} = \boldsymbol{\sigma}\mathrm{B}_{\mathrm{r}}^{2}\mathrm{u}_{\boldsymbol{\theta}} \tag{3.2.5}$$

where $\boldsymbol{\sigma}$ is electrical conductivity.

v. Lorentz force in the r -component, $\mathrm{f_r}$, is obtained from

$$\mathscr{J}_{\mathrm{v}}\times\mathbf{B}$$

Using equations (3.2.2) and equation (3.2.4)

$$\mathscr{J}_{\mathrm{v}} = \boldsymbol{\sigma}(\mathbf{u}\times\mathbf{B}) = \boldsymbol{\sigma}\begin{vmatrix} \hat{\boldsymbol{\rho}}_{\mathbf{r}} & \hat{\boldsymbol{\rho}}_{\boldsymbol{\theta}} & \hat{\boldsymbol{\rho}}_{\mathbf{z}} \\ \mathrm{u_r} & \mathrm{u}_{\boldsymbol{\theta}} & 0 \\ 0 & \mathrm{B}_{\boldsymbol{\theta}} & 0 \end{vmatrix} = \boldsymbol{\sigma}\mathrm{B}_{\boldsymbol{\theta}}\mathrm{u_r}\hat{\boldsymbol{\rho}}_{\mathbf{z}}$$

so that

$$\mathscr{J}_{\mathrm{v}} \times \mathbf{B} = \begin{vmatrix} \hat{\boldsymbol{\rho}}_{\mathbf{r}} & \hat{\boldsymbol{\rho}}_{\boldsymbol{\theta}} & \hat{\boldsymbol{\rho}}_{\mathbf{z}} \\ 0 & 0 & \boldsymbol{\sigma}\mathrm{B}_{\boldsymbol{\theta}}\mathrm{u}_{\mathrm{r}} \\ 0 & \mathrm{B}_{\boldsymbol{\theta}} & 0 \end{vmatrix} = -\boldsymbol{\sigma}\mathrm{B}_{\boldsymbol{\theta}}^{2}\mathrm{u}_{\mathrm{r}}\hat{\boldsymbol{\rho}}_{\mathbf{r}}$$

Lorentz force become

$$\mathrm{f}_{\mathrm{r}} = -\boldsymbol{\sigma}\mathrm{B}_{\boldsymbol{\theta}}^{2}\mathrm{u}_{\mathrm{r}} \tag{3.2.6}$$

vi. Thermodynamic temperature of fluid vary in the directions $\boldsymbol{\theta}$ and r but is zero in z. Temperature, simply, is then:

$$\mathrm{T} = \{\mathrm{T}_{\mathrm{r}}, \mathrm{T}_{\boldsymbol{\theta}}, 0\} \tag{3.2.7}$$

where T_{r} and $\mathrm{T}_{\boldsymbol{\theta}}$ are fluid temperatures in r and $\boldsymbol{\theta}$ directions respectively.

vii. The electric current density, $\mathscr{J}_{\mathrm{t}}$, for temperature is obtained as follows, when worked out in cylindrical coordinates, $(\hat{\boldsymbol{\rho}}_{\mathbf{r}}, \hat{\boldsymbol{\rho}}_{\boldsymbol{\theta}}, \hat{\boldsymbol{\rho}}_{\mathbf{z}})$; From Ohm's law of electromagnetism, equation (3.3.5),

$$\mathscr{J}_{\mathrm{t}} = \boldsymbol{\sigma}\left(\mathbf{E} + \mathbf{u} \times \mathbf{B}\right)$$

when $\mathbf{E} = 0$, it is considered that the electric force created by $\mathbf{E}$ is much much smaller than Lorentz force created by magnetic field $\mathbf{B}$. Otherwise a different formulation is required. Using equations (3.2.3) and (3.2.4)

$$\mathscr{J}_{\mathrm{t}} = \boldsymbol{\sigma}(\mathbf{u} \times \mathbf{B}) = \boldsymbol{\sigma}\begin{vmatrix} \hat{\boldsymbol{\rho}}_{\mathbf{r}} & \hat{\boldsymbol{\rho}}_{\boldsymbol{\theta}} & \hat{\boldsymbol{\rho}}_{\mathbf{z}} \\ \mathrm{u}_{\mathrm{r}} & \mathrm{u}_{\boldsymbol{\theta}} & 0 \\ \mathrm{B}_{\mathrm{r}} & \mathrm{B}_{\boldsymbol{\theta}} & 0 \end{vmatrix} = \boldsymbol{\sigma}\left(\mathrm{B}_{\boldsymbol{\theta}}\mathrm{u}_{\mathrm{r}} - \mathrm{B}_{\mathrm{r}}\mathrm{u}_{\boldsymbol{\theta}}\right)\hat{\boldsymbol{\rho}}_{\mathbf{z}}$$

so that

$$\mathscr{J}_{\mathrm{t}}^{2} = (\sigma)^{2}\left(\mathrm{B}_{\theta}\mathrm{u}_{\mathrm{r}} - \mathrm{B}_{\mathrm{r}}\mathrm{u}_{\theta}\right)^{2} \tag{3.2.8}$$

viii. The flow is steady i.e the velocity of the fluid at a particular fixed point does not change with time. This means that time is not considered in this study.

ix. There is no viscous dissipation of energy i.e there is no conversion of kinetic energy into internal energy by work done against the viscous stresses which would increase the initial temperature of the fluid. The research considered the original initial fluid temperature.

x. The Hall effect is negligible. Hall effect tends to accelerate fluid velocity. The study took into account initial fluid velocity.

xi. There are gravitational forces, $\rho\mathbf{g}$ while pressure fields p are negligible, where $\mathbf{g}$ and ρ are gravitational field strength and density of fluid respectively. This is because modeling is to be done with fluid being driven by gravitational force only

3.3 Governing Equations

The governing equations are:

3.3.1 Elliptical cross section of pipe

Taking into account a pipe of elliptical cross section, the centre will be at the origin. The length r is measured from the ellipse's centre and depends on the central angle θ as shown in figure 3.3.1. θ is measured in the anticlockwise direction in radians. Length r is given by

$$\mathrm{r}^{2} = \frac{\mathrm{a}^{2}\mathrm{b}^{2}}{\mathrm{a}^{2}\sin^{2}\theta + \mathrm{b}^{2}\cos^{2}\theta} \tag{3.3.1}$$

where a and b are half of the ellipse's major and minor axes respectively. The fluid will flow in the z-direction.

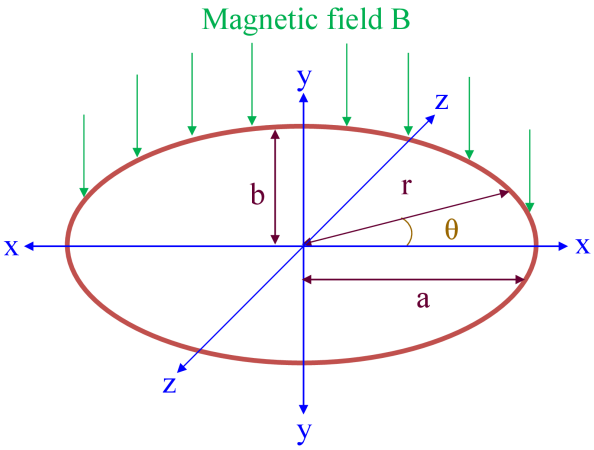

Figure 3.3.1: Elliptical cross section of pipe

3.3.2 Equation of continuity

From assumption (iii), in cylindrical coordinates $(\mathrm{r}, \theta, \mathrm{z})$, the equation of continuity for an incompressible fluid is given by

$$\frac{1}{\mathrm{r}}\frac{\partial}{\partial \mathrm{r}}\left(\mathrm{r u_r}\right) + \frac{1}{\mathrm{r}}\frac{\partial}{\partial \theta}\left(\mathrm{u}_\theta\right) = 0 \tag{3.3.2}$$

Where $\mathrm{u_r}$ and u_θ are components of fluid velocity, $\mathbf{u}$, in r and θ directions respectively.

3.3.3 Navier-Stokes equations

From assumptions (iii), (viii) and (xi), Navier-Stokes equations of motion for an incompressible fluid are given in cylindrical coordinates $(\mathrm{r}, \theta, \mathrm{z})$ for the θ and r -components as:

θ -component

$$\rho\left(\mathrm{u_r}\frac{\partial \mathrm{u}_\theta}{\partial \mathrm{r}} + \frac{\mathrm{u}_\theta}{\mathrm{r}}\frac{\partial \mathrm{u}_\theta}{\partial \theta} + \frac{\mathrm{u}_\theta \mathrm{u_r}}{\mathrm{r}}\right)$$

$$= \mu \left[\frac{1}{\mathrm{r}} \frac{\partial}{\partial \mathrm{r}} \left(\mathrm{r} \frac{\partial \mathrm{u}_\theta}{\partial \mathrm{r}} \right) + \frac{1}{\mathrm{r}^2} \frac{\partial^2 \mathrm{u}_\theta}{\partial \theta^2} + \frac{2}{\mathrm{r}^2} \frac{\partial \mathrm{u}_\mathrm{r}}{\partial \theta} - \frac{\mathrm{u}_\theta}{\mathrm{r}^2} \right] + \mathrm{f}_\theta + \rho \mathrm{g}_\theta \tag{3.3.3}$$

and r-component:

$$\rho \left(\mathrm{u}_\mathrm{r} \frac{\partial \mathrm{u}_\mathrm{r}}{\partial \mathrm{r}} + \frac{\mathrm{u}_\theta}{\mathrm{r}} \frac{\partial \mathrm{u}_\mathrm{r}}{\partial \theta} - \frac{\mathrm{u}_\theta^2}{\mathrm{r}} \right)$$

$$= \mu \left[\frac{1}{\mathrm{r}} \frac{\partial}{\partial \mathrm{r}} \left(\mathrm{r} \frac{\partial \mathrm{u}_\mathrm{r}}{\partial \mathrm{r}} \right) + \frac{1}{\mathrm{r}^2} \frac{\partial^2 \mathrm{u}_\mathrm{r}}{\partial \theta^2} - \frac{\mathrm{u}_\mathrm{r}}{\mathrm{r}^2} - \frac{2}{\mathrm{r}^2} \frac{\partial \mathrm{u}_\theta}{\partial \theta} \right] + \mathrm{f}_\mathrm{r} + \rho \mathrm{g}_\mathrm{r} \tag{3.3.4}$$

respectively.

3.3.4 Ohm's law of electromagnetism

Ohm's law asserts that the total electric current flowing in a conductor is proportional to the total electric field. In addition to the field **E** acting on a fluid at rest, a fluid moving with velocity **u** in the presence of a magnetic field **B** acquires an additional electric field $\mathbf{u} \times \mathbf{B}$. Ohm's law then becomes

$$\mathscr{J} = \sigma(\mathbf{E} + \mathbf{u} \times \mathbf{B}) \tag{3.3.5}$$

where σ is electrical conductivity

3.3.5 Heat energy equation

When assumptions (vi) and (ix) are considered, heat energy equation is written in cylindrical coordinates as

$$\frac{1}{\rho \mathrm{c_p}} \left(\frac{\mathrm{k}}{\mathrm{r}} \frac{\partial \mathrm{T}}{\partial \mathrm{r}} + \mathrm{k} \frac{\partial^2 \mathrm{T}}{\partial \mathrm{r}^2} + \frac{\mathrm{k}}{\mathrm{r}^2} \frac{\partial^2 \mathrm{T}}{\partial \theta^2} + \frac{\mathscr{J}_\mathrm{t}^2}{\sigma} \right) = 0 \tag{3.3.6}$$

Where $\mathrm{c_p}$ is specific heat capacity of fluid and k is thermal conductivity of fluid.

3.4 Non-dimensionalisation

Non-dimensionalisation, Josef [21], is done to simplify equations by reducing the number of variables used. The technique introduces dimensionless quantities like Hartmann number and Prandtl number whose magnitude influence temperature and velocity distributions differently.

3.4.1 Non-dimensionalisation of Navier-Stokes equations

To non-dimensionalise Navier-Stokes equations (3.3.3) and (3.3.4), the following non-dimensional parameters are used: $\mathrm{r} = \mathrm{r}^{\star}\mathrm{R}, \theta = \theta^{\star}, \mathrm{u_r} = \mathrm{u_r^{\star}U_0}, \mathrm{u_\theta} = \mathrm{u_\theta^{\star}U_0}$, kinematic viscosity: $\nu = \frac{\mu}{\rho}$, Reynolds number: $\mathrm{Re} = \frac{\mathrm{RU_0}}{\nu}$, Hartmann number: $\mathrm{Ha} = \mathrm{BR}\left(\frac{\sigma}{\mu}\right)^{\frac{1}{2}}$ and Stuart number (interaction parameter): $\mathrm{N} = \frac{\sigma \mathrm{B}^2 \mathrm{R}}{\rho \mathrm{U_0}} = \frac{\mathrm{Ha}^2}{\mathrm{Re}}$, where $\mathrm{U_0}$ and R are characteristic velocity scale and characteristic length from the centre of ellipse respectively. Quantities with superscript stars are dimensionless quantities. For equation (3.3.3);

$$\mathrm{u_r}\frac{\partial \mathrm{u_\theta}}{\partial \mathrm{r}} = \mathrm{u_r^{\star}U_0}\left(\frac{\partial \mathrm{u_\theta}}{\partial \mathrm{u_\theta^{\star}}}\frac{\partial \mathrm{r}^{\star}}{\partial \mathrm{r}}\frac{\partial \mathrm{u_\theta^{\star}}}{\partial \mathrm{r}^{\star}}\right) = \frac{\mathrm{U_0^2}}{\mathrm{R}}\mathrm{u_r^{\star}}\frac{\partial \mathrm{u_\theta^{\star}}}{\partial \mathrm{r}^{\star}}$$

$$\frac{\mathrm{u_\theta}}{\mathrm{r}}\frac{\partial \mathrm{u_\theta}}{\partial \theta} = \frac{\mathrm{u_\theta^{\star}U_0}}{\mathrm{r}^{\star}\mathrm{R}}\left(\frac{\partial \mathrm{u_\theta}}{\partial \mathrm{u_\theta^{\star}}}\frac{\partial \theta^{\star}}{\partial \theta}\frac{\partial \mathrm{u_\theta^{\star}}}{\partial \theta^{\star}}\right) = \frac{\mathrm{U_0^2}}{\mathrm{R}}\frac{\mathrm{u_\theta^{\star}}}{\mathrm{r}^{\star}}\frac{\partial \mathrm{u_\theta^{\star}}}{\partial \theta^{\star}}$$

$$\frac{\mathrm{u_\theta u_r}}{\mathrm{r}} = \frac{\mathrm{u_{\theta^{\star}}U_0 u_r^{\star}U_0}}{\mathrm{r}^{\star}\mathrm{R}} = \frac{\mathrm{U_0^2}}{\mathrm{R}}\frac{\mathrm{u_\theta^{\star}u_r^{\star}}}{\mathrm{r}^{\star}}$$

$$\frac{1}{\mathrm{r}}\frac{\partial \mathrm{u_\theta}}{\partial \mathrm{r}} = \frac{1}{\mathrm{r}^{\star}\mathrm{R}}\left(\frac{\partial \mathrm{u_\theta}}{\partial \mathrm{u_\theta^{\star}}}\frac{\partial \mathrm{r}^{\star}}{\partial \mathrm{r}}\frac{\partial \mathrm{u_\theta^{\star}}}{\partial \mathrm{r}^{\star}}\right) = \frac{\mathrm{U_0}}{\mathrm{R}^2}\frac{1}{\mathrm{r}^{\star}}\frac{\partial \mathrm{u_\theta^{\star}}}{\partial \mathrm{r}^{\star}}$$

$$\frac{\partial^2 \mathrm{u_\theta}}{\partial \mathrm{r}^2} = \frac{\partial}{\partial \mathrm{r}^{\star}}\left(\frac{\partial \mathrm{u_\theta}}{\partial \mathrm{r}}\right)\frac{\partial \mathrm{r}^{\star}}{\partial \mathrm{r}} = \frac{\mathrm{U_0}}{\mathrm{R}^2}\frac{\partial^2 \mathrm{u_\theta^{\star}}}{\partial \mathrm{r}^{\star 2}}$$

$$\frac{1}{\mathrm{r}^2}\frac{\partial^2 \mathrm{u_\theta}}{\partial \theta^2} = \frac{1}{\mathrm{r}^{\star 2}\mathrm{R}^2}\frac{\partial}{\partial \theta^{\star}}\left(\frac{\partial \mathrm{u_\theta}}{\partial \mathrm{u_\theta^{\star}}}\frac{\partial \theta^{\star}}{\partial \theta}\frac{\partial \mathrm{u_\theta^{\star}}}{\partial \theta^{\star}}\right)\frac{\partial \theta^{\star}}{\partial \theta} = \frac{\mathrm{U_0}}{\mathrm{R}^2\mathrm{r}^{\star 2}}\frac{\partial^2 \mathrm{u_\theta^{\star}}}{\partial \theta^{\star 2}}$$

$$\frac{2}{r^2}\frac{\partial u_r}{\partial \theta} = \frac{2}{r^{\star 2}R^2}\left(\frac{\partial u_r}{\partial u_r^\star}\frac{\partial \theta^\star}{\partial \theta}\frac{\partial u_r^\star}{\partial \theta^\star}\right) = \frac{2U_0}{R^2 r^{\star 2}}\frac{\partial u_r^\star}{\partial \theta^\star}$$

$$\frac{u_\theta}{r^2} = \frac{U_0}{R^2}\frac{u_\theta^\star}{r^{\star 2}}$$

Substituting the terms above and equation (3.2.5) in equation (3.3.3), it becomes

$$\rho\left(\frac{U_0^2}{R}u_r^\star\frac{\partial u_\theta^\star}{\partial r^\star} + \frac{U_0^2}{R}\frac{u_\theta^\star}{r^\star}\frac{\partial u_\theta^\star}{\partial \theta^\star} + \frac{U_0^2}{R}\frac{u_\theta^\star u_r^\star}{r^\star}\right) =$$

$$\mu\left[\frac{U_0}{R^2}\frac{1}{r^\star}\frac{\partial u_\theta^\star}{\partial r^\star} + \frac{U_0}{R^2}\frac{\partial^2 u_\theta^\star}{\partial r^{\star 2}} + \frac{U_0}{R^2 r^{\star 2}}\frac{\partial^2 u_\theta^\star}{\partial \theta^{\star 2}} + \frac{2U_0}{R^2 r^{\star 2}}\frac{\partial u_r^\star}{\partial \theta^\star} - \frac{U_0}{R^2}\frac{u_\theta^\star}{r^{\star 2}}\right] + \sigma B^2 U_0 u_\theta^\star + \rho g_\theta$$

$$\rho\frac{U_0^2}{R}\left(u_r^\star\frac{\partial u_\theta^\star}{\partial r^\star} + \frac{u_\theta^\star}{r^\star}\frac{\partial u_\theta^\star}{\partial \theta^\star} + \frac{u_\theta^\star u_r^\star}{r^\star}\right) =$$

$$\mu\frac{U_0}{R^2}\left[\frac{1}{r^\star}\frac{\partial u_\theta^\star}{\partial r^\star} + \frac{\partial^2 u_\theta^\star}{\partial r^{\star 2}} + \frac{1}{r^{\star 2}}\frac{\partial^2 u_\theta^\star}{\partial \theta^{\star 2}} + \frac{2}{r^{\star 2}}\frac{\partial u_r^\star}{\partial \theta^\star} - \frac{u_\theta^\star}{r^{\star 2}}\right] + \sigma B^2 U_0 u_\theta^\star + \rho g_\theta$$

Multiplying both sides of the above expression by $\frac{R}{U_0^2\rho}$, gives

$$u_r^\star\frac{\partial u_\theta^\star}{\partial r^\star} + \frac{u_\theta^\star}{r^\star}\frac{\partial u_\theta^\star}{\partial \theta^\star} + \frac{u_\theta^\star u_r^\star}{r^\star} =$$

$$\frac{\nu}{RU_0}\left[\frac{1}{r^\star}\frac{\partial u_\theta^\star}{\partial r^\star} + \frac{\partial^2 u_\theta^\star}{\partial r^{\star 2}} + \frac{1}{r^{\star 2}}\frac{\partial^2 u_\theta^\star}{\partial \theta^{\star 2}} + \frac{2}{r^{\star 2}}\frac{\partial u_r^\star}{\partial \theta^\star} - \frac{u_\theta^\star}{r^{\star 2}}\right] + \frac{\sigma B^2 R}{U_0\rho}u_\theta^\star + \frac{R}{U_0^2}g_\theta$$

Upon introducing Reynolds and Stuart numbers in the above expression leads to

$$u_r^\star\frac{\partial u_\theta^\star}{\partial r^\star} + \frac{u_\theta^\star}{r^\star}\frac{\partial u_\theta^\star}{\partial \theta^\star} + \frac{u_\theta^\star u_r^\star}{r^\star} =$$

$$\frac{1}{Re}\left[\frac{1}{r^\star}\frac{\partial u_\theta^\star}{\partial r^\star} + \frac{\partial^2 u_\theta^\star}{\partial r^{\star 2}} + \frac{1}{r^{\star 2}}\frac{\partial^2 u_\theta^\star}{\partial \theta^{\star 2}} + \frac{2}{r^{\star 2}}\frac{\partial u_r^\star}{\partial \theta^\star} - \frac{u_\theta^\star}{r^{\star 2}}\right] + Nu_\theta^\star + \frac{R}{U_0^2}g_\theta$$

Neglecting $\star$'s and letting $\frac{\mathrm{R}}{\mathrm{U}_0^2}\mathrm{g}_\theta = \gamma_\theta$, gravitational force in the $\theta-$ component

$$\mathrm{u_r}\frac{\partial \mathrm{u}_\theta}{\partial \mathrm{r}} + \frac{\mathrm{u}_\theta}{\mathrm{r}}\frac{\partial \mathrm{u}_\theta}{\partial \theta} + \frac{\mathrm{u}_\theta \mathrm{u_r}}{\mathrm{r}} =$$

$$\frac{1}{\mathrm{Re}}\left[\frac{1}{\mathrm{r}}\frac{\partial \mathrm{u}_\theta}{\partial \mathrm{r}} + \frac{\partial^2 \mathrm{u}_\theta}{\partial \mathrm{r}^2} + \frac{1}{\mathrm{r}^2}\frac{\partial^2 \mathrm{u}_\theta}{\partial \theta^2} + \frac{2}{\mathrm{r}^2}\frac{\partial \mathrm{u_r}}{\partial \theta} - \frac{\mathrm{u}_\theta}{\mathrm{r}^2}\right] + \mathrm{Nu}_\theta + \gamma_\theta \tag{3.4.1}$$

Repeating process for equation (3.3.4);

$$\mathrm{u_r}\frac{\partial \mathrm{u_r}}{\partial \mathrm{r}} = \mathrm{u_r^\star U_0}\left(\frac{\partial \mathrm{u_r}}{\partial \mathrm{u_r^\star}}\frac{\partial \mathrm{r}^\star}{\partial \mathrm{r}}\frac{\partial \mathrm{u_r^\star}}{\partial \mathrm{r}^\star}\right) = \frac{\mathrm{U_0^2}}{\mathrm{R}}\mathrm{u_r^\star}\frac{\partial \mathrm{u_r^\star}}{\partial \mathrm{r}^\star}$$

$$\frac{\mathrm{u}_\theta}{\mathrm{r}}\frac{\partial \mathrm{u_r}}{\partial \theta} = \frac{\mathrm{u}_\theta^\star \mathrm{U_0}}{\mathrm{r}^\star \mathrm{R}}\left(\frac{\partial \mathrm{u_r}}{\partial \mathrm{u_r^\star}}\frac{\partial \theta^\star}{\partial \theta}\frac{\partial \mathrm{u_r^\star}}{\partial \theta^\star}\right) = \frac{\mathrm{U_0^2}}{\mathrm{R}}\frac{\mathrm{u}_\theta^\star}{\mathrm{r}^\star}\frac{\partial \mathrm{u_r^\star}}{\partial \theta^\star}$$

$$\frac{\mathrm{u}_\theta^2}{\mathrm{r}} = \frac{\mathrm{u}_\theta^{\star 2}\mathrm{U_0^2}}{\mathrm{r}^\star \mathrm{R}}$$

$$\frac{1}{\mathrm{r}}\frac{\partial \mathrm{u_r}}{\partial \mathrm{r}} = \frac{1}{\mathrm{r}^\star \mathrm{R}}\left(\frac{\partial \mathrm{u_r}}{\partial \mathrm{u_r^\star}}\frac{\partial \mathrm{r}^\star}{\partial \mathrm{r}}\frac{\partial \mathrm{u_r^\star}}{\partial \mathrm{r}^\star}\right) = \frac{\mathrm{U_0}}{\mathrm{R}^2}\frac{1}{\mathrm{r}^\star}\frac{\partial \mathrm{u_r^\star}}{\partial \mathrm{r}^\star}$$

$$\frac{\partial^2 \mathrm{u_r}}{\partial \mathrm{r}^2} = \frac{\partial}{\partial \mathrm{r}^\star}\left(\frac{\partial \mathrm{u_r}}{\partial \mathrm{u_r^\star}}\frac{\partial \mathrm{r}^\star}{\partial \mathrm{r}}\frac{\partial \mathrm{u_r^\star}}{\partial \mathrm{r}^\star}\right)\frac{\partial \mathrm{r}^\star}{\partial \mathrm{r}} = \frac{\mathrm{U_0}}{\mathrm{R}^2}\frac{\partial^2 \mathrm{u_r^\star}}{\partial \mathrm{r}^{\star 2}}$$

$$\frac{1}{\mathrm{r}^2}\frac{\partial^2 \mathrm{u_r}}{\partial \theta^2} = \frac{1}{\mathrm{r}^{\star 2}\mathrm{R}^2}\frac{\partial}{\partial \theta^\star}\left(\frac{\partial \mathrm{u_r}}{\partial \mathrm{u_r^\star}}\frac{\partial \theta^\star}{\partial \theta}\frac{\partial \mathrm{u_r^\star}}{\partial \theta^\star}\right)\frac{\partial \theta^\star}{\partial \theta} = \frac{\mathrm{U_0}}{\mathrm{R}^2\mathrm{r}^{\star 2}}\frac{\partial^2 \mathrm{u_r^\star}}{\partial \theta^{\star 2}}$$

$$\frac{\mathrm{u_r}}{\mathrm{r}^2} = \frac{\mathrm{U_0}}{\mathrm{R}^2}\frac{\mathrm{u_r^\star}}{\mathrm{r}^{\star 2}}$$

$$\frac{2}{\mathrm{r}^2}\frac{\partial \mathrm{u}_\theta}{\partial \theta} = \frac{2}{\mathrm{r}^{\star 2}\mathrm{R}^2}\left(\frac{\partial \mathrm{u}_\theta}{\partial \mathrm{u}_\theta^\star}\frac{\partial \theta^\star}{\partial \theta}\frac{\partial \mathrm{u}_\theta^\star}{\partial \theta^\star}\right) = \frac{2\mathrm{U_0}}{\mathrm{R}^2\mathrm{r}^{\star 2}}\frac{\partial \mathrm{u}_\theta^\star}{\partial \theta^\star}$$

Substituting the terms above and equation (3.2.6) in equation (3.3.4), it delivers

$$\rho\left(\frac{\mathrm{U_0^2}}{\mathrm{R}}\mathrm{u_r^\star}\frac{\partial \mathrm{u_r^\star}}{\partial \mathrm{r}^\star} + \frac{\mathrm{U_0^2}}{\mathrm{R}}\frac{\mathrm{u}_\theta^\star}{\mathrm{r}^\star}\frac{\partial \mathrm{u_r^\star}}{\partial \theta^\star} - \frac{\mathrm{U_0^2}}{\mathrm{R}}\frac{\mathrm{u}_\theta^{\star 2}}{\mathrm{r}^\star}\right) =$$

$$\mu\left[\frac{\mathrm{U_0}}{\mathrm{R}^2}\frac{1}{\mathrm{r}^\star}\frac{\partial \mathrm{u_r^\star}}{\partial \mathrm{r}^\star} + \frac{\mathrm{U_0}}{\mathrm{R}^2}\frac{\partial^2 \mathrm{u_r^\star}}{\partial \mathrm{r}^{\star 2}} + \frac{\mathrm{U_0}}{\mathrm{R}^2\mathrm{r}^{\star 2}}\frac{\partial^2 \mathrm{u_r^\star}}{\partial \theta^{\star 2}} - \frac{2\mathrm{U_0}}{\mathrm{R}^2\mathrm{r}^{\star 2}}\frac{\partial \mathrm{u}_\theta^\star}{\partial \theta^\star} - \frac{\mathrm{U_0}}{\mathrm{R}^2}\frac{\mathrm{u_r^\star}}{\mathrm{r}^{\star 2}}\right] - \sigma \mathrm{B}^2 \mathrm{U_0}\mathrm{u_r^\star} + \rho \mathrm{g_r}$$

Then,

$$\rho\frac{\mathrm{U}_0^2}{\mathrm{R}}\left(\mathrm{u_r^\star}\frac{\partial \mathrm{u_r^\star}}{\partial \mathrm{r^\star}}+\frac{\mathrm{u_\theta^\star}}{\mathrm{r^\star}}\frac{\partial \mathrm{u_r^\star}}{\partial \boldsymbol{\theta}^\star}-\frac{\mathrm{u_\theta^{\star 2}}}{\mathrm{r^\star}}\right)=$$

$$\mu\frac{\mathrm{U}_0}{\mathrm{R}^2}\left[\frac{1}{\mathrm{r^\star}}\frac{\partial \mathrm{u_r^\star}}{\partial \mathrm{r^\star}}+\frac{\partial^2 \mathrm{u_r^\star}}{\partial \mathrm{r^{\star 2}}}+\frac{1}{\mathrm{r^{\star 2}}}\frac{\partial^2 \mathrm{u_r^\star}}{\partial \boldsymbol{\theta}^{\star 2}}-\frac{2}{\mathrm{r^{\star 2}}}\frac{\partial \mathrm{u_\theta^\star}}{\partial \boldsymbol{\theta}^\star}-\frac{\mathrm{u_r^\star}}{\mathrm{r^{\star 2}}}\right]-\sigma\mathrm{B}^2\mathrm{U}_0\mathrm{u_r^\star}+\rho\mathrm{g_r}$$

Multiplying both sides of the above expression by $\frac{\mathrm{R}}{\mathrm{U}_0^2\rho}$, gives

$$\mathrm{u_r^\star}\frac{\partial \mathrm{u_r^\star}}{\partial \mathrm{r^\star}}+\frac{\mathrm{u_\theta^\star}}{\mathrm{r^\star}}\frac{\partial \mathrm{u_r^\star}}{\partial \boldsymbol{\theta}^\star}-\frac{\mathrm{u_\theta^{\star 2}}}{\mathrm{r^\star}}=$$

$$\frac{\nu}{\mathrm{RU}_0}\left[\frac{1}{\mathrm{r^\star}}\frac{\partial \mathrm{u_r^\star}}{\partial \mathrm{r^\star}}+\frac{\partial^2 \mathrm{u_r^\star}}{\partial \mathrm{r^{\star 2}}}+\frac{1}{\mathrm{r^{\star 2}}}\frac{\partial^2 \mathrm{u_r^\star}}{\partial \boldsymbol{\theta}^{\star 2}}-\frac{2}{\mathrm{r^{\star 2}}}\frac{\partial \mathrm{u_\theta^\star}}{\partial \boldsymbol{\theta}^\star}-\frac{\mathrm{u_r^\star}}{\mathrm{r^{\star 2}}}\right]-\frac{\sigma\mathrm{B}^2\mathrm{R}}{\mathrm{U}_0\rho}\mathrm{u_r^\star}+\frac{\mathrm{R}}{\mathrm{U}_0^2}\mathrm{g_r}$$

Which shortens to

$$\mathrm{u_r^\star}\frac{\partial \mathrm{u_r^\star}}{\partial \mathrm{r^\star}}+\frac{\mathrm{u_\theta^\star}}{\mathrm{r^\star}}\frac{\partial \mathrm{u_r^\star}}{\partial \boldsymbol{\theta}^\star}-\frac{\mathrm{u_\theta^{\star 2}}}{\mathrm{r^\star}}=$$

$$\frac{1}{\mathrm{Re}}\left[\frac{1}{\mathrm{r^\star}}\frac{\partial \mathrm{u_r^\star}}{\partial \mathrm{r^\star}}+\frac{\partial^2 \mathrm{u_r^\star}}{\partial \mathrm{r^{\star 2}}}+\frac{1}{\mathrm{r^{\star 2}}}\frac{\partial^2 \mathrm{u_r^\star}}{\partial \boldsymbol{\theta}^{\star 2}}-\frac{2}{\mathrm{r^{\star 2}}}\frac{\partial \mathrm{u_\theta^\star}}{\partial \boldsymbol{\theta}^\star}-\frac{\mathrm{u_r^\star}}{\mathrm{r^{\star 2}}}\right]-\mathrm{Nu_r^\star}+\frac{\mathrm{R}}{\mathrm{U}_0^2}\mathrm{g_r}$$

Neglecting $\star$'s and letting $\frac{\mathrm{R}}{\mathrm{U}_0^2}\mathrm{g_r}=\gamma_\mathrm{r}$, gravitational force in the r– component

$$\mathrm{u_r}\frac{\partial \mathrm{u_r}}{\partial \mathrm{r}}+\frac{\mathrm{u_\theta}}{\mathrm{r}}\frac{\partial \mathrm{u_r}}{\partial \boldsymbol{\theta}}-\frac{\mathrm{u_\theta^2}}{\mathrm{r}}=$$

$$\frac{1}{\mathrm{Re}}\left[\frac{1}{\mathrm{r}}\frac{\partial \mathrm{u_r}}{\partial \mathrm{r}}+\frac{\partial^2 \mathrm{u_r}}{\partial \mathrm{r^2}}+\frac{1}{\mathrm{r^2}}\frac{\partial^2 \mathrm{u_r}}{\partial \boldsymbol{\theta}^2}-\frac{2}{\mathrm{r^2}}\frac{\partial \mathrm{u_\theta}}{\partial \boldsymbol{\theta}}-\frac{\mathrm{u_r}}{\mathrm{r^2}}\right]-\mathrm{Nu_r}+\gamma_\mathrm{r} \tag{3.4.2}$$

3.4.2 Non-dimensionalisation of heat energy equation

To non-dimensionalise heat energy equation (3.3.6), the following non-dimensional parameters are used, Josef [21]: $\mathrm{r}=\mathrm{r^\star R}$, $\boldsymbol{\theta}=\boldsymbol{\theta}^\star$, $\mathrm{u_r}=\mathrm{u_r^\star U}_0$, $\mathrm{u_\theta}=\mathrm{u_\theta^\star U}_0$, $\mathrm{T}=\mathrm{T^\star}(\mathrm{T}_0-\mathrm{T}_1)+\mathrm{T}_1$, Prandtl number: $\mathrm{Pr}=\frac{\mu c_\mathrm{p}}{\mathrm{k}}$, Hartmann number: $\mathrm{Ha}=\mathrm{BR}\left(\frac{\sigma}{\mu}\right)^{\frac{1}{2}}$, Eckert number: $\mathrm{Ec}=\frac{\mathrm{U}_0^2}{\mathrm{c_p}(\mathrm{T}_0-\mathrm{T}_1)}$, where U_0 and R are a characteristic velocity and a characteristic length from the centre of ellipse respectively

. T_0 and T_1 are temperatures at the centre and periphery of pipe respectively. Quantities with superscript star are dimensionless quantities. Then

$$\frac{\partial \mathrm{T}}{\partial \mathrm{r}} = \frac{\partial \mathrm{r}^\star}{\partial \mathrm{r}} \frac{\partial \mathrm{T}}{\partial \mathrm{T}^\star} \frac{\partial \mathrm{T}^\star}{\partial \mathrm{r}^\star} = \frac{(\mathrm{T}_0 - \mathrm{T}_1)}{\mathrm{R}} \frac{\partial \mathrm{T}^\star}{\partial \mathrm{r}^\star}$$

$$\frac{\partial^2 \mathrm{T}}{\partial \mathrm{r}^2} = \frac{\partial}{\partial \mathrm{r}^\star} \left(\frac{\partial \mathrm{T}}{\partial \mathrm{r}} \right) \frac{\partial \mathrm{r}^\star}{\partial \mathrm{r}} = \frac{(\mathrm{T}_0 - \mathrm{T}_1)}{\mathrm{R}^2} \frac{\partial^2 \mathrm{T}^\star}{\partial \mathrm{r}^{\star 2}}$$

$$\frac{\partial \mathrm{T}}{\partial \boldsymbol{\theta}} = \frac{\partial \boldsymbol{\theta}^\star}{\partial \boldsymbol{\theta}} \frac{\partial \mathrm{T}}{\partial \mathrm{T}^\star} \frac{\partial \mathrm{T}^\star}{\partial \boldsymbol{\theta}^\star} = (\mathrm{T}_0 - \mathrm{T}_1) \frac{\partial \mathrm{T}^\star}{\partial \boldsymbol{\theta}^\star}$$

$$\frac{\partial^2 \mathrm{T}}{\partial \boldsymbol{\theta}^2} = \frac{\partial}{\partial \boldsymbol{\theta}^\star} \left(\frac{\partial \mathrm{T}}{\partial \boldsymbol{\theta}} \right) \frac{\partial \boldsymbol{\theta}^\star}{\partial \boldsymbol{\theta}} = (\mathrm{T}_0 - \mathrm{T}_1) \frac{\partial^2 \mathrm{T}^\star}{\partial \boldsymbol{\theta}^{\star 2}}$$

Putting these terms and equation (3.2.8) in equation (3.3.6), it converts to

$$\frac{\mathrm{k}}{\boldsymbol{\rho} \mathrm{c}_\mathrm{p}} \left[\frac{(\mathrm{T}_0 - \mathrm{T}_1)}{\mathrm{r}^\star \mathrm{R}^2} \frac{\partial \mathrm{T}^\star}{\partial \mathrm{r}^\star} + \frac{(\mathrm{T}_0 - \mathrm{T}_1)}{\mathrm{R}^2} \frac{\partial^2 \mathrm{T}^\star}{\partial \mathrm{r}^{\star 2}} + \frac{(\mathrm{T}_0 - \mathrm{T}_1)}{(\mathrm{R}\mathrm{r}^\star)^2} \frac{\partial^2 \mathrm{T}^\star}{\partial \boldsymbol{\theta}^{\star 2}} \right] + \frac{\boldsymbol{\sigma} \mathrm{B}^2 \mathrm{U}_0^2}{\boldsymbol{\rho} \mathrm{c}_\mathrm{p}} (\mathrm{u}_\mathrm{r}^\star - \mathrm{u}_{\boldsymbol{\theta}}^\star)^2 = 0$$

so that

$$\frac{\mathrm{k}(\mathrm{T}_0 - \mathrm{T}_1)}{\boldsymbol{\rho} \mathrm{c}_\mathrm{p} \mathrm{R}^2} \left[\frac{1}{\mathrm{r}^\star} \frac{\partial \mathrm{T}^\star}{\partial \mathrm{r}^\star} + \frac{\partial^2 \mathrm{T}^\star}{\partial \mathrm{r}^{\star 2}} + \frac{1}{\mathrm{r}^{\star 2}} \frac{\partial^2 \mathrm{T}^\star}{\partial \boldsymbol{\theta}^{\star 2}} \right] + \frac{\boldsymbol{\sigma} \mathrm{B}^2 \mathrm{U}_0^2}{\boldsymbol{\rho} \mathrm{c}_\mathrm{p}} (\mathrm{u}_\mathrm{r}^\star - \mathrm{u}_{\boldsymbol{\theta}}^\star)^2 = 0 \tag{3.4.3}$$

Multiplying through equation (3.4.3) by $\frac{\boldsymbol{\rho} \mathrm{R}^2}{\mathrm{T}_0 - \mathrm{T}_1}$, it delivers

$$\frac{\mathrm{k}}{\mathrm{c}_\mathrm{p}} \left[\frac{1}{\mathrm{r}^\star} \frac{\partial \mathrm{T}^\star}{\partial \mathrm{r}^\star} + \frac{\partial^2 \mathrm{T}^\star}{\partial \mathrm{r}^{\star 2}} + \frac{1}{\mathrm{r}^{\star 2}} \frac{\partial^2 \mathrm{T}^\star}{\partial \boldsymbol{\theta}^{\star 2}} \right] + \frac{\boldsymbol{\sigma} \mathrm{B}^2 \mathrm{U}_0^2 \mathrm{R}^2}{\mathrm{c}_\mathrm{p}(\mathrm{T}_0 - \mathrm{T}_1)} (\mathrm{u}_\mathrm{r}^\star - \mathrm{u}_{\boldsymbol{\theta}}^\star)^2 = 0$$

Dividing through by dynamic viscosity $\boldsymbol{\mu}$ gives

$$\frac{\mathrm{k}}{\boldsymbol{\mu} \mathrm{c}_\mathrm{p}} \left[\frac{1}{\mathrm{r}^\star} \frac{\partial \mathrm{T}^\star}{\partial \mathrm{r}^\star} + \frac{\partial^2 \mathrm{T}^\star}{\partial \mathrm{r}^{\star 2}} + \frac{1}{\mathrm{r}^{\star 2}} \frac{\partial^2 \mathrm{T}^\star}{\partial \boldsymbol{\theta}^{\star 2}} \right] + \frac{\boldsymbol{\sigma} \mathrm{B}^2 \mathrm{U}_0^2 \mathrm{R}^2}{\boldsymbol{\mu} \mathrm{c}_\mathrm{p}(\mathrm{T}_0 - \mathrm{T}_1)} (\mathrm{u}_\mathrm{r}^\star - \mathrm{u}_{\boldsymbol{\theta}}^\star)^2 = 0 \tag{3.4.4}$$

Inserting the dimensionless numbers in equation (3.4.4), it transforms to

$$\frac{1}{\mathrm{Pr}}\left[\frac{1}{\mathrm{r}^\star}\frac{\partial \mathrm{T}^\star}{\partial \mathrm{r}^\star}+\frac{\partial^2 \mathrm{T}^\star}{\partial \mathrm{r}^{\star 2}}+\frac{1}{\mathrm{r}^{\star 2}}\frac{\partial^2 \mathrm{T}^\star}{\partial \theta^{\star 2}}\right]+\mathrm{EcHa}^2(\mathrm{u}_\mathrm{r}^\star-\mathrm{u}_\theta^\star)^2=0$$

Neglecting the $\star$'s gives

$$\frac{1}{\mathrm{Pr}}\left[\frac{1}{\mathrm{r}}\frac{\partial \mathrm{T}}{\partial \mathrm{r}}+\frac{\partial^2 \mathrm{T}}{\partial \mathrm{r}^2}+\frac{1}{\mathrm{r}^2}\frac{\partial^2 \mathrm{T}}{\partial \theta^2}\right]+\mathrm{EcHa}^2(\mathrm{u}_\mathrm{r}-\mathrm{u}_\theta)^2=0 \tag{3.4.5}$$

3.5 Equations in terms of stream function

Stream function which is represented by ψ, Nikolaos [22], is introduced in equations (3.4.1), (3.4.2) and (3.4.5) to reduce the number of dependent variables from two to one. This is effected by using the relations $\mathrm{u}_\mathrm{r}=\frac{1}{\mathrm{r}}\frac{\partial \psi}{\partial \theta}$ and $\mathrm{u}_\theta=-\frac{\partial \psi}{\partial \mathrm{r}}$,

3.5.1 Navier-Stokes equations in terms of stream function

For equation (3.4.1);

$$\mathrm{u}_\mathrm{r}\frac{\partial \mathrm{u}_\theta}{\partial \mathrm{r}}=-\frac{1}{\mathrm{r}}\frac{\partial \psi}{\partial \theta}\frac{\partial^2 \psi}{\partial \mathrm{r}^2}$$

$$\frac{\mathrm{u}_\theta}{\mathrm{r}}\frac{\partial \mathrm{u}_\theta}{\partial \theta}=\frac{1}{\mathrm{r}}\left(-\frac{\partial \psi}{\partial \mathrm{r}}\right)\frac{\partial}{\partial \theta}\left(-\frac{\partial \psi}{\partial \mathrm{r}}\right)=\frac{1}{\mathrm{r}}\frac{\partial \psi}{\partial \mathrm{r}}\frac{\partial^2 \psi}{\partial \mathrm{r}\partial \theta}$$

$$\frac{\mathrm{u}_\mathrm{r}\mathrm{u}_\theta}{\mathrm{r}}=\frac{1}{\mathrm{r}^2}\frac{\partial \psi}{\partial \theta}\left(-\frac{\partial \psi}{\partial \mathrm{r}}\right)=-\frac{1}{\mathrm{r}^2}\frac{\partial \psi}{\partial \theta}\frac{\partial \psi}{\partial \mathrm{r}}$$

$$\frac{1}{\mathrm{r}}\frac{\partial \mathrm{u}_\theta}{\partial \mathrm{r}}=\frac{1}{\mathrm{r}}\frac{\partial}{\partial \mathrm{r}}\left(-\frac{\partial \psi}{\partial \mathrm{r}}\right)=-\frac{1}{\mathrm{r}}\frac{\partial^2 \psi}{\partial \mathrm{r}^2}$$

$$\frac{\partial^2 \mathrm{u}_\theta}{\partial \mathrm{r}^2}=\frac{\partial}{\partial \mathrm{r}}\frac{\partial}{\partial \mathrm{r}}\left(-\frac{\partial \psi}{\partial \mathrm{r}}\right)=-\frac{\partial^3 \psi}{\partial \mathrm{r}^3}$$

$$\frac{1}{\mathrm{r}^2}\frac{\partial^2 \mathrm{u}_\theta}{\partial \theta^2}=\frac{1}{\mathrm{r}^2}\frac{\partial}{\partial \theta}\frac{\partial}{\partial \theta}\left(-\frac{\partial \psi}{\partial \mathrm{r}}\right)=-\frac{1}{\mathrm{r}^2}\frac{\partial^3 \psi}{\partial \theta^2 \partial \mathrm{r}}$$

$$\frac{2}{r^2}\frac{\partial u_r}{\partial \theta} = \frac{2}{r^2}\frac{\partial}{\partial \theta}\left(\frac{1}{r}\frac{\partial \psi}{\partial \theta}\right) = \frac{2}{r^3}\frac{\partial^2 \psi}{\partial \theta^2}$$

$$-\frac{u_\theta}{r^2} = -\frac{1}{r^2}\left(-\frac{\partial \psi}{\partial r}\right) = \frac{1}{r^2}\frac{\partial \psi}{\partial r}$$

$$Nu_\theta = -N\frac{\partial \psi}{\partial r}$$

Setting the terms above in equation (3.4.1), it hands out

$$\frac{\partial \psi}{\partial r}\frac{\partial^2 \psi}{\partial r \partial \theta} - \frac{\partial \psi}{\partial \theta}\frac{\partial^2 \psi}{\partial r^2} - \frac{1}{r}\frac{\partial \psi}{\partial \theta}\frac{\partial \psi}{\partial r} =$$

$$\frac{1}{Re}\left[\frac{1}{r}\frac{\partial \psi}{\partial r} + \frac{2}{r^2}\frac{\partial^2 \psi}{\partial \theta^2} - \frac{1}{r}\frac{\partial^3 \psi}{\partial \theta^2 \partial r} - r\frac{\partial^3 \psi}{\partial r^3} - \frac{\partial^2 \psi}{\partial r^2}\right] - Nr\frac{\partial \psi}{\partial r} + r\gamma_\theta$$

From assumption (xi), gravitational force is constant and does not vary so that setting the gravitational force, $\lambda_\theta = r\gamma_\theta$, the above expression becomes

$$\frac{\partial \psi}{\partial r}\frac{\partial^2 \psi}{\partial r \partial \theta} - \frac{\partial \psi}{\partial \theta}\frac{\partial^2 \psi}{\partial r^2} - \frac{1}{r}\frac{\partial \psi}{\partial \theta}\frac{\partial \psi}{\partial r} =$$

$$\frac{1}{Re}\left[\frac{1}{r}\frac{\partial \psi}{\partial r} + \frac{2}{r^2}\frac{\partial^2 \psi}{\partial \theta^2} - \frac{1}{r}\frac{\partial^3 \psi}{\partial \theta^2 \partial r} - r\frac{\partial^3 \psi}{\partial r^3} - \frac{\partial^2 \psi}{\partial r^2}\right] - Nr\frac{\partial \psi}{\partial r} + \lambda_\theta \tag{3.5.1}$$

The same procedure is done for equation (3.4.2) so that;

$$u_r\frac{\partial u_r}{\partial r} = -\frac{1}{r^3}\left[\frac{\partial \psi}{\partial \theta}\right]^2$$

$$\frac{u_\theta}{r}\frac{\partial u_r}{\partial \theta} = -\frac{1}{r^2}\frac{\partial \psi}{\partial r}\frac{\partial^2 \psi}{\partial \theta^2}$$

$$\frac{u_\theta^2}{r} = \frac{1}{r}\left[\frac{\partial \psi}{\partial r}\right]^2$$

$$\frac{1}{r}\frac{\partial u_r}{\partial r} = \frac{1}{r^2}\frac{\partial^2 \psi}{\partial r \partial \theta} - \frac{1}{r^3}\frac{\partial \psi}{\partial \theta}$$

$$\frac{\partial^2 \mathrm{u_r}}{\partial \mathrm{r}^2} = \frac{2}{\mathrm{r}^3}\frac{\partial \psi}{\partial \theta}$$

$$\frac{1}{\mathrm{r}^2}\frac{\partial^2 \mathrm{u_r}}{\partial \theta^2} = \frac{1}{\mathrm{r}^3}\frac{\partial^3 \psi}{\partial \theta^3}$$

$$\frac{\mathrm{u_r}}{\mathrm{r}^2} = \frac{1}{\mathrm{r}^3}\frac{\partial \psi}{\partial \theta}$$

$$\frac{2}{\mathrm{r}^2}\frac{\partial \mathrm{u}_\theta}{\partial \theta} = -\frac{2}{\mathrm{r}^2}\frac{\partial^2 \psi}{\partial \theta \partial \mathrm{r}}$$

$$\mathrm{Nu_r} = \mathrm{N}\frac{1}{\mathrm{r}}\frac{\partial \psi}{\partial \theta}$$

Putting the terms above in equation (3.4.2), it becomes

$$-\frac{1}{\mathrm{r}^3}\left[\frac{\partial \psi}{\partial \theta}\right]^2 - \frac{1}{\mathrm{r}^2}\frac{\partial^2 \psi}{\partial \theta^2}\frac{\partial \psi}{\partial \mathrm{r}} - \frac{1}{\mathrm{r}}\left[\frac{\partial \psi}{\partial \mathrm{r}}\right]^2 = \frac{1}{\mathrm{Re}}\left[\frac{3}{\mathrm{r}^2}\frac{\partial^2 \psi}{\partial \mathrm{r}\partial \theta} + \frac{1}{\mathrm{r}^3}\frac{\partial^3 \psi}{\partial \theta^3}\right] - \mathrm{N}\frac{1}{\mathrm{r}}\frac{\partial \psi}{\partial \theta} + \gamma_\mathrm{r} \qquad (3.5.2)$$

3.5.2 Heat energy equation in terms of stream function

Stream function, ψ, is introduced in equation (3.4.5), it turns out to

$$\frac{1}{\mathrm{Pr}}\left[\frac{1}{\mathrm{r}}\frac{\partial \mathrm{T}}{\partial \mathrm{r}} + \frac{\partial^2 \mathrm{T}}{\partial \mathrm{r}^2} + \frac{1}{\mathrm{r}^2}\frac{\partial^2 \mathrm{T}}{\partial \theta^2}\right] + \mathrm{EcHa}^2\left(\frac{1}{\mathrm{r}}\frac{\partial \psi}{\partial \theta} + \frac{\partial \psi}{\partial \mathrm{r}}\right)^2 = 0 \qquad (3.5.3)$$

Equations (3.5.1), (3.5.2) and (3.5.3) are the governing equations to be solved in the domain Ω with boundary conditions;

$$\frac{1}{\mathrm{r}}\frac{\partial \psi}{\partial \theta} = -\frac{\partial \psi}{\partial \mathrm{r}} = 0$$

$$\frac{\partial \mathrm{T}}{\partial \mathrm{r}} = \frac{\partial \mathrm{T}}{\partial \theta} = 0$$

$\mathrm{T} = \mathrm{T}_0$ when $\mathscr{P} = 0, \mathrm{T} = \mathrm{T}_1$ when $\mathscr{P} = \mathrm{r}$ on Γ, where $\mathscr{P}$ is length of r measured from ellipse's centre.

3.6 Similarity Transformation

Similarity transformation, Abbott *et. al* [23], is a methodology for converting a n-independent variable differential equation to a $\mathrm{n}-1$ independent variable differential equation. When $\mathrm{n}=2$, a pde revamps to an ode.

3.6.1 Similarity transformation for Navier-Stokes equation

Equation (3.5.1) with its boundary conditions is a non-linear partial differential equation. It is converted into an ordinary differential equation by using similarity transformation. Abbott *et. al* [23] considered similarity analysis of steady two dimensional, laminar boundary layer equations using similarity transformations of the form $\eta=\frac{\mathrm{y}}{\mathrm{x}^{\mathrm{k}}}, \mathrm{h}(\eta)=\mathrm{x}^{\mathrm{c}}\psi$, where x,y are cartesian coordinates, ψ is stream function, c,k are real numbers. In this study, the similarity transformation used is of the form $\eta=\varepsilon^{\mathrm{r}^{\mathrm{n}}\theta^{\mathrm{n}}}$ such that $\psi=\varepsilon^{\mathrm{r}^{\mathrm{n}}\theta^{\mathrm{n}}}\mathrm{f}(\varepsilon^{\mathrm{r}^{\mathrm{n}}\theta^{\mathrm{n}}})$, where n is an integer and ε is the base of natural logarithm. $\eta=\varepsilon^{\mathrm{r}^{\mathrm{n}}\theta^{\mathrm{n}}}$ is chosen because it is infinitely differentiable and will deliver coefficients of the form $\mathrm{r}^{\mathrm{n}}\theta^{\mathrm{n}}$ after differentiation has taken place to enable pdes to be converted into odes. This transformation also converts non- linear pdes directly into linear odes. When $\mathrm{n}=0$, a constant is formed and its derivative is zero. When $\mathrm{n}\geq 1$, derivatives are obtained but they cannot be integrated in section 3.7.24. When $\mathrm{n}\leq -1$ derivatives are obtained and can be worked out in section 3.7.24. However, as n increases, the expressions obtained become more complex and difficult to work out. Consideration is therefore made for $\mathrm{n}=-1$ so that: since $\psi=\varepsilon^{\mathrm{r}^{-1}\theta^{-1}}\mathrm{f}(\varepsilon^{\mathrm{r}^{-1}\theta^{-1}})$ then

$$\frac{\partial\psi}{\partial\mathrm{r}}=\frac{\partial}{\partial\mathrm{r}}\left(\varepsilon^{\mathrm{r}^{-1}\theta^{-1}}\mathrm{f}(\varepsilon^{\mathrm{r}^{-1}\theta^{-1}})\right)=-\mathrm{r}^{-2}\theta^{-1}\varepsilon^{\mathrm{r}^{-1}\theta^{-1}}\mathrm{f}(\varepsilon^{\mathrm{r}^{-1}\theta^{-1}})-\mathrm{r}^{-2}\theta^{-1}\varepsilon^{2\mathrm{r}^{-1}\theta^{-1}}\mathrm{f}'(\varepsilon^{\mathrm{r}^{-1}\theta^{-1}})$$

$$\frac{\partial \psi}{\partial \theta} = \frac{\partial}{\partial \theta}\left(\varepsilon^{r^{-1}\theta^{-1}} f(\varepsilon^{r^{-1}\theta^{-1}})\right) = -r^{-1}\theta^{-2}\varepsilon^{r^{-1}\theta^{-1}} f(\varepsilon^{r^{-1}\theta^{-1}}) - r^{-1}\theta^{-2}\varepsilon^{2r^{-1}\theta^{-1}} f'(\varepsilon^{r^{-1}\theta^{-1}})$$

$$\frac{\partial^2 \psi}{\partial r \partial \theta} = \frac{\partial}{\partial r}\left(-r^{-1}\theta^{-2}\varepsilon^{r^{-1}\theta^{-1}} f(\varepsilon^{r^{-1}\theta^{-1}}) - r^{-1}\theta^{-2}\varepsilon^{2r^{-1}\theta^{-1}} f'(\varepsilon^{r^{-1}\theta^{-1}})\right) =$$

$$r^{-3}\theta^{-3}\varepsilon^{r^{-1}\theta^{-1}} f(\varepsilon^{r^{-1}\theta^{-1}}) + r^{-2}\theta^{-2}\varepsilon^{r^{-1}\theta^{-1}} f(\varepsilon^{r^{-1}\theta^{-1}}) + 3r^{-3}\theta^{-3}\varepsilon^{2r^{-1}\theta^{-1}} f'(\varepsilon^{r^{-1}\theta^{-1}})$$

$$+ r^{-2}\theta^{-2}\varepsilon^{2r^{-1}\theta^{-1}} f'(\varepsilon^{r^{-1}\theta^{-1}}) + r^{-3}\theta^{-3}\varepsilon^{3r^{-1}\theta^{-1}} f''(\varepsilon^{r^{-1}\theta^{-1}})$$

$$\frac{\partial^2 \psi}{\partial r^2} = r^{-4}\theta^{-2}\varepsilon^{r^{-1}\theta^{-1}} f(\varepsilon^{r^{-1}\theta^{-1}}) + 2r^{-3}\theta^{-1}\varepsilon^{r^{-1}\theta^{-1}} f(\varepsilon^{r^{-1}\theta^{-1}}) + 3r^{-4}\theta^{-2}\varepsilon^{2r^{-1}\theta^{-1}} f'(\varepsilon^{r^{-1}\theta^{-1}})$$

$$+ 2r^{-3}\theta^{-1}\varepsilon^{2r^{-1}\theta^{-1}} f'(\varepsilon^{r^{-1}\theta^{-1}}) + r^{-4}\theta^{-2}\varepsilon^{3r^{-1}\theta^{-1}} f''(\varepsilon^{r^{-1}\theta^{-1}})$$

$$\frac{\partial^2 \psi}{\partial \theta^2} = r^{-2}\theta^{-4}\varepsilon^{r^{-1}\theta^{-1}} f(\varepsilon^{r^{-1}\theta^{-1}}) + 2r^{-1}\theta^{-3}\varepsilon^{r^{-1}\theta^{-1}} f(\varepsilon^{r^{-1}\theta^{-1}}) + 3r^{-2}\theta^{-4}\varepsilon^{2r^{-1}\theta^{-1}} f'(\varepsilon^{r^{-1}\theta^{-1}})$$

$$+ 2r^{-1}\theta^{-3}\varepsilon^{2r^{-1}\theta^{-1}} f'(\varepsilon^{r^{-1}\theta^{-1}}) + r^{-2}\theta^{-4}\varepsilon^{3r^{-1}\theta^{-1}} f''(\varepsilon^{r^{-1}\theta^{-1}})$$

$$\frac{\partial^3 \psi}{\partial r \partial \theta^2} = -r^{-4}\theta^{-5}\varepsilon^{r^{-1}\theta^{-1}} f(\varepsilon^{r^{-1}\theta^{-1}}) - 4r^{-3}\theta^{-4}\varepsilon^{r^{-1}\theta^{-1}} f(\varepsilon^{r^{-1}\theta^{-1}}) - 2r^{-2}\theta^{-3}\varepsilon^{r^{-1}\theta^{-1}} f(\varepsilon^{r^{-1}\theta^{-1}})$$

$$-7r^{-4}\theta^{-5}\varepsilon^{2r^{-1}\theta^{-1}} f'(\varepsilon^{r^{-1}\theta^{-1}}) - 12r^{-3}\theta^{-4}\varepsilon^{2r^{-1}\theta^{-1}} f'(\varepsilon^{r^{-1}\theta^{-1}}) - 2r^{-2}\theta^{-3}\varepsilon^{2r^{-1}\theta^{-1}} f'(\varepsilon^{r^{-1}\theta^{-1}})$$

$$-6r^{-4}\theta^{-5}\varepsilon^{3r^{-1}\theta^{-1}} f''(\varepsilon^{r^{-1}\theta^{-1}}) - 4r^{-3}\theta^{-4}\varepsilon^{3r^{-1}\theta^{-1}} f''(\varepsilon^{r^{-1}\theta^{-1}}) - r^{-4}\theta^{-5}\varepsilon^{4r^{-1}\theta^{-1}} f'''(\varepsilon^{r^{-1}\theta^{-1}})$$

$$\frac{\partial^3 \psi}{\partial r^3} = -r^{-6}\theta^{-3}\varepsilon^{r^{-1}\theta^{-1}} f(\varepsilon^{r^{-1}\theta^{-1}}) - 6r^{-5}\theta^{-2}\varepsilon^{r^{-1}\theta^{-1}} f(\varepsilon^{r^{-1}\theta^{-1}}) - 6r^{-4}\theta^{-1}\varepsilon^{r^{-1}\theta^{-1}} f(\varepsilon^{r^{-1}\theta^{-1}})$$

$$-7r^{-6}\theta^{-3}\varepsilon^{2r^{-1}\theta^{-1}} f'(\varepsilon^{r^{-1}\theta^{-1}}) - 18r^{-5}\theta^{-2}\varepsilon^{2r^{-1}\theta^{-1}} f'(\varepsilon^{r^{-1}\theta^{-1}}) - 6r^{-4}\theta^{-1}\varepsilon^{2r^{-1}\theta^{-1}} f'(\varepsilon^{r^{-1}\theta^{-1}})$$

$$-6r^{-6}\theta^{-3}\varepsilon^{3r^{-1}\theta^{-1}} f''(\varepsilon^{r^{-1}\theta^{-1}}) - 6r^{-5}\theta^{-2}\varepsilon^{3r^{-1}\theta^{-1}} f''(\varepsilon^{r^{-1}\theta^{-1}}) - r^{-6}\theta^{-3}\varepsilon^{4r^{-1}\theta^{-1}} f'''(\varepsilon^{r^{-1}\theta^{-1}})$$

On multiplying terms, we get;

$$\frac{\partial \psi}{\partial r}\frac{\partial^2 \psi}{\partial r \partial \theta} = -r^{-5}\theta^{-4}\varepsilon^{2r^{-1}\theta^{-1}}(f(\varepsilon^{r^{-1}\theta^{-1}}))^2 - r^{-4}\theta^{-3}\varepsilon^{2r^{-1}\theta^{-1}}(f(\varepsilon^{r^{-1}\theta^{-1}}))^2$$

$$-4\mathrm{r}^{-5}\theta^{-4}\varepsilon^{3\mathrm{r}^{-1}\theta^{-1}}\mathrm{f}(\varepsilon^{\mathrm{r}^{-1}\theta^{-1}})\mathrm{f}'(\varepsilon^{\mathrm{r}^{-1}\theta^{-1}})-2\mathrm{r}^{-4}\theta^{-3}\varepsilon^{3\mathrm{r}^{-1}\theta^{-1}}\mathrm{f}(\varepsilon^{\mathrm{r}^{-1}\theta^{-1}})\mathrm{f}'(\varepsilon^{\mathrm{r}^{-1}\theta^{-1}})$$

$$-3\mathrm{r}^{-5}\theta^{-4}\varepsilon^{4\mathrm{r}^{-1}\theta^{-1}}(\mathrm{f}'(\varepsilon^{\mathrm{r}^{-1}\theta^{-1}}))^2-\mathrm{r}^{-4}\theta^{-3}\varepsilon^{4\mathrm{r}^{-1}\theta^{-1}}(\mathrm{f}'(\varepsilon^{\mathrm{r}^{-1}\theta^{-1}}))^2$$

$$-\mathrm{r}^{-5}\theta^{-4}\varepsilon^{4\mathrm{r}^{-1}\theta^{-1}}\mathrm{f}(\varepsilon^{\mathrm{r}^{-1}\theta^{-1}})\mathrm{f}''(\varepsilon^{\mathrm{r}^{-1}\theta^{-1}})-\mathrm{r}^{-5}\theta^{-4}\varepsilon^{5\mathrm{r}^{-1}\theta^{-1}}\mathrm{f}'(\varepsilon^{\mathrm{r}^{-1}\theta^{-1}})\mathrm{f}''(\varepsilon^{\mathrm{r}^{-1}\theta^{-1}})$$

$$-\frac{\partial\psi}{\partial\theta}\frac{\partial^2\psi}{\partial\mathrm{r}^2}=\mathrm{r}^{-5}\theta^{-4}\varepsilon^{2\mathrm{r}^{-1}\theta^{-1}}(\mathrm{f}(\varepsilon^{\mathrm{r}^{-1}\theta^{-1}}))^2+2\mathrm{r}^{-4}\theta^{-3}\varepsilon^{2\mathrm{r}^{-1}\theta^{-1}}(\mathrm{f}(\varepsilon^{\mathrm{r}^{-1}\theta^{-1}}))^2$$

$$+4\mathrm{r}^{-5}\theta^{-4}\varepsilon^{3\mathrm{r}^{-1}\theta^{-1}}\mathrm{f}(\varepsilon^{\mathrm{r}^{-1}\theta^{-1}})\mathrm{f}'(\varepsilon^{\mathrm{r}^{-1}\theta^{-1}})+4\mathrm{r}^{-4}\theta^{-3}\varepsilon^{3\mathrm{r}^{-1}\theta^{-1}}\mathrm{f}(\varepsilon^{\mathrm{r}^{-1}\theta^{-1}})\mathrm{f}'(\varepsilon^{\mathrm{r}^{-1}\theta^{-1}})$$

$$+3\mathrm{r}^{-5}\theta^{-4}\varepsilon^{4\mathrm{r}^{-1}\theta^{-1}}(\mathrm{f}'(\varepsilon^{\mathrm{r}^{-1}\theta^{-1}}))^2+2\mathrm{r}^{-4}\theta^{-3}\varepsilon^{4\mathrm{r}^{-1}\theta^{-1}}(\mathrm{f}'(\varepsilon^{\mathrm{r}^{-1}\theta^{-1}}))^2$$

$$+\mathrm{r}^{-5}\theta^{-4}\varepsilon^{4\mathrm{r}^{-1}\theta^{-1}}\mathrm{f}(\varepsilon^{\mathrm{r}^{-1}\theta^{-1}})\mathrm{f}''(\varepsilon^{\mathrm{r}^{-1}\theta^{-1}})+\mathrm{r}^{-5}\theta^{-4}\varepsilon^{5\mathrm{r}^{-1}\theta^{-1}}\mathrm{f}'(\varepsilon^{\mathrm{r}^{-1}\theta^{-1}})\mathrm{f}''(\varepsilon^{\mathrm{r}^{-1}\theta^{-1}})$$

$$-\frac{1}{\mathrm{r}}\frac{\partial\psi}{\partial\mathrm{r}}\frac{\partial\psi}{\partial\theta}=-\mathrm{r}^{-4}\theta^{-3}\varepsilon^{2\mathrm{r}^{-1}\theta^{-1}}(\mathrm{f}(\varepsilon^{\mathrm{r}^{-1}\theta^{-1}}))^2-2\mathrm{r}^{-4}\theta^{-3}\varepsilon^{3\mathrm{r}^{-1}\theta^{-1}}\mathrm{f}(\varepsilon^{\mathrm{r}^{-1}\theta^{-1}})\mathrm{f}'(\varepsilon^{\mathrm{r}^{-1}\theta^{-1}})$$

$$-\mathrm{r}^{-4}\theta^{-3}\varepsilon^{4\mathrm{r}^{-1}\theta^{-1}}(\mathrm{f}'(\varepsilon^{\mathrm{r}^{-1}\theta^{-1}}))^2$$

$$\frac{1}{\mathrm{r}}\frac{\partial\psi}{\partial\mathrm{r}}=-\mathrm{r}^{-3}\theta^{-1}\varepsilon^{\mathrm{r}^{-1}\theta^{-1}}\mathrm{f}(\varepsilon^{\mathrm{r}^{-1}\theta^{-1}})-\mathrm{r}^{-3}\theta^{-1}\varepsilon^{2\mathrm{r}^{-1}\theta^{-1}}\mathrm{f}'(\varepsilon^{\mathrm{r}^{-1}\theta^{-1}})$$

$$\frac{2}{\mathrm{r}^2}\frac{\partial^2\psi}{\partial\theta^2}=2\mathrm{r}^{-4}\theta^{-4}\varepsilon^{\mathrm{r}^{-1}\theta^{-1}}\mathrm{f}(\varepsilon^{\mathrm{r}^{-1}\theta^{-1}})+4\mathrm{r}^{-3}\theta^{-3}\varepsilon^{\mathrm{r}^{-1}\theta^{-1}}\mathrm{f}(\varepsilon^{\mathrm{r}^{-1}\theta^{-1}})$$

$$+6\mathrm{r}^{-4}\theta^{-4}\varepsilon^{2\mathrm{r}^{-1}\theta^{-1}}\mathrm{f}'(\varepsilon^{\mathrm{r}^{-1}\theta^{-1}})+4\mathrm{r}^{-3}\theta^{-3}\varepsilon^{2\mathrm{r}^{-1}\theta^{-1}}\mathrm{f}'(\varepsilon^{\mathrm{r}^{-1}\theta^{-1}})+2\mathrm{r}^{-4}\theta^{-4}\varepsilon^{3\mathrm{r}^{-1}\theta^{-1}}\mathrm{f}''(\varepsilon^{\mathrm{r}^{-1}\theta^{-1}})$$

$$-\frac{1}{\mathrm{r}}\frac{\partial^3\psi}{\partial\mathrm{r}\partial\theta^2}=\mathrm{r}^{-5}\theta^{-5}\varepsilon^{\mathrm{r}^{-1}\theta^{-1}}\mathrm{f}(\varepsilon^{\mathrm{r}^{-1}\theta^{-1}})+4\mathrm{r}^{-4}\theta^{-4}\varepsilon^{\mathrm{r}^{-1}\theta^{-1}}\mathrm{f}(\varepsilon^{\mathrm{r}^{-1}\theta^{-1}})$$

$$+2\mathrm{r}^{-3}\theta^{-3}\varepsilon^{\mathrm{r}^{-1}\theta^{-1}}\mathrm{f}(\varepsilon^{\mathrm{r}^{-1}\theta^{-1}})+7\mathrm{r}^{-5}\theta^{-5}\varepsilon^{2\mathrm{r}^{-1}\theta^{-1}}\mathrm{f}'(\varepsilon^{\mathrm{r}^{-1}\theta^{-1}})+12\mathrm{r}^{-4}\theta^{-4}\varepsilon^{2\mathrm{r}^{-1}\theta^{-1}}\mathrm{f}'(\varepsilon^{\mathrm{r}^{-1}\theta^{-1}})$$

$$+2\mathrm{r}^{-3}\theta^{-3}\varepsilon^{2\mathrm{r}^{-1}\theta^{-1}}\mathrm{f}'(\varepsilon^{\mathrm{r}^{-1}\theta^{-1}})+6\mathrm{r}^{-5}\theta^{-5}\varepsilon^{3\mathrm{r}^{-1}\theta^{-1}}\mathrm{f}''(\varepsilon^{\mathrm{r}^{-1}\theta^{-1}})+4\mathrm{r}^{-4}\theta^{-4}\varepsilon^{3\mathrm{r}^{-1}\theta^{-1}}\mathrm{f}''(\varepsilon^{\mathrm{r}^{-1}\theta^{-1}})$$

$$+\mathrm{r}^{-5}\theta^{-5}\varepsilon^{4\mathrm{r}^{-1}\theta^{-1}}\mathrm{f}'''(\varepsilon^{\mathrm{r}^{-1}\theta^{-1}})$$

$$-\mathrm{r}\frac{\partial^3\psi}{\partial\mathrm{r}^3}=\mathrm{r}^{-5}\theta^{-3}\varepsilon^{\mathrm{r}^{-1}\theta^{-1}}\mathrm{f}(\varepsilon^{\mathrm{r}^{-1}\theta^{-1}})+6\mathrm{r}^{-4}\theta^{-2}\varepsilon^{\mathrm{r}^{-1}\theta^{-1}}\mathrm{f}(\varepsilon^{\mathrm{r}^{-1}\theta^{-1}})$$

$$+6\mathrm{r}^{-3}\theta^{-1}\varepsilon^{\mathrm{r}^{-1}\theta^{-1}}\mathrm{f}(\varepsilon^{\mathrm{r}^{-1}\theta^{-1}})+7\mathrm{r}^{-5}\theta^{-3}\varepsilon^{2\mathrm{r}^{-1}\theta^{-1}}\mathrm{f}'(\varepsilon^{\mathrm{r}^{-1}\theta^{-1}})+18\mathrm{r}^{-4}\theta^{-2}\varepsilon^{2\mathrm{r}^{-1}\theta^{-1}}\mathrm{f}'(\varepsilon^{\mathrm{r}^{-1}\theta^{-1}})$$

$$+6\mathrm{r}^{-3}\theta^{-1}\varepsilon^{2\mathrm{r}^{-1}\theta^{-1}}\mathrm{f}'(\varepsilon^{\mathrm{r}^{-1}\theta^{-1}})+6\mathrm{r}^{-5}\theta^{-3}\varepsilon^{3\mathrm{r}^{-1}\theta^{-1}}\mathrm{f}''(\varepsilon^{\mathrm{r}^{-1}\theta^{-1}})+6\mathrm{r}^{-4}\theta^{-2}\varepsilon^{3\mathrm{r}^{-1}\theta^{-1}}\mathrm{f}''(\varepsilon^{\mathrm{r}^{-1}\theta^{-1}})$$

$$+\mathrm{r}^{-5}\theta^{-3}\varepsilon^{4\mathrm{r}^{-1}\theta^{-1}}\mathrm{f}'''(\varepsilon^{\mathrm{r}^{-1}\theta^{-1}})$$

$$-\mathrm{Ha}^2\mathrm{r}\frac{\partial\psi}{\partial\mathrm{r}}=\mathrm{r}^{-1}\theta^{-1}\varepsilon^{\mathrm{r}^{-1}\theta^{-1}}\mathrm{Ha}^2\mathrm{f}(\varepsilon^{\mathrm{r}^{-1}\theta^{-1}})+\mathrm{r}^{-1}\theta^{-1}\varepsilon^{2\mathrm{r}^{-1}\theta^{-1}}\mathrm{Ha}^2\mathrm{f}'(\varepsilon^{\mathrm{r}^{-1}\theta^{-1}})$$

Substituting the multiplied terms above in equation (3.5.1), it becomes

$$\mathrm{r}^{-5}\theta^{-3}\varepsilon^{4\mathrm{r}^{-1}\theta^{-1}}\mathrm{f}'''(\varepsilon^{\mathrm{r}^{-1}\theta^{-1}})+\mathrm{r}^{-5}\theta^{-5}\varepsilon^{4\mathrm{r}^{-1}\theta^{-1}}\mathrm{f}'''(\varepsilon^{\mathrm{r}^{-1}\theta^{-1}})+5\mathrm{r}^{-4}\theta^{-2}\varepsilon^{3\mathrm{r}^{-1}\theta^{-1}}\mathrm{f}''(\varepsilon^{\mathrm{r}^{-1}\theta^{-1}})$$

$$+6\mathrm{r}^{-5}\theta^{-3}\varepsilon^{3\mathrm{r}^{-1}\theta^{-1}}\mathrm{f}''(\varepsilon^{\mathrm{r}^{-1}\theta^{-1}})+6\mathrm{r}^{-4}\theta^{-4}\varepsilon^{3\mathrm{r}^{-1}\theta^{-1}}\mathrm{f}''(\varepsilon^{\mathrm{r}^{-1}\theta^{-1}})+6\mathrm{r}^{-5}\theta^{-5}\varepsilon^{3\mathrm{r}^{-1}\theta^{-1}}\mathrm{f}''(\varepsilon^{\mathrm{r}^{-1}\theta^{-1}})$$

$$+3\mathrm{r}^{-3}\theta^{-1}\varepsilon^{2\mathrm{r}^{-1}\theta^{-1}}\mathrm{f}'(\varepsilon^{\mathrm{r}^{-1}\theta^{-1}})+15\mathrm{r}^{-4}\theta^{-2}\varepsilon^{2\mathrm{r}^{-1}\theta^{-1}}\mathrm{f}'(\varepsilon^{\mathrm{r}^{-1}\theta^{-1}})+6\mathrm{r}^{-3}\theta^{-3}\varepsilon^{2\mathrm{r}^{-1}\theta^{-1}}\mathrm{f}'(\varepsilon^{\mathrm{r}^{-1}\theta^{-1}})$$

$$+7\mathrm{r}^{-5}\theta^{-3}\varepsilon^{2\mathrm{r}^{-1}\theta^{-1}}\mathrm{f}'(\varepsilon^{\mathrm{r}^{-1}\theta^{-1}})+18\mathrm{r}^{-4}\theta^{-4}\varepsilon^{2\mathrm{r}^{-1}\theta^{-1}}\mathrm{f}'(\varepsilon^{\mathrm{r}^{-1}\theta^{-1}})+7\mathrm{r}^{-5}\theta^{-5}\varepsilon^{2\mathrm{r}^{-1}\theta^{-1}}\mathrm{f}'(\varepsilon^{\mathrm{r}^{-1}\theta^{-1}})$$

$$+3\mathrm{r}^{-3}\theta^{-1}\varepsilon^{\mathrm{r}^{-1}\theta^{-1}}\mathrm{f}(\varepsilon^{\mathrm{r}^{-1}\theta^{-1}})+5\mathrm{r}^{-4}\theta^{-2}\varepsilon^{\mathrm{r}^{-1}\theta^{-1}}\mathrm{f}(\varepsilon^{\mathrm{r}^{-1}\theta^{-1}})+6\mathrm{r}^{-3}\theta^{-3}\varepsilon^{\mathrm{r}^{-1}\theta^{-1}}\mathrm{f}(\varepsilon^{\mathrm{r}^{-1}\theta^{-1}})$$

$$+\mathrm{r}^{-5}\theta^{-3}\varepsilon^{\mathrm{r}^{-1}\theta^{-1}}\mathrm{f}(\varepsilon^{\mathrm{r}^{-1}\theta^{-1}})+6\mathrm{r}^{-4}\theta^{-4}\varepsilon^{\mathrm{r}^{-1}\theta^{-1}}\mathrm{f}(\varepsilon^{\mathrm{r}^{-1}\theta^{-1}})+\mathrm{r}^{-5}\theta^{-5}\varepsilon^{\mathrm{r}^{-1}\theta^{-1}}\mathrm{f}(\varepsilon^{\mathrm{r}^{-1}\theta^{-1}})$$

$$+\mathrm{r}^{-1}\theta^{-1}\varepsilon^{2\mathrm{r}^{-1}\theta^{-1}}\mathrm{Ha}^2\mathrm{f}'(\varepsilon^{\mathrm{r}^{-1}\theta^{-1}})+\mathrm{r}^{-1}\theta^{-1}\varepsilon^{\mathrm{r}^{-1}\theta^{-1}}\mathrm{Ha}^2\mathrm{f}(\varepsilon^{\mathrm{r}^{-1}\theta^{-1}})+\mathrm{Re}\lambda_\theta=0 \tag{3.6.1}$$

At this stage, only terms whose coefficients are $\mathrm{r}^{-1}\theta^{-1}$ or having their powers multiples of $\mathrm{r}^{-1}\theta^{-1}$ are considered. This is because we started by setting similarity transformation to be of the form $\mathrm{r}^{-1}\theta^{-1}$. It is prudent that we again select only terms of the same formation at the end of similarity transformation. Otherwise expressions formed are complex and difficult to solve. The terms left out in equation (3.6.1) are considered to have negligible effect and have their sum equal to zero.

Equation (3.6.1) become

$$r^{-5}\theta^{-5}\varepsilon^{4r^{-1}\theta^{-1}}f'''(\varepsilon^{r^{-1}\theta^{-1}})+6r^{-4}\theta^{-4}\varepsilon^{3r^{-1}\theta^{-1}}f''(\varepsilon^{r^{-1}\theta^{-1}})+6r^{-5}\theta^{-5}\varepsilon^{3r^{-1}\theta^{-1}}f''(\varepsilon^{r^{-1}\theta^{-1}})$$

$$+6r^{-3}\theta^{-3}\varepsilon^{2r^{-1}\theta^{-1}}f'(\varepsilon^{r^{-1}\theta^{-1}})+18r^{-4}\theta^{-4}\varepsilon^{2r^{-1}\theta^{-1}}f'(\varepsilon^{r^{-1}\theta^{-1}})+7r^{-5}\theta^{-5}\varepsilon^{2r^{-1}\theta^{-1}}f'(\varepsilon^{r^{-1}\theta^{-1}})$$

$$+6r^{-3}\theta^{-3}\varepsilon^{r^{-1}\theta^{-1}}f(\varepsilon^{r^{-1}\theta^{-1}})+6r^{-4}\theta^{-4}\varepsilon^{r^{-1}\theta^{-1}}f(\varepsilon^{r^{-1}\theta^{-1}})+r^{-5}\theta^{-5}\varepsilon^{r^{-1}\theta^{-1}}f(\varepsilon^{r^{-1}\theta^{-1}})$$

$$+r^{-1}\theta^{-1}\varepsilon^{2r^{-1}\theta^{-1}}Ha^2f'(\varepsilon^{r^{-1}\theta^{-1}})+r^{-1}\theta^{-1}\varepsilon^{r^{-1}\theta^{-1}}Ha^2f(\varepsilon^{r^{-1}\theta^{-1}})+Re\lambda_\theta=0 \tag{3.6.2}$$

Since $\eta=\varepsilon^{r^{-1}\theta^{-1}}$, equation (3.6.2) gives

$$\eta^4\log\eta^5f'''(\eta)+6\eta^3\log\eta^4f''(\eta)+6\eta^3\log\eta^5f''(\eta)+6\eta^2\log\eta^3f'(\eta)+18\eta^2\log\eta^4f'(\eta)$$

$$+7\eta^2\log\eta^5f'(\eta)+6\eta\log\eta^3f(\eta)+6\eta\log\eta^4f(\eta)+\eta\log\eta^5f(\eta)+\eta^2\log\eta Ha^2f'(\eta)$$

$$+\eta\log\eta Ha^2f(\eta)+Re\lambda_\theta=0 \tag{3.6.3}$$

Boundary conditions being

$$\frac{1}{r}\frac{\partial\psi}{\partial\theta}=-r^{-2}\theta^{-2}\varepsilon^{2r^{-1}\theta^{-1}}f'(\varepsilon^{r^{-1}\theta^{-1}})-r^{-2}\theta^{-2}\varepsilon^{r^{-1}\theta^{-1}}f(\varepsilon^{r^{-1}\theta^{-1}})$$

$$=f'(\varepsilon^{r^{-1}\theta^{-1}})-f(\varepsilon^{r^{-1}\theta^{-1}})=0$$

$$f'(\eta)-f(\eta)=0$$

on Γ

Similarity transformation technique has been used to convert Navier-Stokes equation (3.5.1), which is a pde into an ode, equation (3.6.3).

3.6.2 Similarity transformation for heat energy equation

Equation (3.5.3) is a partial differential equation which is converted into an ordinary differential equation using similarity transformation, Abbott *et.al* [23]. The similarity transformations embraced are of the form $\tau = \varepsilon^{\eta}$ and $\eta = \mathrm{r}^{-1}\theta^{-1}$ such that $\mathrm{T} = \mathrm{h}(\varepsilon^{\mathrm{r}^{-1}\theta^{-1}})$ and $\psi = \mathrm{f}(\varepsilon^{\mathrm{r}^{-1}\theta^{-1}})$, where ε is the base of the natural logarithm. Then,

$$\frac{\partial \mathrm{T}}{\partial \mathrm{r}} = \frac{\partial}{\partial \mathrm{r}}\left[\mathrm{h}(\varepsilon^{\mathrm{r}^{-1}\theta^{-1}})\right] = -\mathrm{r}^{-2}\theta^{-1}\varepsilon^{\mathrm{r}^{-1}\theta^{-1}}\mathrm{h}'(\varepsilon^{\mathrm{r}^{-1}\theta^{-1}})$$

$$\frac{\partial^2 \mathrm{T}}{\partial \mathrm{r}^2} = \frac{\partial}{\partial \mathrm{r}}\left[-\mathrm{r}^{-2}\theta^{-1}\varepsilon^{\mathrm{r}^{-1}\theta^{-1}}\mathrm{h}'(\varepsilon^{\mathrm{r}^{-1}\theta^{-1}})\right]$$

$$= \mathrm{r}^{-4}\theta^{-2}\varepsilon^{\mathrm{r}^{-1}\theta^{-1}}\mathrm{h}'(\varepsilon^{\mathrm{r}^{-1}\theta^{-1}}) + 2\mathrm{r}^{-3}\theta^{-1}\varepsilon^{\mathrm{r}^{-1}\theta^{-1}}\mathrm{h}'(\varepsilon^{\mathrm{r}^{-1}\theta^{-1}}) + \mathrm{r}^{-4}\theta^{-2}\varepsilon^{2\mathrm{r}^{-1}\theta^{-1}}\mathrm{h}''(\varepsilon^{\mathrm{r}^{-1}\theta^{-1}})$$

$$\frac{\partial \mathrm{T}}{\partial \theta} = \frac{\partial}{\partial \theta}\left[\mathrm{h}(\varepsilon^{\mathrm{r}^{-1}\theta^{-1}})\right] = -\mathrm{r}^{-1}\theta^{-2}\varepsilon^{\mathrm{r}^{-1}\theta^{-1}}\mathrm{h}'(\varepsilon^{\mathrm{r}^{-1}\theta^{-1}})$$

$$\frac{\partial^2 \mathrm{T}}{\partial \theta^2} = \frac{\partial}{\partial \theta}\left[-\mathrm{r}^{-1}\theta^{-2}\varepsilon^{\mathrm{r}^{-1}\theta^{-1}}\mathrm{h}'(\varepsilon^{\mathrm{r}^{-1}\theta^{-1}})\right]$$

$$= \mathrm{r}^{-2}\theta^{-4}\varepsilon^{\mathrm{r}^{-1}\theta^{-1}}\mathrm{h}'(\varepsilon^{\mathrm{r}^{-1}\theta^{-1}}) + 2\mathrm{r}^{-1}\theta^{-3}\varepsilon^{\mathrm{r}^{-1}\theta^{-1}}\mathrm{h}'(\varepsilon^{\mathrm{r}^{-1}\theta^{-1}}) + \mathrm{r}^{-2}\theta^{-4}\varepsilon^{2\mathrm{r}^{-1}\theta^{-1}}\mathrm{h}''(\varepsilon^{\mathrm{r}^{-1}\theta^{-1}})$$

$$\frac{1}{\mathrm{r}}\frac{\partial \mathrm{T}}{\partial \mathrm{r}} = -\mathrm{r}^{-3}\theta^{-1}\varepsilon^{\mathrm{r}^{-1}\theta^{-1}}\mathrm{h}'(\varepsilon^{\mathrm{r}^{-1}\theta^{-1}})$$

$$\frac{1}{\mathrm{r}^2}\frac{\partial^2 \mathrm{T}}{\partial \theta^2} =$$

$$\mathrm{r}^{-4}\theta^{-4}\varepsilon^{\mathrm{r}^{-1}\theta^{-1}}\mathrm{h}'(\varepsilon^{\mathrm{r}^{-1}\theta^{-1}}) + 2\mathrm{r}^{-3}\theta^{-3}\varepsilon^{\mathrm{r}^{-1}\theta^{-1}}\mathrm{h}'(\varepsilon^{\mathrm{r}^{-1}\theta^{-1}}) + \mathrm{r}^{-4}\theta^{-4}\varepsilon^{2\mathrm{r}^{-1}\theta^{-1}}\mathrm{h}''(\varepsilon^{\mathrm{r}^{-1}\theta^{-1}})$$

$$\left(\frac{1}{\mathrm{r}}\frac{\partial \psi}{\partial \theta} + \frac{\partial \psi}{\partial \mathrm{r}}\right)^2 = \frac{1}{\mathrm{r}^2}\left(\frac{\partial \psi}{\partial \theta}\right)^2 + \frac{2}{\mathrm{r}}\frac{\partial \psi}{\partial \theta}\frac{\partial \psi}{\partial \mathrm{r}} + \left(\frac{\partial \psi}{\partial \mathrm{r}}\right)^2$$

$$\frac{\partial \psi}{\partial \mathrm{r}} = \frac{\partial}{\partial \mathrm{r}}\left[\mathrm{f}(\varepsilon^{\mathrm{r}^{-1}\theta^{-1}})\right] = -\mathrm{r}^{-2}\theta^{-1}\varepsilon^{\mathrm{r}^{-1}\theta^{-1}}\mathrm{f}'(\varepsilon^{\mathrm{r}^{-1}\theta^{-1}})$$

$$\frac{\partial \psi}{\partial \theta} = \frac{\partial}{\partial \theta}\left[\mathrm{f}(\varepsilon^{\mathrm{r}^{-1}\theta^{-1}})\right] = -\mathrm{r}^{-1}\theta^{-2}\varepsilon^{\mathrm{r}^{-1}\theta^{-1}}\mathrm{f}'(\varepsilon^{\mathrm{r}^{-1}\theta^{-1}})$$

$$\frac{1}{r^2}\left(\frac{\partial \psi}{\partial \theta}\right)^2 = r^{-4}\theta^{-4}\varepsilon^{2r^{-1}\theta^{-1}}\left[f'(\varepsilon^{r^{-1}\theta^{-1}})\right]^2$$

$$\frac{2}{r}\frac{\partial \psi}{\partial \theta}\frac{\partial \psi}{\partial r} = 2r^{-4}\theta^{-3}\varepsilon^{2r^{-1}\theta^{-1}}\left[f'(\varepsilon^{r^{-1}\theta^{-1}})\right]^2$$

$$\left(\frac{\partial \psi}{\partial r}\right)^2 = r^{-4}\theta^{-2}\varepsilon^{2r^{-1}\theta^{-1}}\left[f'(\varepsilon^{r^{-1}\theta^{-1}})\right]^2$$

Inserting these terms in equation (3.5.3), it produces

$$\frac{1}{Pr}\left[r^{-4}\theta^{-2}\varepsilon^{r^{-1}\theta^{-1}}h'(\varepsilon^{r^{-1}\theta^{-1}}) + r^{-3}\theta^{-1}\varepsilon^{r^{-1}\theta^{-1}}h'(\varepsilon^{r^{-1}\theta^{-1}})\right]$$

$$+$$

$$\frac{1}{Pr}\left[r^{-4}\theta^{-2}\varepsilon^{2r^{-1}\theta^{-1}}h''(\varepsilon^{r^{-1}\theta^{-1}}) + r^{-4}\theta^{-4}\varepsilon^{r^{-1}\theta^{-1}}h'(\varepsilon^{r^{-1}\theta^{-1}}) + 2r^{-3}\theta^{-3}\varepsilon^{r^{-1}\theta^{-1}}h'(\varepsilon^{r^{-1}\theta^{-1}})\right]$$

$$+$$

$$\frac{1}{Pr}\left[r^{-4}\theta^{-4}\varepsilon^{2r^{-1}\theta^{-1}}h''(\varepsilon^{r^{-1}\theta^{-1}})\right] + EcHa^2\left[r^{-4}\theta^{-4}\varepsilon^{2r^{-1}\theta^{-1}}\left[f'(\varepsilon^{r^{-1}\theta^{-1}})\right]^2\right]$$

$$+$$

$$EcHa^2\left[2r^{-4}\theta^{-3}\varepsilon^{2r^{-1}\theta^{-1}}\left[\left(f'(\varepsilon^{r^{-1}\theta^{-1}})\right)\right]^2 + r^{-4}\theta^{-2}\varepsilon^{2r^{-1}\theta^{-1}}\left[\left(f'(\varepsilon^{r^{-1}\theta^{-1}})\right)\right]^2\right] = 0 \qquad (3.6.4)$$

Multiplying both sides of equation (3.6.4) by r^2, delivers

$$\frac{1}{Pr}\left[r^{-2}\theta^{-2}\varepsilon^{r^{-1}\theta^{-1}}h'(\varepsilon^{r^{-1}\theta^{-1}}) + r^{-1}\theta^{-1}\varepsilon^{r^{-1}\theta^{-1}}h'(\varepsilon^{r^{-1}\theta^{-1}})\right]$$

$$+$$

$$\frac{1}{Pr}\left[r^{-2}\theta^{-2}\varepsilon^{2r^{-1}\theta^{-1}}h''(\varepsilon^{r^{-1}\theta^{-1}}) + r^{-2}\theta^{-4}\varepsilon^{r^{-1}\theta^{-1}}h'(\varepsilon^{r^{-1}\theta^{-1}}) + 2r^{-1}\theta^{-3}\varepsilon^{r^{-1}\theta^{-1}}h'(\varepsilon^{r^{-1}\theta^{-1}})\right]$$

$$+$$

$$\frac{1}{\mathrm{Pr}}\left[\mathrm{r}^{-2}\theta^{-4}\varepsilon^{2\mathrm{r}^{-1}\theta^{-1}}\mathrm{h}''(\varepsilon^{\mathrm{r}^{-1}\theta^{-1}})\right]+\mathrm{EcHa}^2\left[\mathrm{r}^{-2}\theta^{-4}\varepsilon^{2\mathrm{r}^{-1}\theta^{-1}}\left[\mathrm{f}'(\varepsilon^{\mathrm{r}^{-1}\theta^{-1}})\right]^2\right]$$

$$+$$

$$\mathrm{EcHa}^2\left[2\mathrm{r}^{-2}\theta^{-3}\varepsilon^{2\mathrm{r}^{-1}\theta^{-1}}\left[\left(\mathrm{f}'(\varepsilon^{\mathrm{r}^{-1}\theta^{-1}})\right)\right]^2+\mathrm{r}^{-2}\theta^{-2}\varepsilon^{2\mathrm{r}^{-1}\theta^{-1}}\left[\left(\mathrm{f}'(\varepsilon^{\mathrm{r}^{-1}\theta^{-1}})\right)\right]^2\right]=0 \qquad (3.6.5)$$

Taking into account terms whose coefficients are $\mathrm{r}^{-1}\theta^{-1}$ or its powers' multiples, dwindles equation (3.6.5) to

$$\frac{1}{\mathrm{Pr}}\left[\mathrm{r}^{-1}\theta^{-1}\mathrm{h}'(\varepsilon^{\mathrm{r}^{-1}\theta^{-1}})+\mathrm{h}'(\varepsilon^{\mathrm{r}^{-1}\theta^{-1}})+\mathrm{r}^{-1}\theta^{-1}\varepsilon^{\mathrm{r}^{-1}\theta^{-1}}\mathrm{h}''(\varepsilon^{\mathrm{r}^{-1}\theta^{-1}})\right]$$

$$+\mathrm{EcHa}^2\left[\mathrm{r}^{-1}\theta^{-1}\varepsilon^{\mathrm{r}^{-1}\theta^{-1}}\left[\left(\mathrm{f}'(\varepsilon^{\mathrm{r}^{-1}\theta^{-1}})\right)\right]^2\right]=0 \qquad (3.6.6)$$

Equation (3.6.6) metamorphoses to

$$\frac{1}{\mathrm{Pr}}\left[\tau\log\tau\mathrm{h}''(\tau)+\mathrm{h}'(\tau)+\log\tau\mathrm{h}'(\tau)\right]+\tau\log\tau\mathrm{EcHa}^2\left[\left[\mathrm{f}'(\tau)\right]^2\right]=0 \qquad (3.6.7)$$

since $\tau=\varepsilon^{\mathrm{r}^{-1}\theta^{-1}}$. Boundary conditions being:

$$\mathrm{f}(\tau)=\mathrm{h}(\tau)=0$$

$$\frac{1}{\mathrm{r}}\frac{\partial\psi}{\partial\theta}=-\mathrm{r}^{-2}\theta^{-2}\varepsilon^{\mathrm{r}^{-1}\theta^{-1}}\mathrm{f}'(\varepsilon^{\mathrm{r}^{-1}\theta^{-1}})=\tau(\log\tau)^2\mathrm{f}'(\tau)=0$$

$$-\frac{\partial\psi}{\partial\mathrm{r}}=-\mathrm{r}^{-2}\theta^{-1}\varepsilon^{\mathrm{r}^{-1}\theta^{-1}}\mathrm{f}'(\varepsilon^{\mathrm{r}^{-1}\theta^{-1}})=\mathrm{f}'(\tau)=0$$

$$\frac{\partial\mathrm{T}}{\partial\theta}=-\mathrm{r}^{-1}\theta^{-2}\varepsilon^{\mathrm{r}^{-1}\theta^{-1}}\mathrm{h}'(\varepsilon^{\mathrm{r}^{-1}\theta^{-1}})=\mathrm{h}'(\tau)=0$$

$$\frac{\partial \mathrm{T}}{\partial \mathrm{r}} = -\mathrm{r}^{-2}\theta^{-1}\varepsilon^{\mathrm{r}^{-1}\theta^{-1}}\mathrm{h}'(\varepsilon^{\mathrm{r}^{-1}\theta^{-1}}) = \mathrm{h}'(\tau) = 0$$

on Γ

At this juncture, similarity transformation technique has been used to convert heat energy equation (3.5.3) which is a pde into an ode, equation (3.6.7).

3.7 Finite Element Method (FEM)

Finite Element Method (FEM), Reddy [24], is a numerical technique for finding approximate solutions to boundary value problems for differential equations. Equation (3.6.3), which is utilized to find velocity profile and equation (3.6.7), which is manipulated to find temperature distribution are solved using FEM. FEM involves:

i. Discretization or subdivision of the domain.

ii. Selection of the interpolation functions, to provide an approximation of the unknown solution within an element.

iii. Formulation of the system of equations

iv. Solution of the system of equations. After the system of equations are solved, results are displayed in form of tables and graphs.

To employ FEM, for equation (3.6.3), Ha, Re and λ_θ are known, $\mathrm{f}(\eta)$ is the scalar unknown,which is to be worked out. For equation (3.6.7), Ha, Pr and Ec are known, $\mathrm{h}(\tau)$ is the scalar unknown. $\mathrm{f}(\tau)$ is also known since it is the value of velocity worked out first when examining velocity profile. It is found to be f. This is shown in subsection 4.1, where velocity profile is worked out first to find f. f is then used to find temperature distribution, h in sub section 4.2. Equation (3.6.7)

revamps to

$$\frac{1}{\mathrm{Pr}}\left[\tau\log\tau \mathrm{h}''(\tau)+\mathrm{h}'(\tau)+\log\tau \mathrm{h}'(\tau)\right]+\tau\log\tau \mathrm{EcHa}^2\mathrm{f}^2=0 \tag{3.7.1}$$

Boundary conditions lessen to

$$\mathrm{h}(\tau)=\mathrm{h}'(\tau)=0$$

The approximate solution is C^0 continuous, i.e only the 0^{th} order solution (the solution itself) is continuous across element interfaces, but not higher order derivatives.

3.7.1 Method of weighted residuals for velocity profile

Equation (3.6.3) is the strong form of the problem. The method of weighted residuals is used to obtain the weak form as follows: The residual of the differential equation is obtained by collecting all the terms on one side of the equation i.e

$$\mathrm{R}(\eta)=\eta^4(\log\eta)^5\mathrm{f}'''(\eta)+6\eta^3(\log\eta)^4\mathrm{f}''(\eta)+6\eta^3(\log\eta)^5\mathrm{f}''(\eta)+6\eta^2(\log\eta)^3\mathrm{f}'(\eta)$$

$$+18\eta^2(\log\eta)^4\mathrm{f}'(\eta)+7\eta^2(\log\eta)^5\mathrm{f}'(\eta)+6\eta(\log\eta)^3\mathrm{f}(\eta)+6\eta(\log\eta)^4\mathrm{f}(\eta)+\eta(\log\eta)^5\mathrm{f}(\eta)$$

$$+\eta^2\log\eta\mathrm{Ha}^2\mathrm{f}'(\eta)+\eta\log\eta\mathrm{Ha}^2\mathrm{f}(\eta)+\mathrm{Re}\lambda_{\theta} \tag{3.7.2}$$

Minimization of the residual is carried out so that

$$\int_{\Omega}\mathrm{w}(\eta)\mathrm{R}(\eta)\mathrm{d}\eta=0 \tag{3.7.3}$$

where $\mathrm{w}(\eta)$ is weight (or test) function. Substituting equation (3.7.2) in equation (3.7.3), it turns out into

$$\int_{\Omega}\left[\eta^{4}\left(\log\eta\right)^{5}\mathrm{w}(\eta)\mathrm{f}'''(\eta)+6\eta^{3}\left(\log\eta\right)^{4}\mathrm{w}(\eta)\mathrm{f}''(\eta)+6\eta^{3}\left(\log\eta\right)^{5}\mathrm{w}(\eta)\mathrm{f}''(\eta)\right]\mathrm{d}\eta$$

$$+\int_{\Omega}\left[6\eta^{2}\left(\log\eta\right)^{3}\mathrm{w}(\eta)\mathrm{f}'(\eta)+18\eta^{2}\left(\log\eta\right)^{4}\mathrm{w}(\eta)\mathrm{f}'(\eta)+7\eta^{2}\left(\log\eta\right)^{5}\mathrm{w}(\eta)\mathrm{f}'(\eta)\right]\mathrm{d}\eta$$

$$+\int_{\Omega}\left[6\eta\left(\log\eta\right)^{3}\mathrm{w}(\eta)\mathrm{f}(\eta)+6\eta\left(\log\eta\right)^{4}\mathrm{w}(\eta)\mathrm{f}(\eta)+\eta\left(\log\eta\right)^{5}\mathrm{w}(\eta)\mathrm{f}(\eta)\right]\mathrm{d}\eta$$

$$+\int_{\Omega}\left[\eta^{2}\log\eta\mathrm{Ha}^{2}\mathrm{w}(\eta)\mathrm{f}'(\eta)+\eta\log\eta\mathrm{Ha}^{2}\mathrm{w}(\eta)\mathrm{f}(\eta)+\mathrm{w}(\eta)\mathrm{Re}\lambda_{\theta}\right]\mathrm{d}\eta=0 \qquad (3.7.4)$$

When a C^{0} continuous solution is used in equation (3.7.4), the third and the second order derivatives can not be evaluated properly. The order of the third and the second derivatives is lowered to one by applying integration by parts to the first three terms on the left of equation (3.7.4) as follows

$$\int_{\Omega}\eta^{4}\left(\log\eta\right)^{5}\mathrm{w}(\eta)\mathrm{f}'''(\eta)\mathrm{d}\eta=-\int_{\Omega}5\eta^{3}\left(\log\eta\right)^{4}\mathrm{w}(\eta)\mathrm{f}''(\eta)\mathrm{d}\eta-\int_{\Omega}4\eta^{3}\left(\log\eta\right)^{5}\mathrm{w}(\eta)\mathrm{f}''(\eta)\mathrm{d}\eta$$

$$-\int_{\Omega}\eta^{4}\left(\log\eta\right)^{5}\mathrm{w}'(\eta)\mathrm{f}''(\eta)\mathrm{d}\eta+\int_{\Gamma}\eta^{4}\left(\log\eta\right)^{5}\mathrm{w}(\eta)\mathrm{f}''(\eta)\mathrm{n}_{\eta}\mathrm{d}\Gamma \qquad (3.7.5)$$

The last term of equation (3.7.5) is the boundary integral and is evaluated at the boundaries Γ of the domain Ω. Where n_{η} is the η component of unit outward normal of boundary. n_{η} is equal to -1 and 1 at the left and right boundaries of the problem domain respectively. Placing equation (3.7.5) in equation (3.7.4), delivers

$$\int_{\Omega}\left[\eta^{3}\left(\log\eta\right)^{4}\mathrm{w}(\eta)\mathrm{f}''(\eta)-\eta^{4}\left(\log\eta\right)^{5}\mathrm{w}'(\eta)\mathrm{f}''(\eta)+2\eta^{3}\left(\log\eta\right)^{5}\mathrm{w}(\eta)\mathrm{f}''(\eta)\right]\mathrm{d}\eta$$

$$+\int_{\Omega}\left[6\eta^{2}\left(\log\eta\right)^{3}\mathrm{w}(\eta)\mathrm{f}'(\eta)+18\eta^{2}\left(\log\eta\right)^{4}\mathrm{w}(\eta)\mathrm{f}'(\eta)+7\eta^{2}\left(\log\eta\right)^{5}\mathrm{w}(\eta)\mathrm{f}'(\eta)\right]\mathrm{d}\eta$$

$$+\int_{\Omega}\left[6\eta\left(\log\eta\right)^{3}\mathrm{w}(\eta)\mathrm{f}(\eta)+6\eta\left(\log\eta\right)^{4}\mathrm{w}(\eta)\mathrm{f}(\eta)+\eta\left(\log\eta\right)^{5}\mathrm{w}(\eta)\mathrm{f}(\eta)+\right]\mathrm{d}\eta$$

$$+\int_{\Omega}\left[\eta^{2}\log\eta\mathrm{Ha}^{2}\mathrm{w}(\eta)\mathrm{f}'(\eta)+\eta\log\eta\mathrm{Ha}^{2}\mathrm{w}(\eta)\mathrm{f}(\eta)+\mathrm{w}(\eta)\mathrm{Re}\lambda_{\theta}\right]\mathrm{d}\eta=$$

$$-\int_{\Gamma}\eta^{4}\left(\log\eta\right)^{5}\mathrm{w}(\eta)\mathrm{f}''(\eta)\mathrm{n}_{\eta}\mathrm{d}\Gamma \tag{3.7.6}$$

Integration by parts is carried out on the first term on the left of equation (3.7.6), it changes to

$$\int_{\Omega}\eta^{3}\left(\log\eta\right)^{4}\mathrm{w}(\eta)\mathrm{f}''(\eta)\mathrm{d}\eta=-\int_{\Omega}4\eta^{2}\left(\log\eta\right)^{3}\mathrm{w}(\eta)\mathrm{f}'(\eta)\mathrm{d}\eta-\int_{\Omega}3\eta^{2}\left(\log\eta\right)^{4}\mathrm{w}(\eta)\mathrm{f}'(\eta)\mathrm{d}\eta$$

$$-\int_{\Omega}\eta^{3}\left(\log\eta\right)^{4}\mathrm{w}'(\eta)\mathrm{f}'(\eta)\mathrm{d}\eta+\int_{\Gamma}\eta^{3}\left(\log\eta\right)^{4}\mathrm{w}(\eta)\mathrm{f}'(\eta)\mathrm{n}_{\eta}\mathrm{d}\Gamma \tag{3.7.7}$$

Settling equation (3.7.7) in equation (3.7.6), results in

$$\int_{\Omega}\left[-\eta^{4}\left(\log\eta\right)^{5}\mathrm{w}'(\eta)\mathrm{f}''(\eta)+2\eta^{3}\left(\log\eta\right)^{5}\mathrm{w}(\eta)\mathrm{f}''(\eta)+2\eta^{2}\left(\log\eta\right)^{3}\mathrm{w}(\eta)\mathrm{f}'(\eta)\right]\mathrm{d}\eta$$

$$+\int_{\Omega}\left[-\eta^{3}\left(\log\eta\right)^{4}\mathrm{w}'(\eta)\mathrm{f}'(\eta)+15\eta^{2}\left(\log\eta\right)^{4}\mathrm{w}(\eta)\mathrm{f}'(\eta)+7\eta^{2}\left(\log\eta\right)^{5}\mathrm{w}(\eta)\mathrm{f}'(\eta)\right]\mathrm{d}\eta$$

$$+\int_{\Omega}\left[6\eta\left(\log\eta\right)^{3}\mathrm{w}(\eta)\mathrm{f}(\eta)+6\eta\left(\log\eta\right)^{4}\mathrm{w}(\eta)\mathrm{f}(\eta)+\eta\left(\log\eta\right)^{5}\mathrm{w}(\eta)\mathrm{f}(\eta)+\right]\mathrm{d}\eta$$

$$+\int_{\Omega}\left[\eta^{2}\log\eta\mathrm{Ha}^{2}\mathrm{w}(\eta)\mathrm{f}'(\eta)+\eta\log\eta\mathrm{Ha}^{2}\mathrm{w}(\eta)\mathrm{f}(\eta)+\mathrm{w}(\eta)\mathrm{Re}\lambda_{\theta}\right]\mathrm{d}\eta=$$

$$-\int_{\Gamma}\eta^{4}\left(\log\eta\right)^{5}\mathrm{w}(\eta)\mathrm{f}''(\eta)\mathrm{n}_{\eta}\mathrm{d}\Gamma-\int_{\Gamma}\eta^{3}\left(\log\eta\right)^{4}\mathrm{w}(\eta)\mathrm{f}'(\eta)\mathrm{n}_{\eta}\mathrm{d}\Gamma \tag{3.7.8}$$

Upon integrating by parts the first term on the left in equation (3.7.8), yields

$$-\int_{\Omega}\eta^{4}\left(\log\eta\right)^{5}\mathrm{w}'(\eta)\mathrm{f}''(\eta)\mathrm{d}\eta=\int_{\Omega}5\eta^{3}\left(\log\eta\right)^{4}\mathrm{w}'(\eta)\mathrm{f}'(\eta)\mathrm{d}\eta+\int_{\Omega}4\eta^{3}\left(\log\eta\right)^{5}\mathrm{w}'(\eta)\mathrm{f}'(\eta)\mathrm{d}\eta$$

$$+\int_{\Omega}\eta^{4}\left(\log\eta\right)^{5}\mathrm{w}''(\eta)\mathrm{f}'(\eta)\mathrm{d}\eta-\int_{\Gamma}\eta^{4}\left(\log\eta\right)^{5}\mathrm{w}'(\eta)\mathrm{f}'(\eta)\mathrm{n}_{\eta}\mathrm{d}\Gamma \tag{3.7.9}$$

$\int_{\Omega}\eta^{4}\left(\log\eta\right)^{5}\mathrm{w}''(\eta)\mathrm{f}'(\eta)\mathrm{d}\eta=0$, since test function $\mathrm{w}(\eta)$ can be differentiated only once. Inserting equation (3.7.9) in equation (3.7.8), delivers

$$\int_{\Omega}\left[2\eta^{3}\left(\log\eta\right)^{5}\mathrm{w}(\eta)\mathrm{f}''(\eta)+2\eta^{2}\left(\log\eta\right)^{3}\mathrm{w}(\eta)\mathrm{f}'(\eta)+4\eta^{3}\left(\log\eta\right)^{4}\mathrm{w}'(\eta)\mathrm{f}'(\eta)\right]\mathrm{d}\eta$$

$$+\int_{\Omega}\left[4\eta^{3}\left(\log\eta\right)^{5}\mathrm{w}'(\eta)\mathrm{f}'(\eta)+15\eta^{2}\left(\log\eta\right)^{4}\mathrm{w}(\eta)\mathrm{f}'(\eta)+7\eta^{2}\left(\log\eta\right)^{5}\mathrm{w}(\eta)\mathrm{f}'(\eta)\right]\mathrm{d}\eta$$

$$+\int_{\Omega}\left[6\eta\left(\log\eta\right)^{3}\mathrm{w}(\eta)\mathrm{f}(\eta)+6\eta\left(\log\eta\right)^{4}\mathrm{w}(\eta)\mathrm{f}(\eta)+\eta\left(\log\eta\right)^{5}\mathrm{w}(\eta)\mathrm{f}(\eta)+\right]\mathrm{d}\eta$$

$$+\int_{\Omega}\left[\eta^{2}\log\eta\mathrm{Ha}^{2}\mathrm{w}(\eta)\mathrm{f}'(\eta)+\eta\log\eta\mathrm{Ha}^{2}\mathrm{w}(\eta)\mathrm{f}(\eta)+\mathrm{w}(\eta)\mathrm{Re}\lambda_{\theta}\right]\mathrm{d}\eta=$$

$$-\int_{\Gamma}\eta^{4}\left(\log\eta\right)^{5}\mathrm{w}(\eta)\mathrm{f}''(\eta)\mathrm{n}_{\eta}\mathrm{d}\Gamma-\int_{\Gamma}\eta^{3}\left(\log\eta\right)^{4}\mathrm{w}(\eta)\mathrm{f}'(\eta)\mathrm{n}_{\eta}\mathrm{d}\Gamma+\int_{\Gamma}\eta^{4}\left(\log\eta\right)^{5}\mathrm{w}'(\eta)\mathrm{f}'(\eta)\mathrm{n}_{\eta}\mathrm{d}\Gamma \tag{3.7.10}$$

When the first term on the left of equation (3.7.10) is integrated by parts, it converts to

$$\int_{\Omega}2\eta^{3}\left(\log\eta\right)^{5}\mathrm{w}(\eta)\mathrm{f}''(\eta)\mathrm{d}\eta=-\int_{\Omega}10\eta^{2}\left(\log\eta\right)^{4}\mathrm{w}(\eta)\mathrm{f}'(\eta)\mathrm{d}\eta-\int_{\Omega}6\eta^{2}\left(\log\eta\right)^{5}\mathrm{w}(\eta)\mathrm{f}'(\eta)\mathrm{d}\eta$$

$$-\int_{\Omega}2\eta^{3}\left(\log\eta\right)^{5}\mathrm{w}'(\eta)\mathrm{f}'(\eta)\mathrm{d}\eta+\int_{\Gamma}2\eta^{3}\left(\log\eta\right)^{5}\mathrm{w}(\eta)\mathrm{f}'(\eta)\mathrm{n}_{\eta}\mathrm{d}\Gamma \tag{3.7.11}$$

Setting equation (3.7.11) in equation (3.7.10), it turns out to

$$\int_{\Omega}\left[2\eta^{2}\left(\log\eta\right)^{3}\mathrm{w}(\eta)\mathrm{f}'(\eta)+5\eta^{2}\left(\log\eta\right)^{4}\mathrm{w}(\eta)\mathrm{f}'(\eta)+\eta^{2}\left(\log\eta\right)^{5}\mathrm{w}(\eta)\mathrm{f}'(\eta)\right]\mathrm{d}\eta$$

$$+\int_{\Omega}\left[4\eta^{3}\left(\log\eta\right)^{4}\mathrm{w}'(\eta)\mathrm{f}'(\eta)+2\eta^{3}\left(\log\eta\right)^{5}\mathrm{w}'(\eta)\mathrm{f}'(\eta)+6\eta\left(\log\eta\right)^{3}\mathrm{w}(\eta)\mathrm{f}(\eta)\right]\mathrm{d}\eta$$

$$+\int_{\Omega}\left[6\eta\left(\log\eta\right)^{4}\mathrm{w}(\eta)\mathrm{f}(\eta)+\eta\left(\log\eta\right)^{5}\mathrm{w}(\eta)\mathrm{f}(\eta)+\eta^{2}\log\eta\mathrm{Ha}^{2}\mathrm{w}(\eta)\mathrm{f}'(\eta)\right]\mathrm{d}\eta$$

$$+\int_{\Omega}\left[\eta\log\eta\mathrm{Ha}^{2}\mathrm{w}(\eta)\mathrm{f}(\eta)+\mathrm{w}(\eta)\mathrm{Re}\lambda_{\theta}\right]\mathrm{d}\eta=-\int_{\Gamma}\eta^{4}\left(\log\eta\right)^{5}\mathrm{w}(\eta)\mathrm{f}''(\eta)\mathrm{n}_{\eta}\mathrm{d}\Gamma$$

$$-\int_{\Gamma}\eta^{3}\left(\log\eta\right)^{4}\mathrm{w}(\eta)\mathrm{f}'(\eta)\mathrm{n}_{\eta}\mathrm{d}\Gamma+\int_{\Gamma}\eta^{4}\left(\log\eta\right)^{5}\mathrm{w}'(\eta)\mathrm{f}'(\eta)\mathrm{n}_{\eta}\mathrm{d}\Gamma-\int_{\Gamma}2\eta^{3}\left(\log\eta\right)^{5}\mathrm{w}(\eta)\mathrm{f}'(\eta)\mathrm{n}_{\eta}\mathrm{d}\Gamma \tag{3.7.12}$$

Equation (3.7.12) is the weak formulation of equation (3.6.3). The weak form enable the working out with C^{0} continuous approximate solutions to take place.

3.7.2 Method of weighted residuals for temperature distribution

Equation (3.7.1) is the strong form of the problem. The residual of the differential equation is given by

$$\mathrm{R}(\tau)=\frac{1}{\mathrm{Pr}}\left[\tau\log\tau\mathrm{h}''(\tau)+\mathrm{h}'(\tau)+\log\tau\mathrm{h}'(\tau)\right]+\tau\log\tau\mathrm{EcHa}^{2}\mathrm{f}^{2} \tag{3.7.13}$$

Minimization on the residual in the weighted integral is done so that

$$\int_{\Omega}\mathrm{w}(\tau)\mathrm{R}(\tau)\mathrm{d}\tau=0 \tag{3.7.14}$$

where $\mathrm{w}(\tau)$ is weight (or test) function. Setting equation (3.7.13) in equation (3.7.14), gives

$$\int_{\Omega}\left(\frac{1}{\mathrm{Pr}}\left[\mathrm{w}(\tau)\tau\log\tau\mathrm{h}''(\tau)+\mathrm{w}(\tau)\mathrm{h}'(\tau)+\mathrm{w}(\tau)\log\tau\mathrm{h}'(\tau)\right]+\mathrm{w}(\tau)\tau\log\tau\mathrm{EcHa}^{2}\mathrm{f}^{2}\right)\mathrm{d}\tau=0 \tag{3.7.15}$$

When a C^{0} continuous solution is used in equation (3.7.15), the second order derivative can not be evaluated properly. To work with the C^{0} continuous solution, the order of the second derivative is lowered to one by administering integration by parts to the first term on the left of equation

(3.7.15) as follows:

$$\frac{1}{\mathrm{Pr}}\int_{\Omega}\mathrm{w}(\tau)\tau\log\tau\mathrm{h}''(\tau)\mathrm{d}\tau=-\frac{1}{\mathrm{Pr}}\int_{\Omega}\mathrm{w}(\tau)\mathrm{h}'(\tau)\mathrm{d}\tau-\frac{1}{\mathrm{Pr}}\int_{\Omega}\mathrm{w}(\tau)\log\tau\mathrm{h}'(\tau)\mathrm{d}\tau$$

$$-\frac{1}{\mathrm{Pr}}\int_{\Omega}\mathrm{w}'(\tau)\tau\log\tau\mathrm{h}'(\tau)\mathrm{d}\tau+\frac{1}{\mathrm{Pr}}\int_{\Gamma}\mathrm{w}(\tau)\tau\log\tau\mathrm{h}'(\tau)\mathrm{n}_{\tau}\mathrm{d}\Gamma \tag{3.7.16}$$

The last term of equation (3.7.16) is the boundary integral and is evaluated at the boundaries Γ of the domain Ω. Where n_{τ} is the τ component of unit outward normal of the boundary. Inserting equation (3.7.16) in equation (3.7.15), grants

$$\int_{\Omega}\left(-\frac{1}{\mathrm{Pr}}\mathrm{w}'(\tau)\tau\log\tau\mathrm{h}'(\tau)+\mathrm{w}(\tau)\tau\log\tau\mathrm{EcHa}^2\mathrm{g}^2\right)\mathrm{d}\tau$$

$$=-\frac{1}{\mathrm{Pr}}\int_{\Gamma}\mathrm{w}(\tau)\tau\log\tau\mathrm{h}'(\tau)\mathrm{n}_{\tau}\mathrm{d}\Gamma \tag{3.7.17}$$

Equation (3.7.17) is the weak formulation of equation (3.6.7).

3.7.3 Boundary conditions for velocity profile

The boundary terms on the right of equation (3.7.12) gives the primary and secondary variables of the problem. The dependent variable of of the problem, f, expressed in the same form as this first term of boundary term is called the primary variable. For this case it is f_0. The second part of the boundary term comprises the rest of the terms with derivatives of f, which is the secondary variable (SV). The primary variable is provided at the boundary of the problem and is known as Essential (Dirichlet) boundary condition. The secondary variable at the boundary is called Natural (Neumann) boundary condition. The boundary conditions for the problem therefore are

Essential boundary condition:

$$\mathrm{f}=\mathrm{f}_0 \tag{3.7.18}$$

Natural boundary condition:

$$-\int_{\Gamma}\eta^{3}\log\eta^{4}\mathrm{w}(\eta)\mathrm{f}'(\eta)\mathrm{d}\Gamma+\int_{\Gamma}\eta^{4}\log\eta^{5}\mathrm{w}'(\eta)\mathrm{f}'(\eta)\mathrm{d}\Gamma-\int_{\Gamma}2\eta^{3}\log\eta^{5}\mathrm{w}(\eta)\mathrm{f}'(\eta)\mathrm{d}\Gamma$$

$$-\int_{\Gamma}\eta^{4}\log\eta^{5}\mathrm{w}(\eta)\mathrm{f}''(\eta)\mathrm{d}\Gamma=\mathrm{q}_{0} \tag{3.7.19}$$

where q_{0} is velocity profile natural boundary condition. Weak formulation also enable the boundary conditions to be included into the formulation. This property of FEM is unique and is not shared with any other technique like Finite Difference or Finite Volume Method. For the Natural boundary condition, the secondary variable inside the boundary integral is simply replaced by the specified q_{0} value as shown below

$$-\int_{\Gamma}\eta^{3}\log\eta^{4}\mathrm{w}(\eta)\mathrm{f}'(\eta)\mathrm{d}\Gamma+\int_{\Gamma}\eta^{4}\log\eta^{5}\mathrm{w}'(\eta)\mathrm{f}'(\eta)\mathrm{d}\Gamma-\int_{\Gamma}2\eta^{3}\log\eta^{5}\mathrm{w}(\eta)\mathrm{f}'(\eta)\mathrm{d}\Gamma$$

$$-\int_{\Gamma}\eta^{4}\log\eta^{5}\mathrm{w}(\eta)\mathrm{f}''(\eta)\mathrm{d}\Gamma=-\int_{\Gamma}\mathrm{w}(\eta)\mathrm{q}_{0}\mathrm{d}\Gamma$$

For the one-dimensional problem, boundary of the problem domain consists of of only two discrete points i.e the right end and the left end nodes of the finite element mesh. Consequently for the one- dimensional problem, there is no need to evaluate integrals as shown above, instead the integrand is evaluated at the boundary node.

3.7.4 Boundary conditions for temperature distribution

The boundary term on the right of equation (3.7.17) gives the primary and secondary variables of the problem. The boundary conditions for the problem therefore are

Essential boundary condition:

$$\mathrm{h}=\mathrm{h}_{0} \tag{3.7.20}$$

Natural boundary condition:

$$\tau \log \tau h'(\tau) n_\tau = p_0 \tag{3.7.21}$$

For the Natural boundary condition, the secondary variable inside the boundary integral is simply replaced by the specified p_0 value as shown below

$$-\int_\Gamma w(\tau)\tau \log \tau h'(\tau) n_\tau d\Gamma = -\int_\Gamma w(\tau) p_0 d\Gamma$$

3.7.5 Constructing an approximate solution using shape functions for velocity profile

When the desired C^0 continuous approximate solution is

$$f_{app}(\eta) = \sum_{j=1}^{N} f_j s_j(\eta) \tag{3.7.22}$$

Where f_{app} is the approximate solution to be found, N is the number of nodes in the finite element mesh, f_j's are the nodal unknown values that will be calculated at the end of finite element solution and s_j's are the shape (basis) functions that are used to construct the approximate solution. The shape functions have compact support i.e they are nonzero only over the elements which touch the node with which they are associated, everywhere else they are equal to zero. They also possess kronecker-delta property i.e

$$s_j(\eta_i) = \delta_{ij} = \begin{cases} 1 & \textit{if} \quad i = j \\ 0 & \textit{if} \quad i \neq j \end{cases} \tag{3.7.23}$$

Setting equation (3.7.22) in equation (3.7.12), it metamorphoses to

$$\int_{\Omega}\left[2\eta^{2}\left(\log\eta\right)^{3}\mathrm{w}(\eta)\sum_{\mathrm{j}=1}^{\mathrm{N}}\mathrm{f_{j}s_{j}'}(\eta)+5\eta^{2}\left(\log\eta\right)^{4}\mathrm{w}(\eta)\sum_{\mathrm{j}=1}^{\mathrm{N}}\mathrm{f_{j}s_{j}'}(\eta)+\eta^{2}\left(\log\eta\right)^{5}\mathrm{w}(\eta)\sum_{\mathrm{j}=1}^{\mathrm{N}}\mathrm{f_{j}s_{j}'}(\eta)\right]\mathrm{d}\eta$$

$$+\int_{\Omega}\left[4\eta^{3}\left(\log\eta\right)^{4}\mathrm{w}'(\eta)\sum_{\mathrm{j}=1}^{\mathrm{N}}\mathrm{f_{j}s_{j}'}(\eta)+2\eta^{3}\left(\log\eta\right)^{5}\mathrm{w}'(\eta)\sum_{\mathrm{j}=1}^{\mathrm{N}}\mathrm{f_{j}s_{j}'}(\eta)+6\eta\left(\log\eta\right)^{3}\mathrm{w}(\eta)\sum_{\mathrm{j}=1}^{\mathrm{N}}\mathrm{f_{j}s_{j}}(\eta)\right]\mathrm{d}\eta$$

$$+\int_{\Omega}\left[6\eta\left(\log\eta\right)^{4}\mathrm{w}(\eta)\sum_{\mathrm{j}=1}^{\mathrm{N}}\mathrm{f_{j}s_{j}}(\eta)+\eta\left(\log\eta\right)^{5}\mathrm{w}(\eta)\sum_{\mathrm{j}=1}^{\mathrm{N}}\mathrm{f_{j}s_{j}}(\eta)+\eta^{2}\log\eta\mathrm{Ha}^{2}\mathrm{w}(\eta)\sum_{\mathrm{j}=1}^{\mathrm{N}}\mathrm{f_{j}s_{j}'}(\eta)\right]\mathrm{d}\eta$$

$$+\int_{\Omega}\left[\eta\log\eta\mathrm{Ha}^{2}\mathrm{w}(\eta)\sum_{\mathrm{j}=1}^{\mathrm{N}}\mathrm{f_{j}s_{j}}(\eta)+\mathrm{w}(\eta)\mathrm{Re}\lambda_{\theta}\right]\mathrm{d}\eta=-\int_{\Gamma}\mathrm{SV}\mathrm{w}(\eta)\mathrm{d}\Gamma \tag{3.7.24}$$

where SV is the sum of secondary variables.

3.7.6 Constructing an approximate solution using shape functions for temperature distribution

When the desired C^{0} continuous approximate solution is

$$\mathrm{h_{app}}(\tau)=\sum_{\mathrm{j}=1}^{\mathrm{N}}\mathrm{h_{j}s_{j}}(\tau) \tag{3.7.25}$$

where $\mathrm{h_{app}}$ is the approximate solution to be found, $\mathrm{h_{j}}$'s are the nodal unknown values that will be calculated at the end of finite element solution. Putting equation (3.7.25) in equation (3.7.17) gives

$$\int_{\Omega}\left(-\frac{1}{\mathrm{Pr}}\mathrm{w}'(\tau)\tau\log\tau\sum_{\mathrm{j}=1}^{\mathrm{N}}\mathrm{h_{j}s_{j}'}(\tau)+\mathrm{w}(\tau)\tau\log\tau\mathrm{EcHa}^{2}\mathrm{f}^{2}\right)\mathrm{d}\tau$$

$$=-\frac{1}{\mathrm{Pr}}\int_{\Gamma}\mathrm{w}(\tau)\mathrm{SV}\mathrm{d}\Gamma \tag{3.7.26}$$

where SV is sum of secondary variables.

3.7.7 Galerkin Finite Element Method for velocity profile

In the Galerkin Finite Element Method, Ioannis [25], weight functions of equation (3.7.24) are selected to be the same as those of the shape functions i.e to get the $\mathrm{i^{th}}$ equation we use

$$\mathrm{w}(\eta) = \mathrm{s_i}(\eta) \tag{3.7.27}$$

Bringing equation (3.7.27) into equation (3.7.24) produces after taking the summation sign outside and the integration sign inside

$$\sum_{\mathrm{j}=1}^{\mathrm{N}} \left[\int_{\Omega} \left\{ 2\eta^2 (\log\eta)^3 \mathrm{s_i}(\eta)\mathrm{s_j'}(\eta) + 5\eta^2 (\log\eta)^4 \mathrm{s_i}(\eta)\mathrm{s_j'}(\eta) + \eta^2 (\log\eta)^5 \mathrm{s_i}(\eta)\mathrm{s_j'}(\eta) \right\} \mathrm{d}\eta \right] \mathrm{f_j}$$

$$+ \sum_{\mathrm{j}=1}^{\mathrm{N}} \left[\int_{\Omega} \left\{ 4\eta^3 (\log\eta)^4 \mathrm{s_i'}(\eta)\mathrm{s_j'}(\eta) + 2\eta^3 (\log\eta)^5 \mathrm{s_i'}(\eta)\mathrm{s_j'}(\eta) + 6\eta (\log\eta)^3 \mathrm{s_i}(\eta)\mathrm{s_j}(\eta) \right\} \mathrm{d}\eta \right] \mathrm{f_j}$$

$$+ \sum_{\mathrm{j}=1}^{\mathrm{N}} \left[\int_{\Omega} \left\{ 6\eta (\log\eta)^4 \mathrm{s_i}(\eta)\mathrm{s_j}(\eta) + \eta (\log\eta)^5 \mathrm{s_i}(\eta)\mathrm{s_j}(\eta) + \eta^2 \log\eta \mathrm{Ha}^2 \mathrm{s_i}(\eta)\mathrm{s_j'}(\eta) \right\} \mathrm{d}\eta \right] \mathrm{f_j}$$

$$+ \sum_{\mathrm{j}=1}^{\mathrm{N}} \left[\int_{\Omega} \left\{ \eta \log\eta \mathrm{Ha}^2 \mathrm{s_i}(\eta)\mathrm{s_j}(\eta) \right\} \mathrm{d}\eta \right] \mathrm{f_j}$$

$$= -\int_{\Omega} \mathrm{s_i}(\eta) \mathrm{Re} \lambda_{\theta} \mathrm{d}\eta - \int_{\Gamma} \mathrm{SVs_i}(\eta) \mathrm{d}\Gamma \qquad \mathrm{i} = 1, 2, ..., \mathrm{N} \tag{3.7.28}$$

3.7.8 Galerkin Finite Element Method for temperature distribution

When the weight functions of equation (3.7.26) are selected to be the same as those of the shape functions i.e to get the $\mathrm{i^{th}}$ equation we employ

$$\mathrm{w}(\tau) = \mathrm{s_i}(\tau) \tag{3.7.29}$$

Placing equation (3.7.29) in equation (3.7.26), grants upon taking the summation sign outside and the integration sign inside

$$\sum_{j=1}^{N}\left[\int_{\Omega}\left(-\frac{1}{Pr}\tau log\tau s_i'(\tau)s_j'(\tau)\right)d\tau\right]h_j$$

$$=-\int_{\Omega}s_i(\tau)\tau log\tau EcHa^2f^2d\tau-\frac{1}{Pr}\int_{\Gamma}s_i(\tau)SVd\Gamma \qquad i=1,2,...,N \tag{3.7.30}$$

3.7.9 Global equation system for velocity profile

Equation (3.7.28) is expressed in the matrix notation given by

$$[W][X]=[Y]+[Z] \tag{3.7.31}$$

which is global equation system, where W is the square stiffness matrix of size $N\times N$, $[X]$ is the vector of nodal unknowns with N entries. $[Y]$ and $[Z]$ are the global force vector and boundary integral vector respectively, each of size $N\times 1$. From equation (3.7.28)

$$W_{ij}=\sum_{j=1}^{N}\left[\int_{\Omega}\left\{2\eta^2(log\eta)^3s_i(\eta)s_j'(\eta)+5\eta^2(log\eta)^4s_i(\eta)s_j'(\eta)+\eta^2(log\eta)^5s_i(\eta)s_j'(\eta)\right\}d\eta\right]f_j$$

$$+\sum_{j=1}^{N}\left[\int_{\Omega}\left\{4\eta^3(log\eta)^4s_i'(\eta)s_j'(\eta)+2\eta^3(log\eta)^5s_i'(\eta)s_j'(\eta)+6\eta(log\eta)^3s_i(\eta)s_j(\eta)\right\}d\eta\right]f_j$$

$$+\sum_{j=1}^{N}\left[\int_{\Omega}\left\{6\eta(log\eta)^4s_i(\eta)s_j(\eta)+\eta(log\eta)^5s_i(\eta)s_j(\eta)+\eta^2log\eta Ha^2s_i(\eta)s_j'(\eta)\right\}d\eta\right]f_j$$

$$+\sum_{j=1}^{N}\left[\int_{\Omega}\left\{\eta log\eta Ha^2s_i(\eta)s_j(\eta)\right\}d\eta\right]f_j, \quad X_j=f_j,$$

$$Y_i=-\int_{\Omega}s_i(\eta)Re\lambda_\theta d\eta \quad \text{and} \quad Z_i=-\int_{\Gamma}s_i(\eta)SVd\Gamma \tag{3.7.32}$$

$[\mathrm{W}]$ and $[\mathrm{Y}]$ are evaluated over the whole problem domain . $[\mathrm{Z}]$ is evaluated only at the problem boundaries.

3.7.10 Global equation system for temperature distribution

Equation (3.7.30) is expressed in global equation system given by

$$[\mathrm{I}]\,[\mathrm{J}] = [\mathrm{K}] + [\mathrm{L}] \tag{3.7.33}$$

where I is the square stiffness matrix of size $\mathrm{N} \times \mathrm{N}$, $[\mathrm{J}]$ is the vector of nodal unknowns with N entries. $[\mathrm{K}]$ and $[\mathrm{L}]$ are the global force vector and boundary integral vector respectively each of size $\mathrm{N} \times 1$. From equations (3.7.30) and (3.7.33)

$$\mathrm{I_{ij}} = \int_{\Omega} \left(-\frac{1}{\mathrm{Pr}} \tau \log\tau \mathrm{s_i'}(\tau) \mathrm{s_j'}(\tau) \right) \mathrm{d}\tau,\ \mathrm{J_j} = \mathrm{h_j},$$

$$\mathrm{K_i} = -\int_{\Omega} \mathrm{s_i}(\tau) \tau \log\tau \mathrm{Ec Ha^2 g^2 d}\tau \quad \text{and} \quad \mathrm{L_i} = -\frac{1}{\mathrm{Pr}} \int_{\Gamma} \mathrm{s_i}(\tau) \mathrm{SV d}\Gamma \tag{3.7.34}$$

$[\mathrm{I}]$ is evaluated over the whole problem. Temperature is considered constant at boundary so that $[\mathrm{L}]$ is also constant at boundaries. $[\mathrm{K}]$ is considered varying over the whole domain since it depends on fluid velocity which is maximum at the centre of pipe but decreases towards periphery of pipe. Let $\mathrm{L_i} = -\frac{1}{\mathrm{Pr}} \mathrm{I_{21}}$, where $\mathrm{I_{21}}$ is defined in subsection 3.7.16 so that $\mathrm{I_{21}} = \int_{\Gamma} \mathrm{s_i}(\tau) \mathrm{SV d}\Gamma$

3.7.11 Velocity elemental systems

Given that shape functions which appear in $[\mathrm{W}]$ integrals have non zero values only over a small portion of the problem domain, these integrals are evaluated as sum of separate integrals over

individual elements i.e

$$[\mathrm{W}] = \sum_{\mathrm{e}=1}^{\mathrm{E}} [\mathrm{W}^{\mathrm{e}}] \tag{3.7.35}$$

where $[\mathrm{W}^{\mathrm{e}}]$ is elemental stiffness matrix. From equation (3.7.32), the elemental stiffness matrix is given by

$$\begin{aligned}
\mathrm{W}_{\mathrm{ij}}^{\mathrm{e}} = & \int_{\Omega} \left\{ 2\eta^2 (\log\eta)^3 \mathrm{s_i}(\eta)\mathrm{s_j'}(\eta) + 5\eta^2 (\log\eta)^4 \mathrm{s_i}(\eta)\mathrm{s_j'}(\eta) + \eta^2 (\log\eta)^5 \mathrm{s_i}(\eta)\mathrm{s_j'}(\eta) \right\} \mathrm{d}\eta \\
& + \int_{\Omega} \left\{ 4\eta^3 (\log\eta)^4 \mathrm{s_i'}(\eta)\mathrm{s_j'}(\eta) + 2\eta^3 (\log\eta)^5 \mathrm{s_i'}(\eta)\mathrm{s_j'}(\eta) + 6\eta (\log\eta)^3 \mathrm{s_i}(\eta)\mathrm{s_j}(\eta) \right\} \mathrm{d}\eta \\
& + \int_{\Omega} \left\{ 6\eta (\log\eta)^4 \mathrm{s_i}(\eta)\mathrm{s_j}(\eta) + \eta (\log\eta)^5 \mathrm{s_i}(\eta)\mathrm{s_j}(\eta) + \eta^2 \log\eta \mathrm{Ha}^2 \mathrm{s_i}(\eta)\mathrm{s_j'}(\eta) \right\} \mathrm{d}\eta \\
& + \int_{\Omega} \left\{ \eta \log\eta \mathrm{Ha}^2 \mathrm{s_i}(\eta)\mathrm{s_j}(\eta) \right\} \mathrm{d}\eta
\end{aligned} \tag{3.7.36}$$

All elements of $\left[\mathrm{W}_{\mathrm{ij}}^{\mathrm{e}}\right]$ are $\mathrm{N} \times \mathrm{N}$ square matrices. However since only two shape functions have non-zero values over each element, there will be contribution to $\left[\mathrm{W}_{\mathrm{ij}}^{\mathrm{e}}\right]$ only from these two shape functions i.e many of the entries of $\mathrm{N} \times \mathrm{N}$ matrix are zeroes. For instance the stiffness matrix $\left[\mathrm{W}_{\mathrm{ij}}^{\mathrm{e}}\right]$ for a single element will be of the form

$$\begin{vmatrix}
0 & 0 & 0 & 0 & 0 \\
0 & 0 & 0 & 0 & 0 \\
0 & 0 & \mathrm{A} & \mathrm{B} & 0 \\
0 & 0 & \mathrm{C} & \mathrm{D} & 0 \\
0 & 0 & 0 & 0 & 0
\end{vmatrix}$$

As seen from the matrix above, two non-zero shape functions over an element will create only four non-zero entries in $\left[\mathrm{W}_{\mathrm{ij}}^{\mathrm{e}}\right]$.

3.7.12 Temperature elemental systems

Given that shape functions which appear in $[\mathrm{I}]$ integrals have non zero values only over a small portion of the problem domain, these integrals are evaluated as sum of separate integrals over individual elements i.e

$$[\mathrm{I}] = \sum_{\mathrm{e}=1}^{\mathrm{E}} [\mathrm{I}^{\mathrm{e}}] \tag{3.7.37}$$

where $[\mathrm{I}^{\mathrm{e}}]$ is elemental stiffness matrix. From equation (3.7.34), the elemental stiffness matrix is given by

$$\mathrm{I}_{\mathrm{ij}}^{\mathrm{e}} = \int_{\Omega} \left(-\frac{1}{\mathrm{Pr}} \tau \log \tau \mathrm{s}_{\mathrm{i}}'(\tau) \mathrm{s}_{\mathrm{j}}'(\tau) \right) \mathrm{d}\tau \tag{3.7.38}$$

Again all elements of $\left[\mathrm{I}_{\mathrm{ij}}^{\mathrm{e}}\right]$ are $\mathrm{N} \times \mathrm{N}$ square matrices. However since only two shape functions have non-zero values over each element, there will be contribution to $\left[\mathrm{I}_{\mathrm{ij}}^{\mathrm{e}}\right]$ only from these two shape functions i.e many of the entries of $\mathrm{N} \times \mathrm{N}$ matrix are zeroes.

3.7.13 Gauss quadrature integration for velocity profile

Gauss quadrature, Timothy [26], a numerical integration technique in which integrals are evaluated between limits of -1 and 1, is utilized as follows:

$$\int_{-1}^{1} \mathrm{f}(\xi) \mathrm{d}\xi = \sum_{\mathrm{k}=1}^{\mathrm{GP}} \mathrm{f}(\xi_{\mathrm{k}}) \mathrm{w}_{\mathrm{k}} \tag{3.7.39}$$

where ξ_{k} are special Gauss quadrature points in the interval $[-1, 1]$, w_{k} are the corresponding Gauss quadrature weights and GP is the number of Gauss quadrature points to be used. Limits of $\mathrm{W}_{\mathrm{ij}}^{\mathrm{e}}$ integral are $\eta = \eta_1^{\mathrm{e}}$ and $\eta = \eta_2^{\mathrm{e}}$ which are the coordinates of the two end points of the element. To evaluate $\mathrm{W}_{\mathrm{ij}}^{\mathrm{e}}$ integral using Gauss quadrature, limits of the integral are changed to be -1 and 1 which require change of variable. This leads to the use of master element in evaluating

elemental integrals. Using the Kroncker-delta property of shape functions, they are written in terms of the master element coordinate ξ as, Timothy [26],

$$s_1 = \frac{1}{2}(1-\xi) \text{ and } \quad s_2 = \frac{1}{2}(1+\xi) \tag{3.7.40}$$

To evaluate W_{ij}^{e} integrals, the global η coordinate is related to ξ coordinate by, Timothy [26],

$$\eta = \frac{h^e}{2}\xi + \frac{\eta_1^e + \eta_2^e}{2} \tag{3.7.41}$$

where h^e is the length of element, e, given by $h^e = \eta_2^e - \eta_1^e$. Equation (3.7.36) is now written using the ξ coordinate and new limits for Gauss quadrature integration and transforms into

$$W_{ij}^{e} = \int_{-1}^{1} \left\{ 2\eta^2 (\log\eta)^3 s_i \frac{ds_j}{d\xi}\frac{d\xi}{d\eta} + 5\eta^2 (\log\eta)^4 s_i \frac{ds_j}{d\xi}\frac{d\xi}{d\eta} + \eta^2 (\log\eta)^5 s_i \frac{ds_j}{d\xi}\frac{d\xi}{d\eta} \right\} \frac{d\eta}{d\xi} d\xi$$

$$+ \int_{-1}^{1} \left\{ 4\eta^3 (\log\eta)^4 \frac{ds_i}{d\xi}\frac{d\xi}{d\eta}\frac{ds_j}{d\xi}\frac{d\xi}{d\eta} + 2\eta^3 (\log\eta)^5 \frac{ds_i}{d\xi}\frac{d\xi}{d\eta}\frac{ds_j}{d\xi}\frac{d\xi}{d\eta} + 6\eta (\log\eta)^3 s_i(\eta) s_j(\eta) \right\} \frac{d\eta}{d\xi} d\xi$$

$$+ \int_{-1}^{1} \left\{ 6\eta (\log\eta)^4 s_i(\eta) s_j(\eta) + \eta (\log\eta)^5 s_i(\eta) s_j(\eta) + \eta^2 \log\eta Ha^2 s_i \frac{ds_j}{d\xi}\frac{d\xi}{d\eta} \right\} \frac{d\eta}{d\xi} d\xi$$

$$+ \int_{-1}^{1} \{ \eta \log\eta Ha^2 s_i(\eta) s_j(\eta) \} \frac{d\eta}{d\xi} d\xi \tag{3.7.42}$$

Upon defining Finite Element Jacobian as $J^e = \frac{d\eta}{d\xi} = \frac{h^e}{2}$, equation (3.7.42) produces

$$W_{ij}^{e} = \int_{-1}^{1} \left\{ 2\eta^2 (\log\eta)^3 s_i \frac{ds_j}{d\xi} + 5\eta^2 (\log\eta)^4 s_i \frac{ds_j}{d\xi} + \eta^2 (\log\eta)^5 s_i \frac{ds_j}{d\xi} + 4\eta^3 (\log\eta)^4 \frac{ds_i}{d\xi}\frac{ds_j}{d\xi}\frac{1}{J^e} \right\} d\xi$$

$$+ \int_{-1}^{1} \left\{ 2\eta^3 (\log\eta)^5 \frac{ds_i}{d\xi}\frac{ds_j}{d\xi}\frac{1}{J^e} + 6\eta (\log\eta)^3 s_i s_j J^e + 6\eta (\log\eta)^4 s_i s_j J^e + \eta (\log\eta)^5 s_i s_j J^e \right\} d\xi$$

$$+ \int_{-1}^{1} \left\{ \eta^2 \log\eta Ha^2 s_i \frac{ds_j}{d\xi} + \eta \log\eta Ha^2 s_i s_j J^e \right\} d\xi \tag{3.7.43}$$

Equation (3.7.43) is the state that is utilized to obtain velocity elemental stiffness matrix

3.7.14 Gauss quadrature integration for temperature distribution

Integrals are evaluated between limits of -1 and 1.

$$\int_{-1}^{1} \mathrm{h}(\xi)\mathrm{d}\xi = \sum_{\mathrm{k}=1}^{\mathrm{GP}} \mathrm{h}(\xi_{\mathrm{k}})\mathrm{w}_{\mathrm{k}} \tag{3.7.44}$$

where ξ_{k} are special Gauss quadrature points in the interval $[-1,1]$, w_{k} are the corresponding Gauss quadrature weights and GP is the number of Gauss quadrature points to be used. Limits of $\mathrm{I}_{\mathrm{ij}}^{\mathrm{e}}$ integral are $\tau = \tau_1^{\mathrm{e}}$ and $\tau = \tau_2^{\mathrm{e}}$ which are the coordinates of the two end points of the element. To evaluate $\mathrm{I}_{\mathrm{ij}}^{\mathrm{e}}$ integral using Gauss quadrature, limits of the integral are changed to be -1 and 1 which require change of variable. This leads to the use of master element in evaluating elemental integrals. Using the Kroncker-delta property of shape functions, they are written in terms of the master element coordinate ξ as, Timothy [26],

$$\mathrm{s}_1 = \frac{1}{2}(1-\xi) \text{ and } \quad \mathrm{s}_2 = \frac{1}{2}(1+\xi) \tag{3.7.45}$$

To evaluate $\mathrm{I}_{\mathrm{ij}}^{\mathrm{e}}$ integrals, the global τ coordinate is related to ξ coordinate by, Timothy [26],

$$\tau = \frac{\mathrm{h}^{\mathrm{e}}}{2}\xi + \frac{\tau_1^{\mathrm{e}} + \tau_2^{\mathrm{e}}}{2} \tag{3.7.46}$$

where h^{e} is the length of element e given by $\mathrm{h}^{\mathrm{e}} = \tau_2^{\mathrm{e}} - \tau_1^{\mathrm{e}}$. Equation (3.7.38) is now written using the ξ coordinate and new limits for Gauss quadrature integration and transforms to

$$\mathrm{I}_{\mathrm{ij}}^{\mathrm{e}} = \int_{-1}^{1} \left(-\frac{1}{\mathrm{Pr}}\tau \log\tau \frac{\mathrm{ds_i}}{\mathrm{d}\xi}\frac{\mathrm{d}\xi}{\mathrm{d}\tau}\frac{\mathrm{ds_j}}{\mathrm{d}\xi}\frac{\mathrm{d}\xi}{\mathrm{d}\tau} \right) \frac{\mathrm{d}\tau}{\mathrm{d}\xi}\mathrm{d}\xi \tag{3.7.47}$$

Upon defining Finite Element Jacobian as $J^e = \frac{d\tau}{d\xi} = \frac{h^e}{2}$, equation (3.7.47) shortens to

$$I_{ij}^e = \int_{-1}^{1} \left(-\frac{1}{Pr} \tau \log\tau \frac{ds_i}{d\xi} \frac{ds_j}{d\xi} \frac{1}{J^e} \right) d\xi \tag{3.7.48}$$

Equation (3.7.48) is the state that is manipulated to obtain temperature elemental stiffness matrix.

3.7.15 Velocity profile assembly process

After calculating small 2×2 elemental stiffness matrices, they are assembled in proper locations of the global system of equations. This is done by first generating a local to global node mapping.

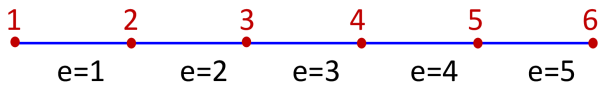

Figure 3.7.1: 5 linear elements with 6 global node numbers

For instance, for a simple mesh of 5 linear elements with shown global node numbers in figure 3.7.1 , local to global node mapping matrix that will be used in the assembly process is

$$L\,to\,G = \begin{bmatrix} 1 & 2 \\ 2 & \mathbf{3} \\ \textit{3} & \mathbf{4} \\ 4 & 5 \\ 5 & 6 \end{bmatrix}$$

where the third element *3* is between the third **3** node and fourth node **4**. The assembly process is now done with the following assembly rule

i. an elemental stiffness matrix W_{ij}^e is assembled into global stiffness matrix W_{IJ}

ii. an elemental boundary integral vector Z_i^e is assembled into the global boundary integral vector Z_I

iii. an elemental force integral vector Y_i is assembled into Y_I

The assembly process results in the following global stiffness matrix, force integral vector and boundary integral vector for 6 node mesh.

$$W = \begin{bmatrix} W_{11}^1 & W_{12}^1 & 0 & 0 & 0 & 0 \\ W_{21}^1 & W_{22}^1 + W_{11}^2 & W_{12}^2 & 0 & 0 & 0 \\ 0 & W_{21}^2 & W_{22}^2 + W_{11}^3 & W_{12}^3 & 0 & 0 \\ 0 & 0 & W_{21}^3 & W_{22}^3 + W_{11}^4 & W_{12}^4 & 0 \\ 0 & 0 & 0 & W_{21}^4 & W_{22}^4 + W_{11}^5 & W_{12}^5 \\ 0 & 0 & 0 & 0 & W_{21}^5 & W_{22}^5 + W_{11}^6 \end{bmatrix},$$

$$[Y] = \begin{bmatrix} Y_1^1 \\ Y_2^1 + Y_1^2 \\ Y_2^2 + Y_1^3 \\ Y_2^3 + Y_1^4 \\ Y_2^4 + Y_1^5 \\ Y_2^5 \end{bmatrix} \quad \text{and} \quad [Z] = \begin{bmatrix} Z_1^1 \\ Z_2^1 + Z_1^2 \\ Z_2^2 + Z_1^3 \\ Z_2^3 + Z_1^4 \\ Z_2^4 + Z_1^5 \\ Z_2^5 \end{bmatrix}$$

For the 6 node mesh, global equation system is given by

$$\begin{bmatrix} \mathrm{W}_{11}^{1} & \mathrm{W}_{12}^{1} & 0 & 0 & 0 & 0 \\ \mathrm{W}_{21}^{1} & \mathrm{W}_{22}^{1}+\mathrm{W}_{11}^{2} & \mathrm{W}_{12}^{2} & 0 & 0 & 0 \\ 0 & \mathrm{W}_{21}^{2} & \mathrm{W}_{22}^{2}+\mathrm{W}_{11}^{3} & \mathrm{W}_{12}^{3} & 0 & 0 \\ 0 & 0 & \mathrm{W}_{21}^{3} & \mathrm{W}_{22}^{3}+\mathrm{W}_{11}^{4} & \mathrm{W}_{12}^{4} & 0 \\ 0 & 0 & 0 & \mathrm{W}_{21}^{4} & \mathrm{W}_{22}^{4}+\mathrm{W}_{11}^{5} & \mathrm{W}_{12}^{5} \\ 0 & 0 & 0 & 0 & \mathrm{W}_{21}^{5} & \mathrm{W}_{22}^{5}+\mathrm{W}_{11}^{6} \end{bmatrix} \begin{bmatrix} \mathrm{f}_{1} \\ \mathrm{f}_{2} \\ \mathrm{f}_{3} \\ \mathrm{f}_{4} \\ \mathrm{f}_{5} \\ \mathrm{f}_{6} \end{bmatrix}$$

$$= \begin{bmatrix} \mathrm{Y}_{1}^{1} \\ \mathrm{Y}_{2}^{1}+\mathrm{Y}_{1}^{2} \\ \mathrm{Y}_{2}^{2}+\mathrm{Y}_{1}^{3} \\ \mathrm{Y}_{2}^{3}+\mathrm{Y}_{1}^{4} \\ \mathrm{Y}_{2}^{4}+\mathrm{Y}_{1}^{5} \\ \mathrm{Y}_{2}^{5} \end{bmatrix} + \begin{bmatrix} \mathrm{Z}_{1}^{1} \\ \mathrm{Z}_{2}^{1}+\mathrm{Z}_{1}^{2} \\ \mathrm{Z}_{2}^{2}+\mathrm{Z}_{1}^{3} \\ \mathrm{Z}_{2}^{3}+\mathrm{Z}_{1}^{4} \\ \mathrm{Z}_{2}^{4}+\mathrm{Z}_{1}^{5} \\ \mathrm{Z}_{2}^{5} \end{bmatrix} \tag{3.7.49}$$

3.7.16 Temperature distribution assembly process

After repeating the procedure for subsection 3.7.15, the assembly process is now done with the following assembly rule

i. an elemental stiffness matrix $\mathrm{I}_{\mathrm{ij}}^{\mathrm{e}}$ is assembled into global stiffness matrix I_{IJ}

ii. an elemental boundary integral vector $\mathrm{L}_{\mathrm{i}}^{\mathrm{e}}$ is assembled into the global boundary integral vector L_{I}

iii. an elemental force integral vector K_{i} is assembled into K_{I}

The assembly process results in the following global stiffness matrix, force integral vector and boundary integral vector for 6 node mesh.

$$\mathrm{I} = \begin{bmatrix} \mathrm{I}_{11}^{1} & \mathrm{I}_{12}^{1} & 0 & 0 & 0 & 0 \\ \mathrm{I}_{21}^{1} & \mathrm{I}_{22}^{1}+\mathrm{I}_{11}^{2} & \mathrm{I}_{12}^{2} & 0 & 0 & 0 \\ 0 & \mathrm{I}_{21}^{2} & \mathrm{I}_{22}^{2}+\mathrm{I}_{11}^{3} & \mathrm{I}_{12}^{3} & 0 & 0 \\ 0 & 0 & \mathrm{I}_{21}^{3} & \mathrm{I}_{22}^{3}+\mathrm{I}_{11}^{4} & \mathrm{I}_{12}^{4} & 0 \\ 0 & 0 & 0 & \mathrm{I}_{21}^{4} & \mathrm{I}_{22}^{4}+\mathrm{I}_{11}^{5} & \mathrm{I}_{12}^{5} \\ 0 & 0 & 0 & 0 & \mathrm{I}_{21}^{5} & \mathrm{I}_{22}^{5}+\mathrm{I}_{11}^{6} \end{bmatrix}$$

$$[\mathrm{K}] = \begin{bmatrix} \mathrm{K}_{1}^{1} \\ \mathrm{K}_{2}^{1}+\mathrm{K}_{1}^{2} \\ \mathrm{K}_{2}^{2}+\mathrm{K}_{1}^{3} \\ \mathrm{K}_{2}^{3}+\mathrm{K}_{1}^{4} \\ \mathrm{K}_{2}^{4}+\mathrm{K}_{1}^{5} \\ \mathrm{K}_{2}^{5} \end{bmatrix} \quad \text{and} \quad [\mathrm{L}] = \begin{bmatrix} \mathrm{L}_{1}^{1} \\ \mathrm{L}_{2}^{1}+\mathrm{L}_{1}^{2} \\ \mathrm{L}_{2}^{2}+\mathrm{L}_{1}^{3} \\ \mathrm{L}_{2}^{3}+\mathrm{L}_{1}^{4} \\ \mathrm{L}_{2}^{4}+\mathrm{L}_{1}^{5} \\ \mathrm{L}_{2}^{5} \end{bmatrix}$$

For the 6 node mesh, global equation system is given by

$$\begin{bmatrix} \mathrm{I}_{11}^{1} & \mathrm{I}_{12}^{1} & 0 & 0 & 0 & 0 \\ \mathrm{I}_{21}^{1} & \mathrm{I}_{22}^{1}+\mathrm{I}_{11}^{2} & \mathrm{I}_{12}^{2} & 0 & 0 & 0 \\ 0 & \mathrm{I}_{21}^{2} & \mathrm{I}_{22}^{2}+\mathrm{I}_{11}^{3} & \mathrm{I}_{12}^{3} & 0 & 0 \\ 0 & 0 & \mathrm{I}_{21}^{3} & \mathrm{I}_{22}^{3}+\mathrm{I}_{11}^{4} & \mathrm{I}_{12}^{4} & 0 \\ 0 & 0 & 0 & \mathrm{I}_{21}^{4} & \mathrm{I}_{22}^{4}+\mathrm{I}_{11}^{5} & \mathrm{I}_{12}^{5} \\ 0 & 0 & 0 & 0 & \mathrm{I}_{21}^{5} & \mathrm{I}_{22}^{5}+\mathrm{I}_{11}^{6} \end{bmatrix} \begin{bmatrix} \mathrm{h}_1 \\ \mathrm{h}_2 \\ \mathrm{h}_3 \\ \mathrm{h}_4 \\ \mathrm{h}_5 \\ \mathrm{h}_6 \end{bmatrix}$$

$$= \begin{bmatrix} \mathrm{K}_1^1 \\ \mathrm{K}_2^1 + \mathrm{K}_1^2 \\ \mathrm{K}_2^2 + \mathrm{K}_1^3 \\ \mathrm{K}_2^3 + \mathrm{K}_1^4 \\ \mathrm{K}_2^4 + \mathrm{K}_1^5 \\ \mathrm{K}_2^5 \end{bmatrix} + \begin{bmatrix} \mathrm{L}_1^1 \\ \mathrm{L}_2^1 + \mathrm{L}_1^2 \\ \mathrm{L}_2^2 + \mathrm{L}_1^3 \\ \mathrm{L}_2^3 + \mathrm{L}_1^4 \\ \mathrm{L}_2^4 + \mathrm{L}_1^5 \\ \mathrm{L}_2^5 \end{bmatrix} \tag{3.7.50}$$

3.7.17 Evaluation of boundary conditions for velocity profile

The boundary integral vector $[\mathrm{Z}]$ is evaluated only at the boundary nodes of the problem domain, not at the inner nodes. For the 6 node mesh $\mathrm{Z}_2 = \mathrm{Z}_3 = \mathrm{Z}_4 = \mathrm{Z}_5 = 0$. The boundary integral vector takes the form

$$[\mathrm{Z}] = \begin{bmatrix} \mathrm{Z}_1^1 \\ 0 \\ 0 \\ 0 \\ 0 \\ \mathrm{Z}_2^5 \end{bmatrix}$$

Taking into account the no-slip condition, $\mathrm{Z}_1 = \mathrm{Z}_6 = 0$, so that the whole boundary integral vector is a null vector and equation (3.7.49) dwindles to

$$\begin{bmatrix} \mathrm{W}_{11}^1 & \mathrm{W}_{12}^1 & 0 & 0 & 0 & 0 \\ \mathrm{W}_{21}^1 & \mathrm{W}_{22}^1 + \mathrm{W}_{11}^2 & \mathrm{W}_{12}^2 & 0 & 0 & 0 \\ 0 & \mathrm{W}_{21}^2 & \mathrm{W}_{22}^2 + \mathrm{W}_{11}^3 & \mathrm{W}_{12}^3 & 0 & 0 \\ 0 & 0 & \mathrm{W}_{21}^3 & \mathrm{W}_{22}^3 + \mathrm{W}_{11}^4 & \mathrm{W}_{12}^4 & 0 \\ 0 & 0 & 0 & \mathrm{W}_{21}^4 & \mathrm{W}_{22}^4 + \mathrm{W}_{11}^5 & \mathrm{W}_{12}^5 \\ 0 & 0 & 0 & 0 & \mathrm{W}_{21}^5 & \mathrm{W}_{22}^5 + \mathrm{W}_{11}^6 \end{bmatrix} \begin{bmatrix} \mathrm{f}_1 \\ \mathrm{f}_2 \\ \mathrm{f}_3 \\ \mathrm{f}_4 \\ \mathrm{f}_5 \\ \mathrm{f}_6 \end{bmatrix}$$

$$= \begin{bmatrix} \mathrm{Y}_1^1 \\ \mathrm{Y}_2^1 + \mathrm{Y}_1^2 \\ \mathrm{Y}_2^2 + \mathrm{Y}_1^3 \\ \mathrm{Y}_2^3 + \mathrm{Y}_1^4 \\ \mathrm{Y}_2^4 + \mathrm{Y}_1^5 \\ \mathrm{Y}_2^5 \end{bmatrix} \tag{3.7.51}$$

3.7.18 Evaluation of boundary conditions for temperature distribution

The boundary integral vector $[\mathrm{L}]$ is evaluated at the boundary nodes of the problem domain. For the 6 node mesh, $\mathrm{L}_1 = \mathrm{L}_2 = \mathrm{L}_3 = \mathrm{L}_4 = \mathrm{L}_5 = \mathrm{L}_6 = -\frac{1}{\mathrm{Pr}}\mathrm{I}_{21}$ since temperature is constant at the

boundary. Putting values of $\mathrm{L_i}$ in equation (3.7.50), it turns out to

$$\begin{bmatrix} \mathrm{I}_{11}^{1} & \mathrm{I}_{12}^{1} & 0 & 0 & 0 & 0 \\ \mathrm{I}_{21}^{1} & \mathrm{I}_{22}^{1}+\mathrm{I}_{11}^{2} & \mathrm{I}_{12}^{2} & 0 & 0 & 0 \\ 0 & \mathrm{I}_{21}^{2} & \mathrm{I}_{22}^{2}+\mathrm{I}_{11}^{3} & \mathrm{I}_{12}^{3} & 0 & 0 \\ 0 & 0 & \mathrm{I}_{21}^{3} & \mathrm{I}_{22}^{3}+\mathrm{I}_{11}^{4} & \mathrm{I}_{12}^{4} & 0 \\ 0 & 0 & 0 & \mathrm{I}_{21}^{4} & \mathrm{I}_{22}^{4}+\mathrm{I}_{11}^{5} & \mathrm{I}_{12}^{5} \\ 0 & 0 & 0 & 0 & \mathrm{I}_{21}^{5} & \mathrm{I}_{22}^{5}+\mathrm{I}_{11}^{6} \end{bmatrix} \begin{bmatrix} \mathrm{h}_1 \\ \mathrm{h}_2 \\ \mathrm{h}_3 \\ \mathrm{h}_4 \\ \mathrm{h}_5 \\ \mathrm{h}_6 \end{bmatrix}$$

$$= \begin{bmatrix} \mathrm{K}_1^1 \\ \mathrm{K}_2^1+\mathrm{K}_1^2 \\ \mathrm{K}_2^2+\mathrm{K}_1^3 \\ \mathrm{K}_2^3+\mathrm{K}_1^4 \\ \mathrm{K}_2^4+\mathrm{K}_1^5 \\ \mathrm{K}_2^5 \end{bmatrix} - \begin{bmatrix} \frac{1}{\mathrm{Pr}}\mathrm{I}_{21} \\ \vdots \\ \vdots \\ \vdots \\ \vdots \\ \vdots \end{bmatrix} \tag{3.7.52}$$

3.7.19 Evaluation of global force vector for velocity profile

From equation (3.7.32), the elemental force vector is given by

$$\mathrm{Y_i} = -\int_{-1}^{1} \mathrm{s_i} \mathrm{Re} \boldsymbol{\lambda_\theta} \mathrm{d}\boldsymbol{\xi}$$

Re and $\boldsymbol{\lambda_\theta}$ are constants. Components of elemental force vector are evaluated as under;

$$\mathrm{Y}_1^{\mathrm{e}} = -\int_{-1}^{1} \frac{1}{2}(1-\boldsymbol{\xi}) \mathrm{Re} \boldsymbol{\lambda_\theta} \mathrm{d}\boldsymbol{\xi} = -\mathrm{Re} \boldsymbol{\lambda_\theta}$$

$$\mathrm{Y}_2^{\mathrm{e}} = -\int_{-1}^{1} \frac{1}{2}(1+\xi)\mathrm{Re}\boldsymbol{\lambda_\theta}\mathrm{d}\xi = -\mathrm{Re}\boldsymbol{\lambda_\theta}$$

When the assembly rule is administered, global force vector lessens to

$$[\mathrm{Y}] = \begin{bmatrix} \mathrm{Y}_1^1 \\ \mathrm{Y}_2^1 + \mathrm{Y}_1^2 \\ \mathrm{Y}_2^2 + \mathrm{Y}_1^3 \\ \mathrm{Y}_2^3 + \mathrm{Y}_1^4 \\ \mathrm{Y}_2^4 + \mathrm{Y}_1^5 \\ \mathrm{Y}_2^5 \end{bmatrix} = \begin{bmatrix} -\mathrm{Re}\boldsymbol{\lambda_\theta} \\ -2\mathrm{Re}\boldsymbol{\lambda_\theta} \\ -2\mathrm{Re}\boldsymbol{\lambda_\theta} \\ -2\mathrm{Re}\boldsymbol{\lambda_\theta} \\ -2\mathrm{Re}\boldsymbol{\lambda_\theta} \\ -\mathrm{Re}\boldsymbol{\lambda_\theta} \end{bmatrix} \tag{3.7.53}$$

Setting equation (3.7.53) in equation (3.7.51), hands out

$$\begin{bmatrix} \mathrm{W}_{11}^1 & \mathrm{W}_{12}^1 & 0 & 0 & 0 & 0 \\ \mathrm{W}_{21}^1 & \mathrm{W}_{22}^1 + \mathrm{W}_{11}^2 & \mathrm{W}_{12}^2 & 0 & 0 & 0 \\ 0 & \mathrm{W}_{21}^2 & \mathrm{W}_{22}^2 + \mathrm{W}_{11}^3 & \mathrm{W}_{12}^3 & 0 & 0 \\ 0 & 0 & \mathrm{W}_{21}^3 & \mathrm{W}_{22}^3 + \mathrm{W}_{11}^4 & \mathrm{W}_{12}^4 & 0 \\ 0 & 0 & 0 & \mathrm{W}_{21}^4 & \mathrm{W}_{22}^4 + \mathrm{W}_{11}^5 & \mathrm{W}_{12}^5 \\ 0 & 0 & 0 & 0 & \mathrm{W}_{21}^5 & \mathrm{W}_{22}^5 + \mathrm{W}_{11}^6 \end{bmatrix} \begin{bmatrix} \mathrm{f}_1 \\ \mathrm{f}_2 \\ \mathrm{f}_3 \\ \mathrm{f}_4 \\ \mathrm{f}_5 \\ \mathrm{f}_6 \end{bmatrix}$$

$$= \begin{bmatrix} -\mathrm{Re}\lambda_\theta \\ -2\mathrm{Re}\lambda_\theta \\ -2\mathrm{Re}\lambda_\theta \\ -2\mathrm{Re}\lambda_\theta \\ -2\mathrm{Re}\lambda_\theta \\ -\mathrm{Re}\lambda_\theta \end{bmatrix} \tag{3.7.54}$$

3.7.20 Evaluation of global force vector for temperature distribution

From equation (3.7.34), the elemental force vector is given by

$$\mathrm{K_i} = -\int_\Omega \mathrm{s_i}(\tau)\tau\log\tau\mathrm{EcHa}^2\mathrm{f}^2\mathrm{d}\xi$$

Ec and Ha are constants while f which is fluid velocity will be a specific value at a specific node. Fluid velocity is maximum at the centre of pipe (core velocity $\mathrm{V_c}$) and then diminishes gradually to zero at the boundary of pipe as is found in velocity profile study results, Gedik *et.al* [10]. Henceforth, f is denoted $\mathrm{f_i}$. The elemental force vector components are evaluated as follows: From equations (3.7.45) and (3.7.46), considering $\mathrm{h^e} = 0.0002$, $\tau_1^\mathrm{e} = 0.0000$ and $\tau_2^\mathrm{e} = 0.0002$ then

$$\tau = 0.0001\xi + 0.0001 \tag{3.7.55}$$

so that

$$\mathrm{K_1^e} = -\int_\Omega \mathrm{s_1}(\tau)\tau\log\tau\mathrm{EcHa}^2\mathrm{f_i^2}\mathrm{d}\xi$$

$$= -\int_{-1}^{1} \frac{1}{2}(1-\xi)(0.0001\xi + 0.0001)\log(0.0001\xi + 0.0001)\mathrm{EcHa}^2\mathrm{f_i^2}\mathrm{d}\xi$$

$$= 0.00062337 \mathrm{EcHa}^2 \mathrm{f}_\mathrm{i}^2 \tag{3.7.56}$$

$$\mathrm{K}_2^\mathrm{e} = -\int_\Omega \mathrm{s}_2(\tau)\tau \log\tau \mathrm{EcHa}^2 \mathrm{f}_\mathrm{i}^2 \mathrm{d}\xi$$

$$= -\int_{-1}^{1} \frac{1}{2}(1+\xi)(0.0001\xi + 0.0001)\log(0.0001\xi + 0.0001)\mathrm{EcHa}^2 \mathrm{f}_\mathrm{i}^2 \mathrm{d}\xi$$

$$= 0.00118007 \mathrm{EcHa}^2 \mathrm{f}_\mathrm{i}^2 \tag{3.7.57}$$

h^e take values of $0.0001 \leq \mathrm{h}^\mathrm{e} \leq 0.0002$ while τ take values of $0.005 \leq \mathrm{h}^\mathrm{e} \leq 0.0001$ to obtain smooth graphs in the results. When the assembly rule is applied utilizing equations (3.7.56) and (3.7.57), global force vector becomes

$$[\mathrm{K}] = \begin{bmatrix} \mathrm{K}_1^1 \\ \mathrm{K}_2^1 + \mathrm{K}_1^2 \\ \mathrm{K}_2^2 + \mathrm{K}_1^3 \\ \mathrm{K}_2^3 + \mathrm{K}_1^4 \\ \mathrm{K}_2^4 + \mathrm{K}_1^5 \\ \mathrm{K}_2^5 \end{bmatrix} = \begin{bmatrix} 0.00062337 \mathrm{EcHa}^2 \mathrm{f}_\mathrm{i}^2 \\ 0.00180344 \mathrm{EcHa}^2 \mathrm{f}_\mathrm{i}^2 \\ 0.00180344 \mathrm{EcHa}^2 \mathrm{f}_\mathrm{i}^2 \\ 0.00180344 \mathrm{EcHa}^2 \mathrm{f}_\mathrm{i}^2 \\ 0.00180344 \mathrm{EcHa}^2 \mathrm{f}_\mathrm{i}^2 \\ 0.00118007 \mathrm{EcHa}^2 \mathrm{f}_\mathrm{i}^2 \end{bmatrix} \tag{3.7.58}$$

Settling equation (3.7.58) in equation (3.7.52), converts it to

$$\begin{bmatrix} \mathrm{I}_{11}^1 & \mathrm{I}_{12}^1 & 0 & 0 & 0 & 0 \\ \mathrm{I}_{21}^1 & \mathrm{I}_{22}^1 + \mathrm{I}_{11}^2 & \mathrm{I}_{12}^2 & 0 & 0 & 0 \\ 0 & \mathrm{I}_{21}^2 & \mathrm{I}_{22}^2 + \mathrm{I}_{11}^3 & \mathrm{I}_{12}^3 & 0 & 0 \\ 0 & 0 & \mathrm{I}_{21}^3 & \mathrm{I}_{22}^3 + \mathrm{I}_{11}^4 & \mathrm{I}_{12}^4 & 0 \\ 0 & 0 & 0 & \mathrm{I}_{21}^4 & \mathrm{I}_{22}^4 + \mathrm{I}_{11}^5 & \mathrm{I}_{12}^5 \\ 0 & 0 & 0 & 0 & \mathrm{I}_{21}^5 & \mathrm{I}_{22}^5 + \mathrm{I}_{11}^6 \end{bmatrix} \begin{bmatrix} \mathrm{h}_1 \\ \mathrm{h}_2 \\ \mathrm{h}_3 \\ \mathrm{h}_4 \\ \mathrm{h}_5 \\ \mathrm{h}_6 \end{bmatrix}$$

$$= \begin{bmatrix} 0.00062337\mathrm{EcHa}^2\mathrm{f}_\mathrm{i}^2 \\ 0.00180344\mathrm{EcHa}^2\mathrm{f}_\mathrm{i}^2 \\ 0.00180344\mathrm{EcHa}^2\mathrm{f}_\mathrm{i}^2 \\ 0.00180344\mathrm{EcHa}^2\mathrm{f}_\mathrm{i}^2 \\ 0.00180344\mathrm{EcHa}^2\mathrm{f}_\mathrm{i}^2 \\ 0.00118007\mathrm{EcHa}^2\mathrm{f}_\mathrm{i}^2 \end{bmatrix} - \begin{bmatrix} \frac{1}{\mathrm{Pr}}\mathrm{I}_{21} \\ \vdots \\ \vdots \\ \vdots \\ \vdots \\ \vdots \end{bmatrix} \tag{3.7.59}$$

3.7.21 Reduction of velocity global equation system

The values f_1 of the first node and f_6 of the last node are known. This leads to reduction in equation (3.7.54), which is done in two steps namely;

i. deleting the first row and the last row of the whole global equation system.

ii. deleting the first column and last column of stiffness matrix.

After trimming has been done, equation (3.7.54) becomes

$$\begin{bmatrix} \mathrm{W}_{22}^1 + \mathrm{W}_{11}^2 & \mathrm{W}_{12}^2 & 0 & 0 \\ \mathrm{W}_{21}^2 & \mathrm{W}_{22}^2 + \mathrm{W}_{11}^3 & \mathrm{W}_{12}^3 & 0 \\ 0 & \mathrm{W}_{21}^3 & \mathrm{W}_{22}^3 + \mathrm{W}_{11}^4 & \mathrm{W}_{12}^4 \\ 0 & 0 & \mathrm{W}_{21}^4 & \mathrm{W}_{22}^4 + \mathrm{W}_{11}^5 \end{bmatrix} \begin{bmatrix} \mathrm{f}_2 \\ \mathrm{f}_3 \\ \mathrm{f}_4 \\ \mathrm{f}_5 \end{bmatrix} = \begin{bmatrix} -2\mathrm{Re}\boldsymbol{\lambda_\theta} \\ \vdots \\ \vdots \\ \vdots \end{bmatrix} \tag{3.7.60}$$

Equation (3.7.60) is the state to be adopted to find approximate solutions to equation (3.6.3), ode.

3.7.22 Trimming temperature global equation system

The value $\mathrm{h_1}$ of the first node and that of the last node $\mathrm{h_6}$ are known. This leads to slashing of the global equation system equation (3.7.59). When reduction is done, equation (3.7.59) becomes

$$\begin{bmatrix} \mathrm{I}_{22}^{1}+\mathrm{I}_{11}^{2} & \mathrm{I}_{12}^{2} & 0 & 0 \\ \mathrm{I}_{21}^{2} & \mathrm{I}_{22}^{2}+\mathrm{I}_{11}^{3} & \mathrm{I}_{12}^{3} & 0 \\ 0 & \mathrm{I}_{21}^{3} & \mathrm{I}_{22}^{3}+\mathrm{I}_{11}^{4} & \mathrm{I}_{12}^{4} \\ 0 & 0 & \mathrm{I}_{21}^{4} & \mathrm{I}_{22}^{4}+\mathrm{I}_{11}^{5} \end{bmatrix} \begin{bmatrix} \mathrm{h}_2 \\ \mathrm{h}_3 \\ \mathrm{h}_4 \\ \mathrm{h}_5 \end{bmatrix}$$

$$= \begin{bmatrix} 0.00180344\mathrm{EcHa}^2\mathrm{f}_\mathrm{i}^2 \\ 0.00180344\mathrm{EcHa}^2\mathrm{f}_\mathrm{i}^2 \\ 0.00180344\mathrm{EcHa}^2\mathrm{f}_\mathrm{i}^2 \\ 0.00180344\mathrm{EcHa}^2\mathrm{g}_\mathrm{i}^2 \end{bmatrix} - \begin{bmatrix} \frac{1}{\mathrm{Pr}}\mathrm{I}_{21} \\ \vdots \\ \vdots \\ \vdots \end{bmatrix} \tag{3.7.61}$$

Equation (3.7.61) is the state to be employed to find approximate solutions to equation (3.6.7), ode.

3.7.23 Discretization of major axis of elliptical cross section of pipe

The major axis of the elliptical cross section of the pipe is sub divided into N-1 elements and N nodes as shown in figure 3.7.2. This is for the purpose of facilitating formation of algebraic equations which will employed to find values of $\mathrm{f_j}$s and $\mathrm{h_j}$s at each of the nodes by engaging equations (3.7.60) and (3.7.61) respectively.

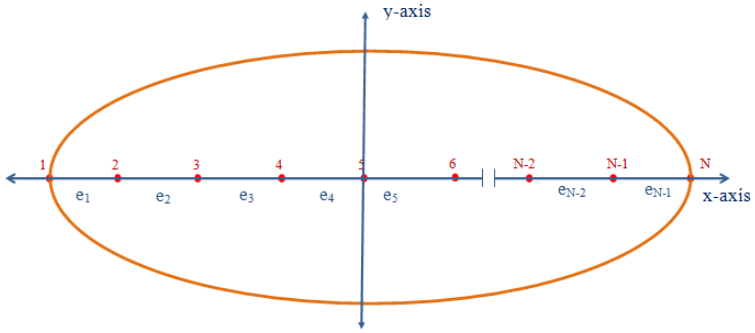

Figure 3.7.2: Discretized major axis of elliptical cross section of pipe

$N = 21$ for circle and $N = 29, 33, 35$ for ellipses.

3.7.24 Calculation of velocity elemental stiffness matrix

Elemental stiffness matrix is evaluated using equations (3.7.40), (3.7.41) and (3.7.43) such that:

Setting $h^e = 0.0002, \eta_1^e = 0.0000$ and $\eta_2^e = 0.0002$ then $\eta = 0.0001\xi + 0.0001$ so that equation (3.7.43) gives

$$W_{11}^1 = -0.5\int_{-1}^{1}(0.0001\xi + 0.0001)^2[\log(0.0001\xi + 0.0001)]^3(1-\xi)d\xi$$

$$-1.25\int_{-1}^{1}(0.0001\xi + 0.0001)^2[\log(0.0001\xi + 0.0001)]^4(1-\xi)d\xi$$

$$-0.25\int_{-1}^{1}(0.0001\xi + 0.0001)^2[\log(0.0001\xi + 0.0001)]^5(1-\xi)d\xi$$

$$+\frac{1}{J^e}\int_{-1}^{1}(0.0001\xi + 0.0001)^3[\log(0.0001\xi + 0.0001)]^4 d\xi$$

$$+\frac{0.5}{J^e}\int_{-1}^{1}(0.0001\xi + 0.0001)^3[\log(0.0001\xi + 0.0001)]^5 d\xi$$

$$+1.5\int_{-1}^{1}(0.0001\xi + 0.0001)[\log(0.0001\xi + 0.0001)]^3(1-\xi)^2 J^e d\xi$$

$$+1.5\int_{-1}^{1}(0.0001\xi + 0.0001)[\log(0.0001\xi + 0.0001)]^4(1-\xi)^2 J^e d\xi$$

$$+0.25\int_{-1}^{1}(0.0001\xi+0.0001)[\log(0.0001\xi+0.0001)]^{5}(1-\xi)^{2}\mathrm{J^{e}}\mathrm{d}\xi$$

$$-0.25\int_{-1}^{1}(0.0001\xi+0.0001)^{2}[\log(0.0001\xi+0.0001)]\mathrm{Ha}^{2}(1-\xi)\mathrm{d}\xi$$

$$+0.25\int_{-1}^{1}(0.0001\xi+0.0001)[\log(0.0001\xi+0.0001)](1-\xi)^{2}\mathrm{Ha}^{2}\mathrm{J^{e}}\mathrm{d}\xi$$

On integrating and simplifying

$$\mathrm{W}_{11}^{1}=1.02009\times10^{-4}+2.03417\times10^{-7}\mathrm{Ha}^{2}-2.99146\times10^{-2}\mathrm{Ha}^{2}\mathrm{J^{e}}-\frac{8.07356\times10^{-8}}{\mathrm{J^{e}}}$$

$$-1.28685\mathrm{J^{e}} \tag{3.7.62}$$

Repeating the processes for $\mathrm{W}_{12}^{1},\mathrm{W}_{21}^{1}$ and W_{22}^{1} results in

$$\mathrm{W}_{12}^{1}=0.5\int_{-1}^{1}(0.0001\xi+0.0001)^{2}[\log(0.0001\xi+0.0001)]^{3}(1-\xi)\mathrm{d}\xi$$

$$+1.25\int_{-1}^{1}(0.0001\xi+0.0001)^{2}[\log(0.0001\xi+0.0001)]^{4}(1-\xi)\mathrm{d}\xi$$

$$+0.25\int_{-1}^{1}(0.0001\xi+0.0001)^{2}[\log(0.0001\xi+0.0001)]^{5}(1-\xi)\mathrm{d}\xi$$

$$-\frac{1}{\mathrm{J^{e}}}\int_{-1}^{1}(0.0001\xi+0.0001)^{3}[\log(0.0001\xi+0.0001)]^{4}\mathrm{d}\xi$$

$$-\frac{0.5}{\mathrm{J^{e}}}\int_{-1}^{1}(0.0001\xi+0.0001)^{3}[\log(0.0001\xi+0.0001)]^{5}\mathrm{d}\xi$$

$$+1.5\int_{-1}^{1}(0.0001\xi+0.0001)[\log(0.0001\xi+0.0001)]^{3}(1-\xi^{2})\mathrm{J^{e}}\mathrm{d}\xi$$

$$+1.5\int_{-1}^{1}(0.0001\xi+0.0001)[\log(0.0001\xi+0.0001)]^{4}(1-\xi^{2})\mathrm{J^{e}}\mathrm{d}\xi$$

$$+0.25\int_{-1}^{1}(0.0001\xi+0.0001)[\log(0.0001\xi+0.0001)]^{5}(1-\xi^{2})\mathrm{J^{e}}\mathrm{d}\xi$$

$$+0.25\int_{-1}^{1}(0.0001\xi+0.0001)^2[\log(0.0001\xi+0.0001)]\mathrm{Ha}^2(1-\xi)\mathrm{d}\xi$$

$$+0.25\int_{-1}^{1}(0.0001\xi+0.0001)[\log(0.0001\xi+0.0001)](1-\xi^2)\mathrm{Ha}^2\mathrm{J}^{\mathrm{e}}\mathrm{d}\xi$$

Upon integrating and simplifying

$$\mathrm{W}_{12}^{1}=-1.02009\times10^{-4}-2.03417\times10^{-8}\mathrm{Ha}^2-2.52849\times10^{-2}\mathrm{Ha}^2\mathrm{J}^{\mathrm{e}}+\frac{8.07356\times10^{-8}}{\mathrm{J}^{\mathrm{e}}}$$

$$-0.889363\mathrm{J}^{\mathrm{e}} \tag{3.7.63}$$

$$\mathrm{W}_{21}^{1}=-0.5\int_{-1}^{1}(0.0001\xi+0.0001)^2[\log(0.0001\xi+0.0001)]^3(1+\xi)\mathrm{d}\xi$$

$$-1.25\int_{-1}^{1}(0.0001\xi+0.0001)^2[\log(0.0001\xi+0.0001)]^4(1+\xi)\mathrm{d}\xi$$

$$-0.25\int_{-1}^{1}(0.0001\xi+0.0001)^2[\log(0.0001\xi+0.0001)]^5(1+\xi)\mathrm{d}\xi$$

$$-\frac{1}{\mathrm{J}^{\mathrm{e}}}\int_{-1}^{1}(0.0001\xi+0.0001)^3[\log(0.0001\xi+0.0001)]^4\mathrm{d}\xi$$

$$-\frac{0.5}{\mathrm{J}^{\mathrm{e}}}\int_{-1}^{1}(0.0001\xi+0.0001)^3[\log(0.0001\xi+0.0001)]^5\mathrm{d}\xi$$

$$+1.5\int_{-1}^{1}(0.0001\xi+0.0001)[\log(0.0001\xi+0.0001)]^3(1-\xi^2)\mathrm{J}^{\mathrm{e}}\mathrm{d}\xi$$

$$+1.5\int_{-1}^{1}(0.0001\xi+0.0001)[\log(0.0001\xi+0.0001)]^4(1-\xi^2)\mathrm{J}^{\mathrm{e}}\mathrm{d}\xi$$

$$+0.25\int_{-1}^{1}(0.0001\xi+0.0001)[\log(0.0001\xi+0.0001)]^5(1-\xi^2)\mathrm{J}^{\mathrm{e}}\mathrm{d}\xi$$

$$-0.25\int_{-1}^{1}(0.0001\xi+0.0001)^2[\log(0.0001\xi+0.0001)]\mathrm{Ha}^2(1+\xi)\mathrm{d}\xi$$

$$+0.25\int_{-1}^{1}(0.0001\xi+0.0001)[\log(0.0001\xi+0.0001)](1-\xi^2)\mathrm{Ha}^2\mathrm{J}^{\mathrm{e}}\mathrm{d}\xi$$

When integration and simplification is done,

$$W_{21}^{1} = -2.39048 \times 10^{-4} + 8.76719 \times 10^{-8} Ha^{2} - 2.52849 \times 10^{-2} Ha^{2} J^{e} + \frac{8.07352 \times 10^{-8}}{J^{e}}$$

$$-0.889363 J^{e} \tag{3.7.64}$$

$$W_{22}^{1} = 0.5 \int_{-1}^{1} (0.0001\xi + 0.0001)^{2} [\log(0.0001\xi + 0.0001)]^{3} (1 + \xi) d\xi$$

$$+1.25 \int_{-1}^{1} (0.0001\xi + 0.0001)^{2} [\log(0.0001\xi + 0.0001)]^{4} (1 + \xi) d\xi$$

$$+0.25 \int_{-1}^{1} (0.0001\xi + 0.0001)^{2} [\log(0.0001\xi + 0.0001)]^{5} (1 + \xi) d\xi$$

$$+\frac{1}{J^{e}} \int_{-1}^{1} (0.0001\xi + 0.0001)^{3} [\log(0.0001\xi + 0.0001)]^{4} d\xi$$

$$+\frac{0.5}{J^{e}} \int_{-1}^{1} (0.0001\xi + 0.0001)^{3} [\log(0.0001\xi + 0.0001)]^{5} d\xi$$

$$+1.5 \int_{-1}^{1} (0.0001\xi + 0.0001) [\log(0.0001\xi + 0.0001)]^{3} (1 + \xi)^{2} J^{e} d\xi$$

$$+1.5 \int_{-1}^{1} (0.0001\xi + 0.0001) [\log(0.0001\xi + 0.0001)]^{4} (1 + \xi)^{2} J^{e} d\xi$$

$$+0.25 \int_{-1}^{1} (0.0001\xi + 0.0001) [\log(0.0001\xi + 0.0001)]^{5} (1 + \xi)^{2} J^{e} d\xi$$

$$+0.25 \int_{-1}^{1} (0.0001\xi + 0.0001)^{2} [\log(0.0001\xi + 0.0001)] Ha^{2} (1 + \xi) d\xi$$

$$+0.25 \int_{-1}^{1} (0.0001\xi + 0.0001) [\log(0.0001\xi + 0.0001)] (1 + \xi)^{2} Ha^{2} J^{e} d\xi$$

Integration and simplification are done and yield

$$W_{22}^{1} = -2.39052 \times 10^{-4} - 8.17592 \times 10^{-8} Ha^{2} - 6.75332 \times 10^{-2} Ha^{2} J^{e} - \frac{8.07356 \times 10^{-8}}{J^{e}}$$

$$-2.0668 J^{e} \tag{3.7.65}$$

The 2×2 $[\mathrm{W}^{\mathrm{e}}]$ elemental matrix is given by

$$\mathrm{W}^{\mathrm{e}} = \begin{bmatrix} \mathrm{W}_{11}^{1} & \mathrm{W}_{12}^{1} \\ \mathrm{W}_{21}^{1} & \mathrm{W}_{22}^{1} \end{bmatrix} \tag{3.7.66}$$

From now henceforth, whenever equation (3.7.66) is mentioned it means it comprises equations (3.7.62) to (3.7.65) which are too large to fit in the matrix. When equation (3.7.66) is put in equation (3.7.60), the solutions of $\mathrm{f_j}$'s are obtained for different values of:

i. Ha while keeping $\boldsymbol{\lambda_\theta}, \mathrm{Re}, \mathrm{a}$ and J^{e} constant

ii. $\boldsymbol{\lambda_\theta}$ while keeping $\mathrm{Ha}, \mathrm{Re}, \mathrm{a}$ and J^{e} fixed

iii. Re while maintaining $\mathrm{Ha}, \mathrm{Re}, \boldsymbol{\lambda_\theta}, \mathrm{a}$ and J^{e}

iv. a while preserving $\mathrm{Ha}, \mathrm{Re}, \boldsymbol{\lambda_\theta}$ and J^{e}

3.7.25 Calculation of temperature elemental stiffness matrix

Placing equation (3.7.55) in equation (3.7.48), it changes to

$$\mathrm{I}_{\mathrm{ij}}^{1} = \int_{-1}^{1} \left(-\frac{1}{\mathrm{Pr}} (0.0001\boldsymbol{\xi} + 0.0001) \log(0.0001\boldsymbol{\xi} + 0.0001) \frac{\mathrm{ds_i}}{\mathrm{d}\boldsymbol{\xi}} \frac{\mathrm{ds_j}}{\mathrm{d}\boldsymbol{\xi}} \frac{1}{\mathrm{J}^{\mathrm{e}}} \right) \mathrm{d}\boldsymbol{\xi} \tag{3.7.67}$$

Equation (3.7.67) is utilized to find components of the elemental stiffness matrix $\mathrm{I}_{11}^{1}, \mathrm{I}_{12}^{1}, \mathrm{I}_{21}^{1}$ and I_{22}^{1} as under:

$$\mathrm{I}_{11}^{1} = \int_{-1}^{1} \left(-\frac{1}{\mathrm{Pr}} (0.0001\boldsymbol{\xi} + 0.0001) \log(0.0001\boldsymbol{\xi} + 0.0001) \frac{\mathrm{ds_1}}{\mathrm{d}\boldsymbol{\xi}} \frac{\mathrm{ds_1}}{\mathrm{d}\boldsymbol{\xi}} \frac{1}{\mathrm{J}^{\mathrm{e}}} \right) \mathrm{d}\boldsymbol{\xi}$$

$$= \int_{-1}^{1} \left(-\frac{1}{\mathrm{Pr}} (0.0001\boldsymbol{\xi} + 0.0001) \log(0.0001\boldsymbol{\xi} + 0.0001) \left(-\frac{1}{2} \right) \left(-\frac{1}{2} \right) \frac{1}{\mathrm{J}^{\mathrm{e}}} \right) \mathrm{d}\boldsymbol{\xi}$$

On integrating and simplifying

$$\mathrm{I}_{11}^{1} = \frac{0.00045086}{\mathrm{Pr}\mathrm{J}^{\mathrm{e}}} \tag{3.7.68}$$

$$\mathrm{I}_{12}^{1} = \int_{-1}^{1} \left(-\frac{1}{\mathrm{Pr}} (0.0001\xi + 0.0001) \log(0.0001\xi + 0.0001) \frac{\mathrm{ds}_1}{\mathrm{d}\xi} \frac{\mathrm{ds}_2}{\mathrm{d}\xi} \frac{1}{\mathrm{J}^{\mathrm{e}}} \right) \mathrm{d}\xi$$

$$= \int_{-1}^{1} \left(-\frac{1}{\mathrm{Pr}} (0.0001\xi + 0.0001) \log(0.0001\xi + 0.0001) \left(-\frac{1}{2} \right) \left(\frac{1}{2} \right) \frac{1}{\mathrm{J}^{\mathrm{e}}} \right) \mathrm{d}\xi$$

Upon integrating and simplifying

$$\mathrm{I}_{12}^{1} = -\frac{0.00045086}{\mathrm{Pr}\mathrm{J}^{\mathrm{e}}} \tag{3.7.69}$$

For I_{21}^{1}

$$\mathrm{I}_{21}^{1} = \int_{-1}^{1} \left(-\frac{1}{\mathrm{Pr}} (0.0001\xi + 0.0001) \log(0.0001\xi + 0.0001) \frac{\mathrm{ds}_2}{\mathrm{d}\xi} \frac{\mathrm{ds}_1}{\mathrm{d}\xi} \frac{1}{\mathrm{J}^{\mathrm{e}}} \right) \mathrm{d}\xi$$

$$= \int_{-1}^{1} \left(-\frac{1}{\mathrm{Pr}} (0.0001\xi + 0.0001) \log(0.0001\xi + 0.0001) \left(\frac{1}{2} \right) \left(-\frac{1}{2} \right) \frac{1}{\mathrm{J}^{\mathrm{e}}} \right) \mathrm{d}\xi$$

Integration and simplification results in

$$\mathrm{I}_{21}^{1} = -\frac{0.00045086}{\mathrm{Pr}\mathrm{J}^{\mathrm{e}}} \tag{3.7.70}$$

For I_{22}^{1}

$$\mathrm{I}_{22}^{1} = \int_{-1}^{1} \left(-\frac{1}{\mathrm{Pr}} (0.0001\xi + 0.0001) \log(0.0001\xi + 0.0001) \frac{\mathrm{ds}_2}{\mathrm{d}\xi} \frac{\mathrm{ds}_2}{\mathrm{d}\xi} \frac{1}{\mathrm{J}^{\mathrm{e}}} \right) \mathrm{d}\xi$$

$$= \int_{-1}^{1} \left(-\frac{1}{\mathrm{Pr}} (0.0001\xi + 0.0001) \log(0.0001\xi + 0.0001) \left(\frac{1}{2} \right) \left(\frac{1}{2} \right) \frac{1}{\mathrm{J}^{\mathrm{e}}} \right) \mathrm{d}\xi$$

Integration and simplification grants

$$\mathrm{I}_{22}^{1}=\frac{0.00045086}{\mathrm{PrJ^{e}}} \tag{3.7.71}$$

The $2\times 2,\quad [\mathrm{I^{e}}]$, elemental matrix is given by

$$\mathrm{I^{e}}=\begin{bmatrix} \mathrm{I}_{11}^{1} & \mathrm{I}_{12}^{1} \\ \mathrm{I}_{21}^{1} & \mathrm{I}_{22}^{1} \end{bmatrix} \tag{3.7.72}$$

Settling equations (3.7.67) to (3.7.71) in equation (3.7.72), it produces

$$\mathrm{I^{e}}=\begin{bmatrix} \frac{0.00045086}{\mathrm{PrJ^{e}}} & -\frac{0.00045086}{\mathrm{PrJ^{e}}} \\ -\frac{0.00045086}{\mathrm{PrJ^{e}}} & \frac{0.00045086}{\mathrm{PrJ^{e}}} \end{bmatrix} \tag{3.7.73}$$

Equation (3.7.73) is used to obtain elemental matrices. On bringing it in equation (3.7.61), solutions of $\mathrm{h_j}$'s are obtained for different values of:

i. Pr while keeping $\mathrm{h^{e}, J^{e}, a, Ec, f_i}$, and Ha constant.

ii. Ha while preserving $\mathrm{Ec, h^{e}, J^{e}, a, f_i}$ and Pr.

iii. Ec while controlling $\mathrm{Ha, h^{e}, J^{e}, Pr, f_i}$ and a.

iv. $\mathrm{f_i}$ while maintaining $\mathrm{Ha, h^{e}, J^{e}, Pr, Ec}$ and a.

v. a while keeping $\mathrm{Ha, h^{e}, J^{e}, Pr, Ec}$ and $\mathrm{f_i}$ fixed.

CHAPTER FOUR

RESULTS AND DISCUSSION

4.1 Results and discussion for velocity profile

In computing the value of f_j's, the values of f at the first and last nodes are known and are both equal to 0.000. From subsection 3.7.13, considering $h^e = 0.0002$, then $J^e = 0.0001$. These four values apply for all the cases worked out in this section.

4.1.1 Varying Hartmann number while controlling gravitational force, distance of major axis, Reynold's number and length of elements

$$(a) \quad \mathbf{Ha = 1.0, J^e = 0.0001, \lambda_\theta = 0.001, Re = 0.5, a = 0.0034}$$

When the above stated values of Ha and J^e are put in equation (3.7.66), it produces

$$W^e = \begin{bmatrix} -0.0008368 & 0.0006139 \\ 0.000955 & -0.0012599 \end{bmatrix} \tag{4.1.1}$$

Using equation (4.1.1), global stiffness matrix W becomes

$$W = \begin{bmatrix} -0.0008368 & 0.0006139 & 0 & 0 & 0 & 0 \\ 0.000955 & -0.0012599 & 0.0006139 & 0 & 0 & 0 \\ 0 & 0.000955 & -0.0012599 & 0.0006139 & 0 & 0 \\ 0 & 0 & 0.000955 & -0.0012599 & 0.0006139 & 0 \\ 0 & 0 & 0 & 0.000955 & -0.0012599 & 0.0006139 \\ 0 & 0 & 0 & 0 & 0.000955 & -0.0012599 \end{bmatrix} \tag{4.1.2}$$

Considering 35 nodes in figure 3.7.2 and then substituting equation (4.1.2), Re and λ_θ in equation (3.7.60), it transforms into

$$\begin{bmatrix} -0.0012599 & 0.0006139 & 0 & 0 & \dots \\ 0.000955 & -0.0012599 & 0.0006139 & 0 & \dots \\ 0 & 0.000955 & -0.0012599 & 0.0006139 & \ddots \\ 0 & 0 & 0.000955 & -0.0012599 & \ddots \\ \vdots & \vdots & \ddots & \ddots & \ddots \end{bmatrix} \begin{bmatrix} f_2 \\ f_3 \\ f_4 \\ \vdots \\ f_{33} \\ f_{34} \end{bmatrix} = \begin{bmatrix} -0.001 \\ -0.001 \\ -0.001 \\ \vdots \\ -0.001 \\ -0.001 \end{bmatrix} \tag{4.1.3}$$

The system of equations formed from equation (4.1.3) are

$$-0.0012599f_2 + 0.0006139f_3 = -0.001 \tag{4.1.4}$$

$$0.000955f_2 - 0.0012599f_3 + 0.0006139f_4 = -0.001 \tag{4.1.5}$$

$$0.000955f_3 - 0.0012599f_4 + 0.0006139f_5 = -0.001 \tag{4.1.6}$$

$$\vdots \tag{4.1.7}$$

$$0.000955f_{31} - 0.0012599f_{32} + 0.0006139f_{33} = -0.001 \tag{4.1.8}$$

$$0.000955f_{32} - 0.0012599f_{33} + 0.0006139f_{34} = -0.001 \tag{4.1.9}$$

$$0.000955f_{33} - 0.0012599f_{34} = -0.001 \tag{4.1.10}$$

Mathematica is used to solve the system of equations (4.1.4) to (4.1.10) and gives solutions of f_j's as

Table 4.1.1: Velocities along the major axis when $\mathrm{Ha} = 1.0$

$\mathrm{f}_1 = 0.000$	$\mathrm{f}_2 = 0.869$	$\mathrm{f}_3 = 1.340$	$\mathrm{f}_4 = 1.594$	$\mathrm{f}_5 = 1.732$
$\mathrm{f}_6 = 1.807$	$\mathrm{f}_7 = 1.847$	$\mathrm{f}_8 = 1.869$	$\mathrm{f}_9 = 1.881$	$\mathrm{f}_{10} = 1.887$
$\mathrm{f}_{11} = 1.891$	$\mathrm{f}_{12} = 1.892$	$\mathrm{f}_{13} = 1.893$	$\mathrm{f}_{14} = 1.894$	$\mathrm{f}_{15} = 1.894$
$\mathrm{f}_{16} = 1.894$	$\mathrm{f}_{17} = 1.895$	$\mathrm{f}_{18} = 1.895$	$\mathrm{f}_{19} = 1.895$	$\mathrm{f}_{20} = 1.895$
$\mathrm{f}_{21} = 1.895$	$\mathrm{f}_{22} = 1.895$	$\mathrm{f}_{23} = 1.895$	$\mathrm{f}_{24} = 1.895$	$\mathrm{f}_{25} = 1.895$
$\mathrm{f}_{26} = 1.895$	$\mathrm{f}_{27} = 1.894$	$\mathrm{f}_{28} = 1.893$	$\mathrm{f}_{29} = 1.891$	$\mathrm{f}_{30} = 1.885$
$\mathrm{f}_{31} = 1.867$	$\mathrm{f}_{32} = 1.815$	$\mathrm{f}_{33} = 1.665$	$\mathrm{f}_{34} = 1.235$	$\mathrm{f}_{35} = 0.000$

The $\mathrm{f_j}$'s are solutions of function f derived from the stream function, ψ, which relates velocities of fluid in the r–component and θ–components. $\mathrm{f_j}$'s will therefore be the velocities of fluid along the major axis of cross section of elliptical pipe.

$$(\mathbf{b}) \quad \mathbf{Ha = 5.0, Re = 0.5, J^e = 0.0001}, \lambda_\theta = \mathbf{0.001, a = 0.0034}$$

Placing the above stated values of Ha and $\mathrm{J^e}$ in equation (3.7.66), it turns out to

$$\mathrm{W^e} = \begin{bmatrix} -0.0009037 & 0.0005527 \\ 0.0008964 & -0.0014240 \end{bmatrix} \tag{4.1.11}$$

Utilizing equation (4.1.11), global stiffness matrix W develops to

$$\mathrm{W} = \begin{bmatrix} -0.0009037 & 0.0005527 & 0 & 0 & 0 & 0 \\ 0.0008964 & -0.0023277 & 0.0005527 & 0 & 0 & 0 \\ 0 & 0.0008964 & -0.0023277 & 0.0005527 & 0 & 0 \\ 0 & 0 & 0.0008964 & -0.0023277 & 0.0005527 & 0 \\ 0 & 0 & 0 & 0.0008964 & -0.0023277 & 0.0005527 \\ 0 & 0 & 0 & 0 & 0.0008964 & -0.0023277 \end{bmatrix} \tag{4.1.12}$$

Taking into account 35 nodes and then inserting equation (4.1.12), Re and λ_θ in equation (3.7.60), it emerges as

$$\begin{bmatrix} -0.0023277 & 0.0005527 & 0 & 0 & \dots \\ 0.0008964 & -0.0023277 & 0.0005527 & 0 & \dots \\ 0 & 0.0008964 & -0.0023277 & 0.0005527 & \ddots \\ 0 & 0 & 0.0008964 & -0.0023277 & \ddots \\ \vdots & \vdots & \ddots & \ddots & \ddots \end{bmatrix} \begin{bmatrix} \mathrm{f}_2 \\ \mathrm{f}_3 \\ \mathrm{f}_4 \\ \vdots \\ \mathrm{f}_{33} \\ \mathrm{f}_{34} \end{bmatrix} = \begin{bmatrix} -0.001 \\ -0.001 \\ -0.001 \\ \vdots \\ -0.001 \\ -0.001 \end{bmatrix} \tag{4.1.13}$$

The structure of equations formed from equation (4.1.13) are

$$-0.0023277\mathrm{f}_2 + 0.0005527\mathrm{f}_3 = -0.001 \tag{4.1.14}$$

$$0.0008964\mathrm{f}_2 - 0.0023277\mathrm{f}_3 + 0.0005527\mathrm{f}_4 = -0.001 \tag{4.1.15}$$

$$0.0008964\mathrm{f}_3 - 0.0023277\mathrm{f}_4 + 0.0005527\mathrm{f}_5 = -0.001 \tag{4.1.16}$$

$$\vdots \tag{4.1.17}$$

$$0.0008964\mathrm{f}_{31} - 0.0023277\mathrm{f}_{32} + 0.0005527\mathrm{f}_{33} = -0.001 \tag{4.1.18}$$

$$0.0008964\mathrm{f}_{32} - 0.0023277\mathrm{f}_{33} + 0.0005527\mathrm{f}_{34} = -0.001 \tag{4.1.19}$$

$$0.0008964\mathrm{f}_{33} - 0.0023277\mathrm{f}_{34} = -0.001 \tag{4.1.20}$$

Algebraic equations (4.1.14) to (4.1.20) are solved by Mathematica which presents solutions of velocities as

Table 4.1.2: Velocities along the major axis when $\mathrm{Ha} = 5.0$

$\mathrm{f}_1 = 0.000$	$\mathrm{f}_2 = 0.650$	$\mathrm{f}_3 = 0.929$	$\mathrm{f}_4 = 1.048$	$\mathrm{f}_5 = 1.100$
$\mathrm{f}_6 = 1.122$	$\mathrm{f}_7 = 1.131$	$\mathrm{f}_8 = 1.135$	$\mathrm{f}_9 = 1.137$	$\mathrm{f}_{10} = 1.138$
$\mathrm{f}_{11} = 1.138$	$\mathrm{f}_{12} = 1.138$	$\mathrm{f}_{13} = 1.138$	$\mathrm{f}_{14} = 1.138$	$\mathrm{f}_{15} = 1.138$
$\mathrm{f}_{16} = 1.138$	$\mathrm{f}_{17} = 1.138$	$\mathrm{f}_{18} = 1.138$	$\mathrm{f}_{19} = 1.138$	$\mathrm{f}_{20} = 1.138$
$\mathrm{f}_{21} = 1.138$	$\mathrm{f}_{22} = 1.138$	$\mathrm{f}_{23} = 1.138$	$\mathrm{f}_{24} = 1.138$	$\mathrm{f}_{25} = 1.138$
$\mathrm{f}_{26} = 1.138$	$\mathrm{f}_{27} = 1.138$	$\mathrm{f}_{28} = 1.138$	$\mathrm{f}_{29} = 1.138$	$\mathrm{f}_{30} = 1.137$
$\mathrm{f}_{31} = 1.133$	$\mathrm{f}_{32} = 1.117$	$\mathrm{f}_{33} = 1.059$	$\mathrm{f}_{34} = 0.837$	$\mathrm{f}_{35} = 0.000$

(c) $\mathbf{Ha = 10.0, Re = 0.5, J^e = 0.0001, \lambda_\theta = 0.001, a = 0.0034}$

On putting the above stated values of Ha and J^{e} in equation (3.7.66), it changes into

$$\mathrm{W}^{\mathrm{e}} = \begin{bmatrix} -0.0011128 & 0.0003615 \\ 0.0007134 & -0.0019366 \end{bmatrix} \tag{4.1.21}$$

Using equation (4.1.21), global stiffness matrix W gives

$$\mathrm{W} = \begin{bmatrix} -0.0011128 & 0.0003615 & 0 & 0 & 0 & 0 \\ 0.0007134 & -0.0030494 & 0.0003615 & 0 & 0 & 0 \\ 0 & 0.0007134 & -0.0030494 & 0.0003615 & 0 & 0 \\ 0 & 0 & 0.0007134 & -0.0030494 & 0.0003615 & 0 \\ 0 & 0 & 0 & 0.0007134 & -0.0030494 & 0.0003615 \\ 0 & 0 & 0 & 0 & 0.0007134 & -0.0030494 \end{bmatrix} \tag{4.1.22}$$

Considering 35 nodes and then substituting equation (4.1.22), Re and λ_θ in equation (3.7.60), it

turns out to

$$\begin{bmatrix} -0.0030494 & 0.0003615 & 0 & 0 & \dots \\ 0.0007134 & -0.0030494 & 0.0003615 & 0 & \dots \\ 0 & 0.0007134 & -0.0030494 & 0.0003615 & \ddots \\ 0 & 0 & 0.0007134 & -0.0030494 & \ddots \\ \vdots & \vdots & \ddots & \ddots & \ddots \end{bmatrix} \begin{bmatrix} f_2 \\ f_3 \\ f_4 \\ \vdots \\ f_{33} \\ f_{34} \end{bmatrix} = \begin{bmatrix} -0.001 \\ -0.001 \\ -0.001 \\ \vdots \\ -0.001 \\ -0.001 \end{bmatrix} \tag{4.1.23}$$

The set of equations formed from equation (4.1.23) are

$$-0.0030494f_2 + 0.0003615f_3 = -0.001 \tag{4.1.24}$$

$$0.0007134f_2 - 0.0030494f_3 + 0.0003615f_4 = -0.001 \tag{4.1.25}$$

$$0.0007134f_3 - 0.0030494f_4 + 0.0003615f_5 = -0.001 \tag{4.1.26}$$

$$\vdots \tag{4.1.27}$$

$$0.0007134f_{31} - 0.0030494f_{32} + 0.0003615f_{33} = -0.001 \tag{4.1.28}$$

$$0.0007134f_{32} - 0.0030494f_{33} + 0.0003615f_{34} = -0.001 \tag{4.1.29}$$

$$0.0007134f_{33} - 0.0030494f_{34} = -0.001 \tag{4.1.30}$$

Equations (4.1.24) to (4.1.30) are solved by Mathematica which provides solutions of velocities as

Table 4.1.3: Velocities along the major axis when $\mathrm{Ha} = 10.0$

$\mathrm{f}_1 = 0.000$	$\mathrm{f}_2 = 0.384$	$\mathrm{f}_3 = 0.477$	$\mathrm{f}_4 = 0.499$	$\mathrm{f}_5 = 0.505$
$\mathrm{f}_6 = 0.506$	$\mathrm{f}_7 = 0.506$	$\mathrm{f}_8 = 0.506$	$\mathrm{f}_9 = 0.506$	$\mathrm{f}_{10} = 0.506$
$\mathrm{f}_{11} = 0.506$	$\mathrm{f}_{12} = 0.506$	$\mathrm{f}_{13} = 0.506$	$\mathrm{f}_{14} = 0.506$	$\mathrm{f}_{15} = 0.506$
$\mathrm{f}_{16} = 0.506$	$\mathrm{f}_{17} = 0.506$	$\mathrm{f}_{18} = 0.506$	$\mathrm{f}_{19} = 0.506$	$\mathrm{f}_{20} = 0.506$
$\mathrm{f}_{21} = 0.506$	$\mathrm{f}_{22} = 0.506$	$\mathrm{f}_{23} = 0.506$	$\mathrm{f}_{24} = 0.506$	$\mathrm{f}_{25} = 0.506$
$\mathrm{f}_{26} = 0.506$	$\mathrm{f}_{27} = 0.506$	$\mathrm{f}_{28} = 0.506$	$\mathrm{f}_{29} = 0.506$	$\mathrm{f}_{30} = 0.506$
$\mathrm{f}_{31} = 0.506$	$\mathrm{f}_{32} = 0.506$	$\mathrm{f}_{33} = 0.499$	$\mathrm{f}_{34} = 0.445$	$\mathrm{f}_{35} = 0.000$

Incorporating velocities in tables 4.1.1, 4.1.2 and 4.1.3 deliver the form in figure 4.1.1

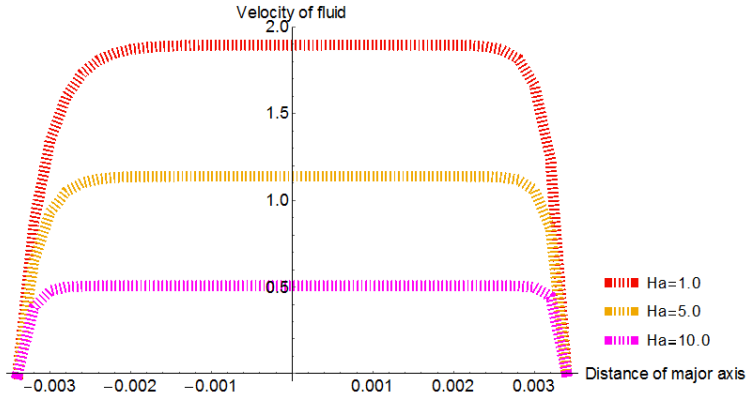

Figure 4.1.1: Combined velocity profiles for $\mathrm{Ha} = 1.0, \mathrm{Ha} = 5.0$ and $\mathrm{Ha} = 10.0$

Hartmann number, Ha, a dimensionless value, is the ratio of electromagnetic force to the viscous force, determines the velocity profile for the flow. As the value of Hartmann number is increased, velocity profile decreases. The effect of the magnetic field is more prominent at the point of core velocity, $\mathrm{V_c}$ i.e $\mathrm{V_c}$ decreases with increase in magnetic field. The presence of magnetic field in an electrically conducting fluid introduces Lorentz force which acts against the flow. This force slows down the fluid velocity as shown in figure 4.1.1 so that the velocity becomes almost constant through the pipe. Again the fluid is viscous so that is sticks on the walls of the pipe so that velocity distribution decreases from the centre of the pipe to the edges. Using different set ups, Gedik *et.al* [10], Nazibuddin and Dutta [27] and Kiema *et.al* [28] also found

that increase in Hartmann number leads to retardation of fluid velocity. Prasanna and Ganesh [17] investigation divulged that velocity profile was flat in the core region of the pipe, this is also the case as indicated in figure 4.1.1. One of the conclusions drawn by Gedik *et.al* [10] who examined a circular pipe was presented in graphical form shown in figure 4.1.2 where B was magnetic flux density while **R** was radius of circular pipe.

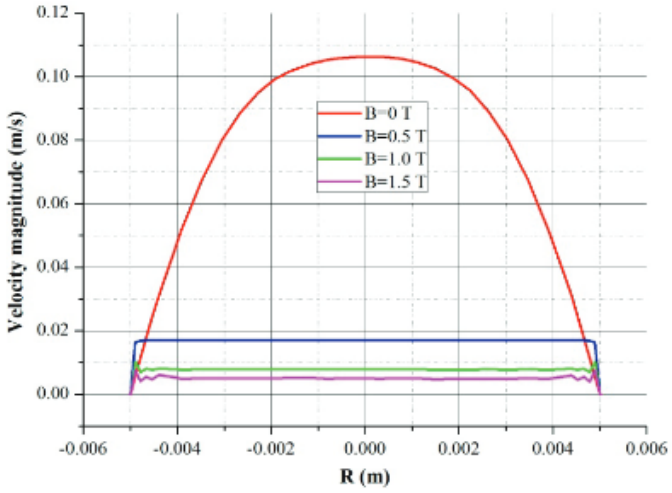

Figure 4.1.2: Velocity form along diameter of pipe when $\mathrm{B} = 0, \mathrm{B} = 0.5, \mathrm{B} = 1.0$ and $\mathrm{B} = 1.5$

The velocity profile for circular pipe figure 4.1.2 are almost similar to those found in this research for a pipe of elliptical cross section in figure 4.1.1. The only difference is that in figure 4.1.2, the shapes are parabolic while in figure 4.1.1 they are almost rectangular.

4.1.2 Altering gravitational force while preserving Hartmann number , distance of major axis, Reynolds number and length of elements

$$\text{(i)} \quad \mathbf{Ha = 1.0, Re = 0.5, J^e = 0.0001, \lambda_\theta = 0.00002, a = 0.0034}$$

The above stated values of Ha and $\mathrm{J^e}$ are put in equation (3.7.66). It produces form which is same as equation (4.1.1). Using equation (4.1.1), global stiffness matrix W, will be equal to equation (4.1.2). Considering 35 nodes in figure 3.7.2 and then substituting equation (4.1.2), Re and λ_θ in

equation (3.7.60), it changes to

$$\begin{bmatrix} -0.0012599 & 0.0006139 & 0 & 0 & \dots \\ 0.000955 & -0.0012599 & 0.0006139 & 0 & \dots \\ 0 & 0.000955 & -0.0012599 & 0.0006139 & \ddots \\ 0 & 0 & 0.000955 & -0.0012599 & \ddots \\ \vdots & \vdots & \ddots & \ddots & \ddots \end{bmatrix} \begin{bmatrix} f_2 \\ f_3 \\ f_4 \\ \vdots \\ f_{33} \\ f_{34} \end{bmatrix} = \begin{bmatrix} -0.00002 \\ -0.00002 \\ -0.00002 \\ \vdots \\ -0.00002 \\ -0.00002 \end{bmatrix} \tag{4.1.31}$$

The collection of equations formed from equation (4.1.31) are

$$-0.0012599f_2 + 0.0006139f_3 = -0.00002 \tag{4.1.32}$$

$$0.000955f_2 - 0.0012599f_3 + 0.0006139f_4 = -0.00002 \tag{4.1.33}$$

$$0.000955f_3 - 0.0012599f_4 + 0.0006139f_5 = -0.00002 \tag{4.1.34}$$

$$\vdots \tag{4.1.35}$$

$$0.000955f_{31} - 0.0012599f_{32} + 0.0006139f_{33} = -0.00002 \tag{4.1.36}$$

$$0.000955f_{32} - 0.0012599f_{33} + 0.0006139f_{34} = -0.00002 \tag{4.1.37}$$

$$0.000955f_{33} - 0.0012599f_{34} = -0.00002 \tag{4.1.38}$$

Mathematica is used to solve equations (4.1.32) to (4.1.38) and conveys solutions of f_j's as

Table 4.1.4: Velocities along the major axis for $\lambda_\theta = 0.00002$

$f_1 = 0.000$	$f_2 = 0.017$	$f_3 = 0.027$	$f_4 = 0.032$	$f_5 = 0.035$
$f_6 = 0.036$	$f_7 = 0.037$	$f_8 = 0.037$	$f_9 = 0.038$	$f_{10} = 0.038$
$f_{11} = 0.038$	$f_{12} = 0.038$	$f_{13} = 0.038$	$f_{14} = 0.038$	$f_{15} = 0.038$
$f_{16} = 0.038$	$f_{17} = 0.038$	$f_{18} = 0.038$	$f_{19} = 0.038$	$f_{20} = 0.038$
$f_{21} = 0.038$	$f_{22} = 0.038$	$f_{23} = 0.038$	$f_{24} = 0.038$	$f_{25} = 0.038$
$f_{26} = 0.038$	$f_{27} = 0.038$	$f_{28} = 0.038$	$f_{29} = 0.038$	$f_{30} = 0.038$
$f_{31} = 0.037$	$f_{32} = 0.036$	$f_{33} = 0.033$	$f_{34} = 0.025$	$f_{35} = 0.000$

(ii) $\mathbf{Ha = 1.0, Re = 0.5, J^e = 0.0001, \lambda_\theta = 0.00004, a = 0.0034}$

When the above stated values of Ha and $\mathrm{J^e}$ are put in equation (3.7.66), it will be the same as equation (4.1.1) since the specifications are equal. Effecting equation (4.1.1), global stiffness matrix W becomes the same as equation (4.1.2). Taking into account 35 nodes and then substituting equation (4.1.2), Re and λ_θ in equation (3.7.60), it grows into

$$\begin{bmatrix} -0.0012599 & 0.0006139 & 0 & 0 & \dots \\ 0.000955 & -0.0012599 & 0.0006139 & 0 & \dots \\ 0 & 0.000955 & -0.0012599 & 0.0006139 & \ddots \\ 0 & 0 & 0.000955 & -0.0012599 & \ddots \\ \vdots & \vdots & \ddots & \ddots & \ddots \end{bmatrix} \begin{bmatrix} f_2 \\ f_3 \\ f_4 \\ \vdots \\ f_{33} \\ f_{34} \end{bmatrix} = \begin{bmatrix} -0.00004 \\ -0.00004 \\ -0.00004 \\ \vdots \\ -0.00004 \\ -0.00004 \end{bmatrix} \tag{4.1.39}$$

The system of equations formed from equation (4.1.39) are

$$-0.0012599\mathrm{f}_2 + 0.0006139\mathrm{f}_3 = -0.00004 \tag{4.1.40}$$

$$0.000955\mathrm{f}_2 - 0.0012599\mathrm{f}_3 + 0.0006139\mathrm{f}_4 = -0.00004 \tag{4.1.41}$$

$$0.000955\mathrm{f}_3 - 0.0012599\mathrm{f}_4 + 0.0006139\mathrm{f}_5 = -0.00004 \tag{4.1.42}$$

$$\vdots \tag{4.1.43}$$

$$0.000955\mathrm{f}_{31} - 0.0012599\mathrm{f}_{32} + 0.0006139\mathrm{f}_{33} = -0.00004 \tag{4.1.44}$$

$$0.000955\mathrm{f}_{32} - 0.0012599\mathrm{f}_{33} + 0.0006139\mathrm{f}_{34} = -0.00004 \tag{4.1.45}$$

$$0.000955\mathrm{f}_{33} - 0.0012599\mathrm{f}_{34} = -0.00004 \tag{4.1.46}$$

Mathematica conveys values in table 4.1.5 when engaged to solve equations (4.1.40) to (4.1.46).

Table 4.1.5: Velocities along the major axis for $\lambda_\theta = 0.00004$

$\mathrm{f}_1 = 0.000$	$\mathrm{f}_2 = 0.034$	$\mathrm{f}_3 = 0.054$	$\mathrm{f}_4 = 0.064$	$\mathrm{f}_5 = 0.069$
$\mathrm{f}_6 = 0.072$	$\mathrm{f}_7 = 0.074$	$\mathrm{f}_8 = 0.075$	$\mathrm{f}_9 = 0.075$	$\mathrm{f}_{10} = 0.075$
$\mathrm{f}_{11} = 0.076$	$\mathrm{f}_{12} = 0.076$	$\mathrm{f}_{13} = 0.076$	$\mathrm{f}_{14} = 0.076$	$\mathrm{f}_{15} = 0.076$
$\mathrm{f}_{16} = 0.076$	$\mathrm{f}_{17} = 0.076$	$\mathrm{f}_{18} = 0.076$	$\mathrm{f}_{19} = 0.076$	$\mathrm{f}_{20} = 0.076$
$\mathrm{f}_{21} = 0.076$	$\mathrm{f}_{22} = 0.076$	$\mathrm{f}_{23} = 0.076$	$\mathrm{f}_{24} = 0.076$	$\mathrm{f}_{25} = 0.076$
$\mathrm{f}_{26} = 0.076$	$\mathrm{f}_{27} = 0.076$	$\mathrm{f}_{28} = 0.076$	$\mathrm{f}_{29} = 0.076$	$\mathrm{f}_{30} = 0.076$
$\mathrm{f}_{31} = 0.075$	$\mathrm{f}_{32} = 0.073$	$\mathrm{f}_{33} = 0.067$	$\mathrm{f}_{34} = 0.049$	$\mathrm{f}_{35} = 0.000$

(iii) $\mathbf{Ha = 1.0, Re = 0.5, J^e = 0.0001, \lambda_\theta = 0.00008, a = 0.0034}$

On placing the above stated values of Ha and J^{e} in equation (3.7.66), it will be the same as equation (4.1.1) since the criterion is the same. Utilizing equation (4.1.1), global stiffness matrix W develop into the same form as equation (4.1.2). Incorporating 35 nodes and then substituting

equation (4.1.2), Re, and λ_θ in equation (3.7.60), it turns out to

$$\begin{bmatrix} & & & & \\ -0.0012599 & 0.0006139 & 0 & 0 & \dots \\ 0.000955 & -0.0012599 & 0.0006139 & 0 & \dots \\ 0 & 0.000955 & -0.0012599 & 0.0006139 & \ddots \\ 0 & 0 & 0.000955 & -0.0012599 & \ddots \\ \vdots & \vdots & \ddots & \ddots & \ddots \end{bmatrix} \begin{bmatrix} \mathrm{f}_2 \\ \mathrm{f}_3 \\ \mathrm{f}_4 \\ \vdots \\ \mathrm{f}_{33} \\ \mathrm{f}_{34} \end{bmatrix} = \begin{bmatrix} -0.00008 \\ -0.00008 \\ -0.00008 \\ \vdots \\ -0.00008 \\ -0.00008 \end{bmatrix} \tag{4.1.47}$$

The set of equations formed from equation (4.1.47) are

$$-0.0012599\mathrm{f}_2 + 0.0006139\mathrm{f}_3 = -0.00008 \tag{4.1.48}$$

$$0.000955\mathrm{f}_2 - 0.0012599\mathrm{f}_3 + 0.0006139\mathrm{f}_4 = -0.00008 \tag{4.1.49}$$

$$0.000955\mathrm{f}_3 - 0.0012599\mathrm{f}_4 + 0.0006139\mathrm{f}_5 = -0.00008 \tag{4.1.50}$$

$$\vdots \tag{4.1.51}$$

$$0.000955\mathrm{f}_{31} - 0.0012599\mathrm{f}_{32} + 0.0006139\mathrm{f}_{33} = -0.00008 \tag{4.1.52}$$

$$0.000955\mathrm{f}_{32} - 0.0012599\mathrm{f}_{33} + 0.0006139\mathrm{f}_{34} = -0.00008 \tag{4.1.53}$$

$$0.000955\mathrm{f}_{33} - 0.0012599\mathrm{f}_{34} = -0.00008 \tag{4.1.54}$$

Mathematica is manipulated to solve equations (4.1.48) to (4.1.54) and dispenses solutions as

Table 4.1.6: Velocities along the major axis for $\lambda_\theta = 0.00008$

$f_1 = 0.000$	$f_2 = 0.069$	$f_3 = 0.107$	$f_4 = 0.128$	$f_5 = 0.139$
$f_6 = 0.145$	$f_7 = 0.148$	$f_8 = 0.150$	$f_9 = 0.150$	$f_{10} = 0.151$
$f_{11} = 0.151$	$f_{12} = 0.151$	$f_{13} = 0.151$	$f_{14} = 0.151$	$f_{15} = 0.151$
$f_{16} = 0.151$	$f_{17} = 0.151$	$f_{18} = 0.151$	$f_{19} = 0.151$	$f_{20} = 0.151$
$f_{21} = 0.151$	$f_{22} = 0.151$	$f_{23} = 0.151$	$f_{24} = 0.151$	$f_{25} = 0.151$
$f_{26} = 0.151$	$f_{27} = 0.151$	$f_{28} = 0.151$	$f_{29} = 0.151$	$f_{30} = 0.151$
$f_{31} = 0.149$	$f_{32} = 0.145$	$f_{33} = 0.133$	$f_{34} = 0.099$	$f_{35} = 0.000$

Putting together velocities in table 4.1.4, table 4.1.5 and table 4.1.6 gives

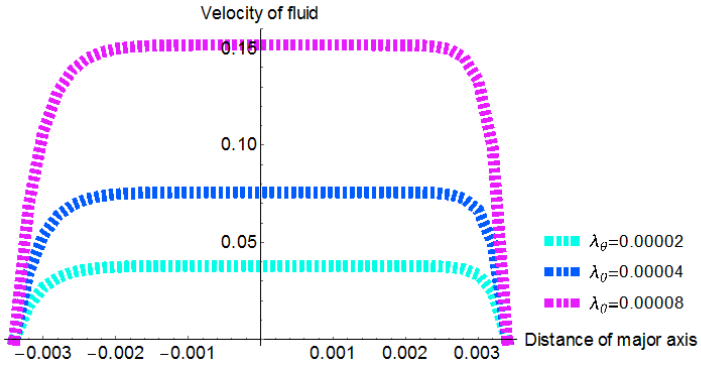

Figure 4.1.3: Merged velocity profiles for $\lambda_\theta = 0.00002, \lambda_\theta = 0.00004$ and $\lambda_\theta = 0.00008$

Increase in gravitational force leads to increase in fluid velocity at the centre of ellipse. The velocity decreases towards the edges of the pipe and is zero at the boundary so that the solution satisfies the no-slip boundary condition, figure 4.1.3. Increase in potential energy leads to increase in kinetic energy which increases velocity.

4.1.3 Modifying Reynolds number while keeping Hartmann number, gravitational force, distance of major axis and length of elements fixed

(i) $\mathbf{Ha = 1.0, Re = 2.0, J^e = 0.0001, \lambda_\theta = 0.0005, a = 0.0034}$

Once the above stated values of Ha and $\mathrm{J^e}$ are placed in equation (3.7.66), it produces form which

is same as equation (4.1.1). Employing equation (4.1.1), global stiffness matrix W be equal to equation (4.1.2). Taking into account 35 nodes in figure 3.7.2 and then substituting equation (4.1.2), Re and λ_θ in equation (3.7.60), it changes to

$$\begin{bmatrix} -0.0012599 & 0.0006139 & 0 & 0 & \dots \\ 0.000955 & -0.0012599 & 0.0006139 & 0 & \dots \\ 0 & 0.000955 & -0.0012599 & 0.0006139 & \ddots \\ 0 & 0 & 0.000955 & -0.0012599 & \ddots \\ \vdots & \vdots & \ddots & \ddots & \ddots \end{bmatrix} \begin{bmatrix} f_2 \\ f_3 \\ f_4 \\ \vdots \\ f_{33} \\ f_{34} \end{bmatrix} = \begin{bmatrix} -0.002 \\ -0.002 \\ -0.002 \\ \vdots \\ -0.002 \\ -0.002 \end{bmatrix} \tag{4.1.55}$$

The algebraic equations formed from equation (4.1.55) are

$$-0.0012599f_2 + 0.0006139f_3 = -0.002 \tag{4.1.56}$$

$$0.000955f_2 - 0.0012599f_3 + 0.0006139f_4 = -0.002 \tag{4.1.57}$$

$$0.000955f_3 - 0.0012599f_4 + 0.0006139f_5 = -0.002 \tag{4.1.58}$$

$$\vdots \tag{4.1.59}$$

$$0.000955f_{31} - 0.0012599f_{32} + 0.0006139f_{33} = -0.002 \tag{4.1.60}$$

$$0.000955f_{32} - 0.0012599f_{33} + 0.0006139f_{34} = -0.002 \tag{4.1.61}$$

$$0.000955f_{33} - 0.0012599f_{34} = -0.002 \tag{4.1.62}$$

Mathematica is used to solve the set of equations (4.1.56) to (4.1.62) and conveys solutions of f_j's as

Table 4.1.7: Velocities along the major axis with $\mathrm{Re} = 2.0$

$\mathrm{f}_1 = 0.000$	$\mathrm{f}_2 = 1.738$	$\mathrm{f}_3 = 2.679$	$\mathrm{f}_4 = 3.188$	$\mathrm{f}_5 = 3.464$
$\mathrm{f}_6 = 3.613$	$\mathrm{f}_7 = 3.694$	$\mathrm{f}_8 = 3.738$	$\mathrm{f}_9 = 3.761$	$\mathrm{f}_{10} = 3.774$
$\mathrm{f}_{11} = 3.781$	$\mathrm{f}_{12} = 3.785$	$\mathrm{f}_{13} = 3.787$	$\mathrm{f}_{14} = 3.788$	$\mathrm{f}_{15} = 3.789$
$\mathrm{f}_{16} = 3.789$	$\mathrm{f}_{17} = 3.789$	$\mathrm{f}_{18} = 3.789$	$\mathrm{f}_{19} = 3.789$	$\mathrm{f}_{20} = 3.789$
$\mathrm{f}_{21} = 3.789$	$\mathrm{f}_{22} = 3.789$	$\mathrm{f}_{23} = 3.789$	$\mathrm{f}_{24} = 3.789$	$\mathrm{f}_{25} = 3.789$
$\mathrm{f}_{26} = 3.789$	$\mathrm{f}_{27} = 3.789$	$\mathrm{f}_{28} = 3.787$	$\mathrm{f}_{29} = 3.783$	$\mathrm{f}_{30} = 3.770$
$\mathrm{f}_{31} = 3.733$	$\mathrm{f}_{32} = 3.630$	$\mathrm{f}_{33} = 3.331$	$\mathrm{f}_{34} = 2.471$	$\mathrm{f}_{35} = 0.000$

(ii) $\mathbf{Ha = 1.0, Re = 4.0, J^e = 0.0001, \lambda_\theta = 0.0005, a = 0.0034}$

On setting the above stated values of Ha and J^{e} in equation (3.7.66), it will be the same as equation (4.1.1) since the restrictions are equal. Utilizing equation (4.1.1), global stiffness matrix W becomes the same as equation (4.1.2). On considering 35 nodes and then substituting equation (4.1.2), Re and λ_θ in equation (3.7.60), it delivers

$$\begin{bmatrix} & & & & \\ -0.0012599 & 0.0006139 & 0 & 0 & \dots \\ 0.000955 & -0.0012599 & 0.0006139 & 0 & \dots \\ 0 & 0.000955 & -0.0012599 & 0.0006139 & \ddots \\ 0 & 0 & 0.000955 & -0.0012599 & \ddots \\ \vdots & \vdots & \ddots & \ddots & \ddots \end{bmatrix} \begin{bmatrix} \mathrm{f}_2 \\ \mathrm{f}_3 \\ \mathrm{f}_4 \\ \vdots \\ \mathrm{f}_{33} \\ \mathrm{f}_{34} \end{bmatrix} = \begin{bmatrix} -0.004 \\ -0.004 \\ -0.004 \\ \vdots \\ -0.004 \\ -0.004 \end{bmatrix} \tag{4.1.63}$$

The collection of equations formed from equation (4.1.63) are

$$-0.0012599\mathrm{f}_2 + 0.0006139\mathrm{f}_3 = -0.004 \tag{4.1.64}$$

$$0.000955\mathrm{f}_2 - 0.0012599\mathrm{f}_3 + 0.0006139\mathrm{f}_4 = -0.004 \tag{4.1.65}$$

$$0.000955\mathrm{f}_3 - 0.0012599\mathrm{f}_4 + 0.0006139\mathrm{f}_5 = -0.004 \tag{4.1.66}$$

$$\vdots \tag{4.1.67}$$

$$0.000955\mathrm{f}_{31} - 0.0012599\mathrm{f}_{32} + 0.0006139\mathrm{f}_{33} = -0.004 \tag{4.1.68}$$

$$0.000955\mathrm{f}_{32} - 0.0012599\mathrm{f}_{33} + 0.0006139\mathrm{f}_{34} = -0.004 \tag{4.1.69}$$

$$0.000955\mathrm{f}_{33} - 0.0012599\mathrm{f}_{34} = -0.004 \tag{4.1.70}$$

Mathematica provides values in table 4.1.8 when employed to solve equations (4.1.64) to (4.1.70).

Table 4.1.8: Velocities along the major axis with $\mathrm{Re} = 4.0$

$\mathrm{f}_1 = 0.000$	$\mathrm{f}_2 = 3.477$	$\mathrm{f}_3 = 5.358$	$\mathrm{f}_4 = 6.377$	$\mathrm{f}_5 = 6.928$
$\mathrm{f}_6 = 7.227$	$\mathrm{f}_7 = 7.388$	$\mathrm{f}_8 = 7.476$	$\mathrm{f}_9 = 7.523$	$\mathrm{f}_{10} = 7.548$
$\mathrm{f}_{11} = 7.562$	$\mathrm{f}_{12} = 7.570$	$\mathrm{f}_{13} = 7.574$	$\mathrm{f}_{14} = 7.576$	$\mathrm{f}_{15} = 7.577$
$\mathrm{f}_{16} = 7.578$	$\mathrm{f}_{17} = 7.578$	$\mathrm{f}_{18} = 7.578$	$\mathrm{f}_{19} = 7.579$	$\mathrm{f}_{20} = 7.579$
$\mathrm{f}_{21} = 7.579$	$\mathrm{f}_{22} = 7.579$	$\mathrm{f}_{23} = 7.579$	$\mathrm{f}_{24} = 7.579$	$\mathrm{f}_{25} = 7.578$
$\mathrm{f}_{26} = 7.578$	$\mathrm{f}_{27} = 7.577$	$\mathrm{f}_{28} = 7.574$	$\mathrm{f}_{29} = 7.565$	$\mathrm{f}_{30} = 7.540$
$\mathrm{f}_{31} = 7.468$	$\mathrm{f}_{32} = 7.259$	$\mathrm{f}_{33} = 6.661$	$\mathrm{f}_{34} = 4.942$	$\mathrm{f}_{35} = 0.000$

(iii) $\mathbf{Ha = 1.0, Re = 8.0, J^e = 0.0001, \lambda_\theta = 0.0005, a = 0.0034}$

When the aforementioned values of Ha and J^{e} are set in equation (3.7.66), it will be the same as equation (4.1.1) since the constants are the same. Effecting equation (4.1.1), global stiffness matrix W transforms into the same form as equation (4.1.2). Incorporating 35 nodes and then

substituting equation (4.1.2), Re, and λ_θ in equation (3.7.60), it turns to

$$\begin{bmatrix} -0.0012599 & 0.0006139 & 0 & 0 & \dots \\ 0.000955 & -0.0012599 & 0.0006139 & 0 & \dots \\ 0 & 0.000955 & -0.0012599 & 0.0006139 & \ddots \\ 0 & 0 & 0.000955 & -0.0012599 & \ddots \\ \vdots & \vdots & \ddots & \ddots & \ddots \end{bmatrix} \begin{bmatrix} \mathrm{f}_2 \\ \mathrm{f}_3 \\ \mathrm{f}_4 \\ \vdots \\ \mathrm{f}_{33} \\ \mathrm{f}_{34} \end{bmatrix} = \begin{bmatrix} -0.008 \\ -0.008 \\ -0.008 \\ \vdots \\ -0.008 \\ -0.008 \end{bmatrix} \tag{4.1.71}$$

The set of equations formed from equation (4.1.71) are

$$-0.0012599\mathrm{f}_2 + 0.0006139\mathrm{f}_3 = -0.008 \tag{4.1.72}$$

$$0.000955\mathrm{f}_2 - 0.0012599\mathrm{f}_3 + 0.0006139\mathrm{f}_4 = -0.008 \tag{4.1.73}$$

$$0.000955\mathrm{f}_3 - 0.0012599\mathrm{f}_4 + 0.0006139\mathrm{f}_5 = -0.008 \tag{4.1.74}$$

$$\vdots \tag{4.1.75}$$

$$0.000955\mathrm{f}_{31} - 0.0012599\mathrm{f}_{32} + 0.0006139\mathrm{f}_{33} = -0.008 \tag{4.1.76}$$

$$0.000955\mathrm{f}_{32} - 0.0012599\mathrm{f}_{33} + 0.0006139\mathrm{f}_{34} = -0.008 \tag{4.1.77}$$

$$0.000955\mathrm{f}_{33} - 0.0012599\mathrm{f}_{34} = -0.008 \tag{4.1.78}$$

Mathematica is used to solve equations (4.1.72) to (4.1.78) and hands out solutions as

Table 4.1.9: Velocities along the major axis with $\mathrm{Re} = 8.0$

$f_1 = 0.000$	$f_2 = 6.953$	$f_3 = 10.717$	$f_4 = 12.754$	$f_5 = 13.856$
$f_6 = 14.453$	$f_7 = 14.776$	$f_8 = 14.951$	$f_9 = 15.056$	$f_{10} = 15.097$
$f_{11} = 15.125$	$f_{12} = 15.140$	$f_{13} = 15.148$	$f_{14} = 15.152$	$f_{15} = 15.154$
$f_{16} = 15.156$	$f_{17} = 15.156$	$f_{18} = 15.157$	$f_{19} = 15.157$	$f_{20} = 15.157$
$f_{21} = 15.157$	$f_{22} = 15.157$	$f_{23} = 15.157$	$f_{24} = 15.157$	$f_{25} = 15.157$
$f_{26} = 15.156$	$f_{27} = 15.154$	$f_{28} = 15.148$	$f_{29} = 15.130$	$f_{30} = 15.080$
$f_{31} = 14.935$	$f_{32} = 14.519$	$f_{33} = 13.322$	$f_{34} = 9.884$	$f_{35} = 0.000$

Bringing together velocities in table 4.1.7, table 4.1.8 and table 4.1.9 produces the figuration in figure 4.1.4.

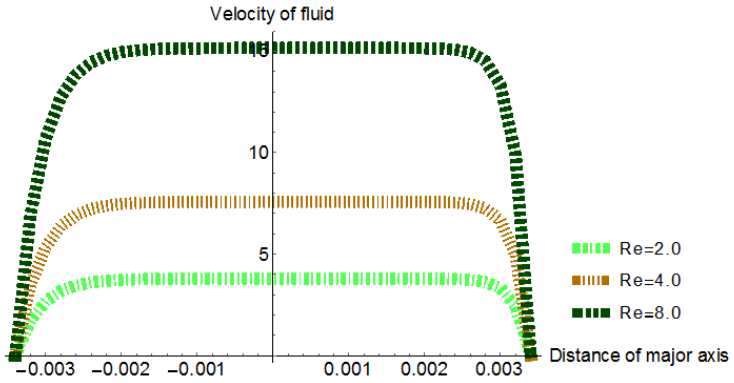

Figure 4.1.4: Linked velocity contours for $\mathrm{Re} = 2.0, \mathrm{Re} = 4.0$ and $\mathrm{Re} = 8.0$

Reynolds number, Re, the ratio of inertial forces to viscous forces within a fluid, is also dimensionless quantity. It is used to predict transition from laminar to turbulent flow. Laminar flow occur at low Reynolds numbers where viscous forces are dominant and is characterized by smooth fluid motion ($\mathrm{Re} \leq 2300$). Turbulent flow occur at high Reynolds number ($\mathrm{Re} \geq 2900$) and is dominated by inertial forces which produce chaotic eddies. From figure 4.1.4 when Re is increased, velocity increases at the centre of pipe and then decreases towards the edges of the pipe. This because the inertial forces overshadow viscous forces. Usman *et.al* [16], embracing a different set up reported that increase in Reynolds number results in increase in fluid temperature. In this study, increase in Reynolds number increases velocity which in turn increases temperature.

Even with low values of Reynolds number such as 2.0 , some level of turbulence sets in. Major axis of pipe of elliptical cross section has its centre of symmetry at the origin. It is therefore expected that velocities $f_2 = f_{34}$, $f_7 = f_{29}$ etc. However, from table 4.1.10 (numerals extracted from tables 4.1.7, 4.1.8 and 4.1.9) this is not the case. When Reynolds number is increased from 4.0 to 8.0, absolute difference increases by 100%. This is evidence that turbulence is setting in. Fluid flow is gradually changing from laminar flow to turbulent flow.

Table 4.1.10: Absolute differences for f_7 and f_{29} when $Re = 2.0, 4.0, 8.0$

Re	f_7	f_{29}	$\lvert f_7 - f_{29} \rvert$
2.0	3.694	3.783	0.0089
4.0	7.388	7.565	0.177
8.0	14.776	15.130	0.354

4.1.4 Changing distance of major axis while maintaining Hartmann number, gravitational force, Reynolds number and length of elements fixed

Varying length of major axis of the pipe entails increasing the number of nodal points while keeping the element length constant. Consideration will be done for 21, 29 and 33 nodes so that $a = 0.0020, a = 0.0028$ and $a = 0.0032$ respectively. When half major axis $a = 0.002$ and half minor axis $b = 0.002$, circular cross section forms. When $a = 0.0028, 0.0032$, while half minor axis remains constant, $b = 0.002$, as shown in figure 4.1.5, elliptical cross sections are formed.

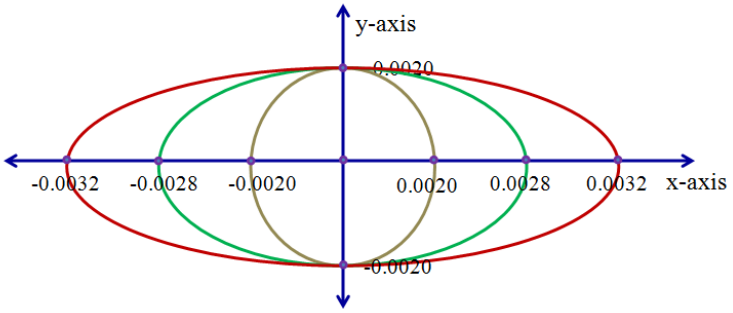

Figure 4.1.5: Change of cross section area of pipe from circular to elliptical.

Aspect ratio, $\alpha = \frac{a}{b}$, increases i.e $1 \leq \alpha \leq 1.6$.

$$(\mathbf{I}) \quad \mathbf{Ha = 1.0, Re = 0.5, J^e = 0.0001}, \lambda_\theta = \mathbf{0.025, a = 0.002}$$

When the above mentioned values of Ha and $\mathrm{J^e}$ are placed in equation (3.7.66), it produces form which is same as equation (4.1.1). Using equation (4.1.1), global stiffness matrix W be equal to equation (4.1.2). Taking into account 21 nodes in figure 3.7.2 and then substituting equation (4.1.2), Re and λ_θ in equation (3.7.60), it becomes

$$\begin{bmatrix} & & & & \\ -0.0012599 & 0.0006139 & 0 & 0 & \dots \\ 0.000955 & -0.0012599 & 0.0006139 & 0 & \dots \\ 0 & 0.000955 & -0.0012599 & 0.0006139 & \ddots \\ 0 & 0 & 0.000955 & -0.0012599 & \ddots \\ \vdots & \vdots & \ddots & \ddots & \ddots \end{bmatrix} \begin{bmatrix} \mathrm{f}_2 \\ \mathrm{f}_3 \\ \mathrm{f}_4 \\ \vdots \\ \mathrm{f}_{19} \\ \mathrm{f}_{20} \end{bmatrix} = \begin{bmatrix} -0.025 \\ -0.025 \\ -0.025 \\ \vdots \\ -0.025 \\ -0.025 \end{bmatrix} \tag{4.1.79}$$

The group of equations formed from equation (4.1.79) are

$$-0.0012599\mathrm{f}_2 + 0.0006139\mathrm{f}_3 = -0.025 \tag{4.1.80}$$

$$0.000955\mathrm{f}_2 - 0.0012599\mathrm{f}_3 + 0.0006139\mathrm{f}_4 = -0.025 \tag{4.1.81}$$

$$0.000955\mathrm{f}_3 - 0.0012599\mathrm{f}_4 + 0.0006139\mathrm{f}_5 = -0.025 \tag{4.1.82}$$

$$\vdots \tag{4.1.83}$$

$$0.000955\mathrm{f}_{17} - 0.0012599\mathrm{f}_{18} + 0.0006139\mathrm{f}_{19} = -0.025 \tag{4.1.84}$$

$$0.000955\mathrm{f}_{18} - 0.0012599\mathrm{f}_{19} + 0.0006139\mathrm{f}_{20} = -0.025 \tag{4.1.85}$$

$$0.000955\mathrm{f}_{19} - 0.0012599\mathrm{f}_{20} = -0.025 \tag{4.1.86}$$

Applying Mathematica to solve algebraic equations (4.1.80) to (4.1.86) conveys solutions of $\mathrm{f_j}$'s as

Table 4.1.11: Velocities along the major axis when $\mathrm{a} = 0.002$

$\mathrm{f}_1 = 0.000$	$\mathrm{f}_2 = 21.729$	$\mathrm{f}_3 = 33.490$	$\mathrm{f}_4 = 39.856$	$\mathrm{f}_5 = 43.301$
$\mathrm{f}_6 = 45.166$	$\mathrm{f}_7 = 46.176$	$\mathrm{f}_8 = 46.722$	$\mathrm{f}_9 = 47.017$	$\mathrm{f}_{10} = 47.177$
$\mathrm{f}_{11} = 47.263$	$\mathrm{f}_{12} = 47.308$	$\mathrm{f}_{13} = 47.326$	$\mathrm{f}_{14} = 47.321$	$\mathrm{f}_{15} = 47.274$
$\mathrm{f}_{16} = 47.120$	$\mathrm{f}_{17} = 46.670$	$\mathrm{f}_{18} = 45.370$	$\mathrm{f}_{19} = 41.632$	$\mathrm{f}_{20} = 30.886$
$\mathrm{f}_{21} = 0.000$	–	–	–	–

$$(\mathbf{II}) \quad \mathbf{Ha = 1.0, Re = 0.5, J^e = 0.0001}, \lambda_\theta = \mathbf{0.025, a = 0.0028}$$

On putting the above stated values of Ha and $\mathrm{J^e}$ in equation (3.7.66), it will be the same as equation (4.1.1) since the criterion is the same. Using equation (4.1.1), global stiffness matrix W becomes the same as equation (4.1.2). Considering 29 nodes and then substituting equation

(4.1.2), Re and λ_θ in equation (3.7.60), it converts to

$$\begin{bmatrix} -0.0012599 & 0.0006139 & 0 & 0 & \dots \\ 0.000955 & -0.0012599 & 0.0006139 & 0 & \dots \\ 0 & 0.000955 & -0.0012599 & 0.0006139 & \ddots \\ 0 & 0 & 0.000955 & -0.0012599 & \ddots \\ \vdots & \vdots & \ddots & \ddots & \ddots \end{bmatrix} \begin{bmatrix} \mathrm{f}_2 \\ \mathrm{f}_3 \\ \mathrm{f}_4 \\ \vdots \\ \mathrm{f}_{27} \\ \mathrm{f}_{28} \end{bmatrix} = \begin{bmatrix} -0.025 \\ -0.025 \\ -0.025 \\ \vdots \\ -0.025 \\ -0.025 \end{bmatrix} \tag{4.1.87}$$

The system of equations formed from equation (4.1.87) are

$$-0.0012599\mathrm{f}_2 + 0.0006139\mathrm{f}_3 = -0.025 \tag{4.1.88}$$

$$0.000955\mathrm{f}_2 - 0.0012599\mathrm{f}_3 + 0.0006139\mathrm{f}_4 = -0.025 \tag{4.1.89}$$

$$0.000955\mathrm{f}_3 - 0.0012599\mathrm{f}_4 + 0.0006139\mathrm{f}_5 = -0.025 \tag{4.1.90}$$

$$\vdots \tag{4.1.91}$$

$$0.000955\mathrm{f}_{25} - 0.0012599\mathrm{f}_{26} + 0.0006139\mathrm{f}_{27} = -0.025 \tag{4.1.92}$$

$$0.000955\mathrm{f}_{26} - 0.0012599\mathrm{f}_{27} + 0.0006139\mathrm{f}_{28} = -0.025 \tag{4.1.93}$$

$$0.000955\mathrm{f}_{27} - 0.0012599\mathrm{f}_{28} = -0.025 \tag{4.1.94}$$

When Mathematica is manipulated to solve the group of equations (4.1.88) to (4.1.94), it delivers solutions of velocities as

Table 4.1.12: Velocities along the major axis when $\mathrm{a} = 0.0028$

$\mathrm{f}_1 = 0.000$	$\mathrm{f}_2 = 21.729$	$\mathrm{f}_3 = 33.490$	$\mathrm{f}_4 = 39.856$	$\mathrm{f}_5 = 43.301$
$\mathrm{f}_6 = 45.166$	$\mathrm{f}_7 = 46.176$	$\mathrm{f}_8 = 46.722$	$\mathrm{f}_9 = 47.018$	$\mathrm{f}_{10} = 47.178$
$\mathrm{f}_{11} = 47.264$	$\mathrm{f}_{12} = 47.311$	$\mathrm{f}_{13} = 47.337$	$\mathrm{f}_{14} = 47.350$	$\mathrm{f}_{15} = 47.358$
$\mathrm{f}_{16} = 47.362$	$\mathrm{f}_{17} = 47.364$	$\mathrm{f}_{18} = 47.365$	$\mathrm{f}_{19} = 47.364$	$\mathrm{f}_{20} = 47.362$
$\mathrm{f}_{21} = 47.356$	$\mathrm{f}_{22} = 47.337$	$\mathrm{f}_{23} = 47.282$	$\mathrm{f}_{24} = 47.125$	$\mathrm{f}_{25} = 46.672$
$\mathrm{f}_{26} = 45.371$	$\mathrm{f}_{27} = 41.632$	$\mathrm{f}_{28} = 30.886$	$\mathrm{f}_{29} = 0.000$	–

(III) $\mathbf{Ha = 1.0, Re = 0.5, J^e = 0.0001, \lambda_\theta = 0.025, a = 0.0032}$

On assigning the above mentioned values of Ha and J^{e} in equation (3.7.66), it will be the same as equation (4.1.1) since the parameters are the same. Effecting equation (4.1.1), global stiffness matrix W transforms into the same form as equation (4.1.2). Incorporating 33 nodes and then substituting equation (4.1.2), Re, and λ_θ in equation (3.7.60), it produces

$$\begin{bmatrix} -0.0012599 & 0.0006139 & 0 & 0 & \dots \\ 0.000955 & -0.0012599 & 0.0006139 & 0 & \dots \\ 0 & 0.000955 & -0.0012599 & 0.0006139 & \ddots \\ 0 & 0 & 0.000955 & -0.0012599 & \ddots \\ \vdots & \vdots & \ddots & \ddots & \ddots \end{bmatrix} \begin{bmatrix} \mathrm{f}_2 \\ \mathrm{f}_3 \\ \mathrm{f}_4 \\ \vdots \\ \mathrm{f}_{31} \\ \mathrm{f}_{32} \end{bmatrix} = \begin{bmatrix} -0.025 \\ -0.025 \\ -0.025 \\ \vdots \\ -0.025 \\ -0.025 \end{bmatrix} \tag{4.1.95}$$

The set of equations formed from equation (4.1.95) are

$$-0.0012599\mathrm{f}_2 + 0.0006139\mathrm{f}_3 = -0.025 \tag{4.1.96}$$

$$0.000955\mathrm{f}_2 - 0.0012599\mathrm{f}_3 + 0.0006139\mathrm{f}_4 = -0.025 \tag{4.1.97}$$

$$0.000955\mathrm{f}_3 - 0.0012599\mathrm{f}_4 + 0.0006139\mathrm{f}_5 = -0.025 \tag{4.1.98}$$

$$\vdots \tag{4.1.99}$$

$$0.000955\mathrm{f}_{29} - 0.0012599\mathrm{f}_{30} + 0.0006139\mathrm{f}_{31} = -0.025 \tag{4.1.100}$$

$$0.000955\mathrm{f}_{30} - 0.0012599\mathrm{f}_{31} + 0.0006139\mathrm{f}_{32} = -0.025 \tag{4.1.101}$$

$$0.000955\mathrm{f}_{31} - 0.0012599\mathrm{f}_{32} = -0.025 \tag{4.1.102}$$

On engaging Mathematica to solve algebraic equations (4.1.96) to (4.1.102), it provides solutions of velocities as

Table 4.1.13: Velocities along the major axis when $\mathrm{a} = 0.0032$

$\mathrm{f}_1 = 0.000$	$\mathrm{f}_2 = 21.729$	$\mathrm{f}_3 = 33.490$	$\mathrm{f}_4 = 39.856$	$\mathrm{f}_5 = 43.301$
$\mathrm{f}_6 = 45.166$	$\mathrm{f}_7 = 46.176$	$\mathrm{f}_8 = 46.722$	$\mathrm{f}_9 = 47.018$	$\mathrm{f}_{10} = 47.178$
$\mathrm{f}_{11} = 47.264$	$\mathrm{f}_{12} = 47.311$	$\mathrm{f}_{13} = 47.337$	$\mathrm{f}_{14} = 47.350$	$\mathrm{f}_{15} = 47.358$
$\mathrm{f}_{16} = 47.362$	$\mathrm{f}_{17} = 47.364$	$\mathrm{f}_{18} = 47.365$	$\mathrm{f}_{19} = 47.366$	$\mathrm{f}_{20} = 47.366$
$\mathrm{f}_{21} = 47.366$	$\mathrm{f}_{22} = 47.366$	$\mathrm{f}_{23} = 47.365$	$\mathrm{f}_{24} = 47.363$	$\mathrm{f}_{25} = 47.356$
$\mathrm{f}_{26} = 47.337$	$\mathrm{f}_{27} = 47.282$	$\mathrm{f}_{28} = 47.125$	$\mathrm{f}_{29} = 46.672$	$\mathrm{f}_{30} = 45.371$
$\mathrm{f}_{31} = 41.632$	$\mathrm{f}_{32} = 30.886$	$\mathrm{f}_{33} = 0.000$	–	–

Constructing together velocities in table 4.1.11, table 4.1.12 and table 4.1.13 delivers the sketch in figure 4.1.6.

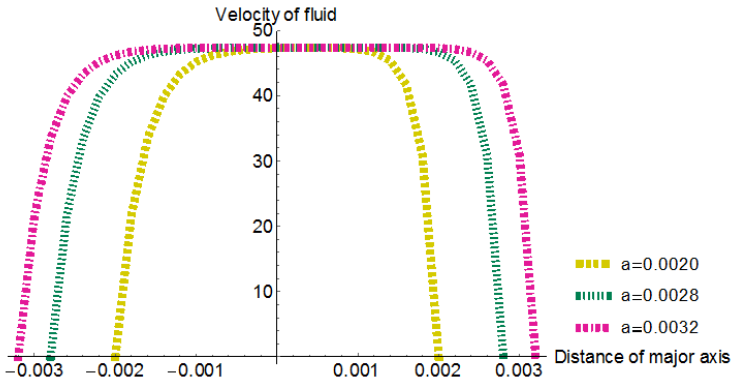

Figure 4.1.6: Combined velocity forms for $\mathrm{a} = 0.0020, \mathrm{a} = 0.0028$ and $\mathrm{a} = 0.0032$

On increasing the distance of the major axis (increasing aspect ratio), the velocity of the fluid at the origin of the pipe also increases marginally. The velocity almost become constant with most of fluid particles acquiring velocity close to that of the core, $\mathrm{V_c}$. The velocity again decreases from the centre of the pipe towards the boundary where it is zero, figure 4.1.6. As the magnetic field strength is kept constant, it means that Lorentz force acting on each conducting particle reduces leading to increase in velocity. When aspect ratio is increased, cross section of pipe changes from circular to elliptical. The velocity profiles as shown in figure 4.1.6 changes from parabolic to almost rectangular shape. This shows that there is more torque at the curved surface of the elliptical pipe, Moffatt [8], than the circular pipe. It is this torque which makes fluid velocity to rise faster from the edges towards the centre in the elliptical pipe than circular pipe.

4.2 Results and discussion for temperature distribution

The values of h for the first and last nodes of the discretized length of major axis are known and are $\mathrm{h_1} = \mathrm{h_N} = 0.000$. This criterion will be implied in this sector. In working out results for different values of dimensionless quantities Pr, Ha and Ec, fluid velocity is maximum at the centre of pipe, core velocity

($\mathrm{V_c}$), as found in subsection 4.1. Fluid velocity then decreases from the centre of pipe towards the edges as shown in table 4.1.1. Values in table 4.1.1 will be adopted in finding $\mathrm{h_i}$'s in subsections 4.2.1, 4.2.2 and 4.2.3. In this particular table, $\mathrm{V_c} = 1.895$.

4.2.1 Changing Prandtl number while keeping Hartmann number, Eckert number, velocity of fluid, distance of major axis and length of elements constant

(a) $\mathbf{Ha = 1.0, J^e = 0.0001, Pr = 0.5, a = 0.0034, Ec = 1.0, V_c = 1.895}$

When the above stated values of Pr and $\mathrm{J^e}$ are put in equation (3.7.73), it becomes

$$\mathrm{I^e} = \begin{bmatrix} 9.017 & -9.017 \\ -9.017 & 9.017 \end{bmatrix} \tag{4.2.1}$$

Using equation (4.2.1), global stiffness matrix I becomes

$$\mathrm{I} = \begin{bmatrix} 9.017 & -9.017 & 0 & 0 & 0 & 0 \\ -9.017 & 18.034 & -9.017 & 0 & 0 & 0 \\ 0 & -9.017 & 18.034 & -9.017 & 0 & 0 \\ 0 & 0 & -9.017 & 18.034 & -9.017 & 0 \\ 0 & 0 & 0 & -9.017 & 18.034 & -9.017 \\ 0 & 0 & 0 & 0 & -9.017 & 18.034 \end{bmatrix} \tag{4.2.2}$$

Considering 35 nodes in figure 3.7.2, substituting parameters $\mathrm{Ha}, \mathrm{Ec}, \mathrm{f_i}$ (table 4.1.1) and equation (4.2.2) in equation (3.7.61) results in

$$\begin{bmatrix} 18.034 & -9.017 & 0 & 0 & \dots \\ -9.017 & 18.034 & -9.017 & 0 & \dots \\ 0 & -9.017 & 18.034 & -9.017 & \ddots \\ 0 & 0 & -9.017 & 18.034 & \ddots \\ \vdots & \vdots & \ddots & \ddots & \ddots \end{bmatrix} \begin{bmatrix} h_2 \\ h_3 \\ h_4 \\ \vdots \\ h_{33} \\ h_{34} \end{bmatrix} = \begin{bmatrix} 18.035 \\ 18.037 \\ 18.039 \\ \vdots \\ 18.039 \\ 18.037 \end{bmatrix} \tag{4.2.3}$$

The system of equations formed from equation (4.2.3) are

$$18.034h_2 - 9.01h_3 = 18.035 \tag{4.2.4}$$

$$-9.01h_2 + 18.034h_3 - 9.01h_4 = 18.037 \tag{4.2.5}$$

$$-9.01h_3 + 18.034h_4 - 9.01h_5 = 18.039 \tag{4.2.6}$$

$$\vdots \tag{4.2.7}$$

$$-9.01h_{31} + 18.034h_{32} - 9.01h_{33} = 18.040 \tag{4.2.8}$$

$$-9.01h_{32} + 18.034h_{33} - 9.01h_{34} = 18.039 \tag{4.2.9}$$

$$-9.01h_{33} + 18.034h_{34} = 18.037 \tag{4.2.10}$$

Mathematica is used to solve the system of equations (4.2.4) to (4.1.10) and give solutions of h_j's as

Table 4.2.1: Temperatures along the major axis for $\mathrm{Pr} = 0.5$

$\mathrm{h}_1 = 0.000$	$\mathrm{h}_2 = 33.010$	$\mathrm{h}_3 = 64.020$	$\mathrm{h}_4 = 93.029$	$\mathrm{h}_5 = 120.039$
$\mathrm{h}_6 = 145.046$	$\mathrm{h}_7 = 168.054$	$\mathrm{h}_8 = 189.061$	$\mathrm{h}_9 = 208.068$	$\mathrm{h}_{10} = 225.073$
$\mathrm{h}_{11} = 240.078$	$\mathrm{h}_{12} = 253.083$	$\mathrm{h}_{13} = 264.068$	$\mathrm{h}_{14} = 273.089$	$\mathrm{h}_{15} = 280.092$
$\mathrm{h}_{16} = 285.093$	$\mathrm{h}_{17} = 288.095$	$\mathrm{h}_{18} = 289.095$	$\mathrm{h}_{19} = 288.095$	$\mathrm{h}_{20} = 285.094$
$\mathrm{h}_{21} = 280.092$	$\mathrm{h}_{22} = 273.090$	$\mathrm{h}_{23} = 264.087$	$\mathrm{h}_{24} = 253.083$	$\mathrm{h}_{25} = 240.079$
$\mathrm{h}_{26} = 225.074$	$\mathrm{h}_{27} = 208.068$	$\mathrm{h}_{28} = 189.062$	$\mathrm{h}_{29} = 168.055$	$\mathrm{h}_{30} = 145.047$
$\mathrm{h}_{31} = 120.039$	$\mathrm{h}_{32} = 93.030$	$\mathrm{h}_{33} = 64.021$	$\mathrm{h}_{34} = 33.011$	$\mathrm{h}_{35} = 0.000$

The $\mathrm{h_j}$'s are solutions of function h derived from the temperature function which relates temperatures of fluid in the r–component and θ–components. $\mathrm{h_j}$'s will therefore be the temperatures of fluid on the major axis of cross section of elliptical pipe when plotted against the nodes which are actually points on the major axis of the pipe.

$$(\mathbf{b}) \quad \mathbf{Ha = 1.0, J^e = 0.0001, Pr = 1.0, a = 0.0034, Ec = 1.0, V_c = 1.895}$$

Setting the above mentioned values of Pr and $\mathrm{J^e}$ in equation (3.7.73), leads to

$$\mathrm{I^e} = \begin{bmatrix} 4.509 & -4.509 \\ -4.509 & 4.509 \end{bmatrix} \tag{4.2.11}$$

Employing equation (4.2.11), global stiffness matrix I turns out to

$$\mathrm{I} = \begin{bmatrix} 4.509 & -4.509 & 0 & 0 & 0 & 0 \\ -4.509 & 9.018 & -4.509 & 0 & 0 & 0 \\ 0 & -4.509 & 9.018 & -4.509 & 0 & 0 \\ 0 & 0 & -4.509 & 9.018 & -4.509 & 0 \\ 0 & 0 & 0 & -4.509 & 9.018 & -4.509 \\ 0 & 0 & 0 & 0 & -4.509 & 9.018 \end{bmatrix} \tag{4.2.12}$$

Taking into account 35 nodes in figure 3.7.2, substituting values $\mathrm{Ha}, \mathrm{Ec}, \mathrm{f_i}$ (table 4.1.1) and equation (4.2.12) in equation (3.7.61), results in

$$\begin{bmatrix} 9.018 & -4.509 & 0 & 0 & \dots \\ -4.509 & 9.018 & -4.509 & 0 & \dots \\ 0 & -4.509 & 9.018 & -4.509 & \ddots \\ 0 & 0 & -4.509 & 9.018 & \ddots \\ \vdots & \vdots & \ddots & \ddots & \ddots \end{bmatrix} \begin{bmatrix} \mathrm{h_2} \\ \mathrm{h_3} \\ \mathrm{h_4} \\ \vdots \\ \mathrm{h_{33}} \\ \mathrm{h_{34}} \end{bmatrix} = \begin{bmatrix} 4.510 \\ 4.512 \\ 4.514 \\ \vdots \\ 4.514 \\ 4.512 \end{bmatrix} \tag{4.2.13}$$

The structure of equations formed from equation (4.2.13) are

$$9.018h_2 - 4.509h_3 = 4.510 \tag{4.2.14}$$

$$-4.509h_2 + 9.018h_3 - 4.509h_4 = 4.512 \tag{4.2.15}$$

$$-4.509h_3 + 9.018h_4 - 4.509h_5 = 4.514 \tag{4.2.16}$$

$$\vdots \tag{4.2.17}$$

$$-4.509h_{31} + 9.018h_{32} - 4.509h_{33} = 4.515 \tag{4.2.18}$$

$$-4.509h_{32} + 9.018h_{33} - 4.509h_{34} = 4.514 \tag{4.2.19}$$

$$-4.509h_{33} + 9.018h_{34} = 4.512 \tag{4.2.20}$$

Mathematica is manipulated to solve the system of equations (4.2.14) to (4.2.20) and delivers solutions of h_j's as

Table 4.2.2: Temperatures along the major axis for $Pr = 1.0$

$h_1 = 0.000$	$h_2 = 16.520$	$h_3 = 32.039$	$h_4 = 46.558$	$h_5 = 60.076$
$h_6 = 72.593$	$h_7 = 84.108$	$h_8 = 94.622$	$h_9 = 104.135$	$h_{10} = 112.646$
$h_{11} = 120.157$	$h_{12} = 126.665$	$h_{13} = 132.173$	$h_{14} = 136.679$	$h_{15} = 140.183$
$h_{16} = 142.687$	$h_{17} = 144.189$	$h_{18} = 144.690$	$h_{19} = 144.189$	$h_{20} = 142.687$
$h_{21} = 140.184$	$h_{22} = 136.679$	$h_{23} = 132.174$	$h_{24} = 126.666$	$h_{25} = 120.158$
$h_{26} = 112.648$	$h_{27} = 104.137$	$h_{28} = 94.624$	$h_{29} = 84.110$	$h_{30} = 72.595$
$h_{31} = 60.078$	$h_{32} = 46.561$	$h_{33} = 32.041$	$h_{34} = 16.521$	$h_{35} = 0.000$

(c) $\mathbf{Ha = 1.0, J^e = 0.0001, Pr = 2.0, a = 0.0034, Ec = 1.0, V_c = 1.895}$

Placing the aforementioned values of Pr and $\mathrm{J^e}$ in equation (3.7.73), transforms to

$$\mathrm{I^e} = \begin{bmatrix} 2.254 & -2.254 \\ -2.254 & 2.254 \end{bmatrix} \tag{4.2.21}$$

Effecting equation (4.2.21), global stiffness matrix I converts to

$$\mathrm{I} = \begin{bmatrix} 2.254 & -2.254 & 0 & 0 & 0 & 0 \\ -2.254 & 4.508 & -2.254 & 0 & 0 & 0 \\ 0 & -2.254 & 4.508 & -2.254 & 0 & 0 \\ 0 & 0 & -2.254 & 4.508 & -2.254 & 0 \\ 0 & 0 & 0 & -2.254 & 4.508 & -2.254 \\ 0 & 0 & 0 & 0 & -2.254 & 4.508 \end{bmatrix} \tag{4.2.22}$$

Upon considering 35 nodes in figure 3.7.2, substituting parameters $\mathrm{Ha}, \mathrm{Ec}, \mathrm{f_i}$ (table 4.1.1) and equation (4.2.22) in equation (3.7.61), grants

$$\begin{bmatrix} 4.508 & -2.254 & 0 & 0 & \dots \\ -2.254 & 4.508 & -2.254 & 0 & \dots \\ 0 & -2.254 & 4.508 & -2.254 & \ddots \\ 0 & 0 & -2.254 & 4.508 & \ddots \\ \vdots & \vdots & \ddots & \ddots & \ddots \end{bmatrix} \begin{bmatrix} \mathrm{h_2} \\ \mathrm{h_3} \\ \mathrm{h_4} \\ \vdots \\ \mathrm{h_{33}} \\ \mathrm{h_{34}} \end{bmatrix} = \begin{bmatrix} 1.128 \\ 1.130 \\ 1.132 \\ \vdots \\ 1.132 \\ 1.130 \end{bmatrix} \tag{4.2.23}$$

The set of equations formed from equation (4.2.23) are

$$4.508h_2 - 2.254h_3 = 1.128 \tag{4.2.24}$$

$$-2.254h_2 + 4.508h_3 - 2.254h_4 = 1.130 \tag{4.2.25}$$

$$-2.254h_3 + 4.508h_4 - 2.254h_5 = 1.132 \tag{4.2.26}$$

$$\vdots \tag{4.2.27}$$

$$-2.254h_{31} + 4.508h_{32} - 2.254h_{33} = 1.133 \tag{4.2.28}$$

$$-2.254h_{32} + 4.508h_{33} - 2.254h_{34} = 1.132 \tag{4.2.29}$$

$$-2.254h_{33} + 4.508h_{34} = 1.130 \tag{4.2.30}$$

Mathematica is utilized to solve the system of equations (4.2.24) to (4.2.30) and provides solutions of h_j's as

Table 4.2.3: Temperatures along the major axis for $Pr = 2.0$

$h_1 = 0.000$	$h_2 = 8.286$	$h_3 = 16.075$	$h_4 = 23.363$	$h_5 = 30.149$
$h_6 = 36.433$	$h_7 = 42.214$	$h_8 = 47.492$	$h_9 = 52.657$	$h_{10} = 56.540$
$h_{11} = 60.311$	$h_{12} = 63.578$	$h_{13} = 66.343$	$h_{14} = 68.605$	$h_{15} = 70.365$
$h_{16} = 71.622$	$h_{17} = 72.376$	$h_{18} = 72.628$	$h_{19} = 72.377$	$h_{20} = 71.623$
$h_{21} = 70.367$	$h_{22} = 68.608$	$h_{23} = 66.346$	$h_{24} = 63.582$	$h_{25} = 60.314$
$h_{26} = 56.546$	$h_{27} = 52.272$	$h_{28} = 47.497$	$h_{29} = 42.220$	$h_{30} = 36.439$
$h_{31} = 30.156$	$h_{32} = 23.371$	$h_{33} = 16.082$	$h_{34} = 8.292$	$h_{35} = 0.000$

Fusing temperatures in tables 4.2.1, 4.2.2 and 4.2.3 gives form in figure 4.2.1.

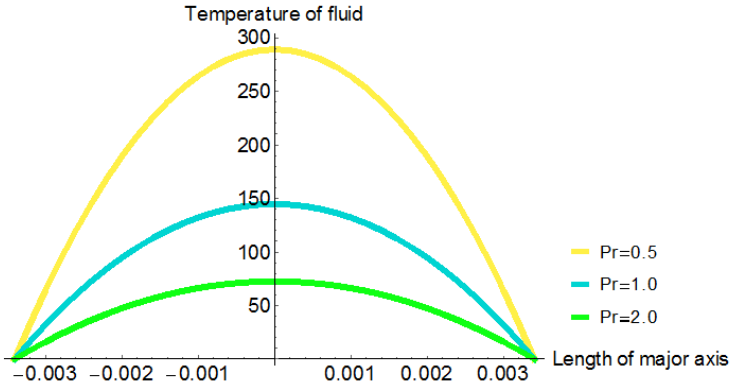

Figure 4.2.1: Combined temperature distributions for $\mathrm{Pr} = 0.5, \mathrm{Pr} = 1.0$ and $\mathrm{Pr} = 2.0$

Prandtl number, Pr, a dimensionless number which is the ratio of momentum diffusivity to thermal diffusivity determines the temperature distribution for the flow. It is observed that when Prandtl number is increased by 100% i.e $\mathrm{Pr} = 0.5$ to $\mathrm{Pr} = 1.0$ or $\mathrm{Pr} = 1.0$ to $\mathrm{Pr} = 2.0$, core temperature decreases by 50%. This also applies to the rest of values apart from the values at the first and last nodes which are zero. This is because the fluid has the ability to transport the momentum faster through the fluid as compared to the heat transfer by conduction as shown in figure 4.2.1. This means that convection dominates over conduction. The effect of Prandtl number is more pronounced at the core temperature. For a given value of Prandtl number, temperature is maximum at the centre of pipe and minimum at the boundary. Using a different arrangement, Dipjyoti *et.al* [15] affirmed contrary i.e increase in Prandtl numbers result in increase in temperature of the flow. On the other hand, in the research done by Anwar *et.al* [29], using also different set up, they found that increase in Prandtl number, resulted in decline in fluid temperature.

4.2.2 Diversifying Hartmann number while keeping Prandtl number, Eckert number, distance of major axis, velocity of fluid and length of elements fixed

(i) $\mathbf{Ha = 5.0, J^e = 0.0001, Pr = 1.0, Ec = 1.0, a = 0.0034, V_c = 1.895}$

Inserting the above stated values of Pr and $\mathrm{J^e}$ in equation (3.7.73), it hands out

$$\mathrm{I^e} = \begin{bmatrix} 4.509 & -4.509 \\ -4.509 & 4.509 \end{bmatrix} \tag{4.2.31}$$

Effecting equation (4.2.31), global stiffness matrix I turns out to

$$\mathrm{I} = \begin{bmatrix} 4.509 & -4.509 & 0 & 0 & 0 & 0 \\ -4.509 & 9.018 & -4.509 & 0 & 0 & 0 \\ 0 & -4.509 & 9.018 & -4.509 & 0 & 0 \\ 0 & 0 & -4.509 & 9.018 & -4.509 & 0 \\ 0 & 0 & 0 & -4.509 & 9.018 & -4.509 \\ 0 & 0 & 0 & 0 & -4.509 & 9.018 \end{bmatrix} \tag{4.2.32}$$

When 35 nodes are considered, replacing values of $\mathrm{Ha}, \mathrm{Ec}, \mathrm{f_i}$ (table 4.1.1) and equation (4.2.32)

in equation (3.7.61), it metamorphoses to

$$\begin{bmatrix} 9.018 & -4.509 & 0 & 0 & \dots \\ -4.509 & 9.018 & -4.509 & 0 & \dots \\ 0 & -4.509 & 9.018 & -4.509 & \ddots \\ 0 & 0 & -4.509 & 9.018 & \ddots \\ \vdots & \vdots & \ddots & \ddots & \ddots \end{bmatrix} \begin{bmatrix} h_2 \\ h_3 \\ h_4 \\ \vdots \\ h_{33} \\ h_{34} \end{bmatrix} = \begin{bmatrix} 4.543 \\ 4.590 \\ 4.624 \\ \vdots \\ 4.634 \\ 4.598 \end{bmatrix} \tag{4.2.33}$$

The structure of equations formed from equation (4.2.33) are

$$9.018h_2 - 4.509h_3 = 4.543 \tag{4.2.34}$$

$$-4.509h_2 + 9.018h_3 - 4.509h_4 = 4.590 \tag{4.2.35}$$

$$-4.509h_3 + 9.018h_4 - 4.509h_5 = 4.624 \tag{4.2.36}$$

$$\vdots \tag{4.2.37}$$

$$-4.509h_{31} + 9.018h_{32} - 4.509h_{33} = 4.658 \tag{4.2.38}$$

$$-4.509h_{32} + 9.018h_{33} - 4.509h_{34} = 4.634 \tag{4.2.39}$$

$$-4.509h_{33} + 9.018h_{34} = 4.598 \tag{4.2.40}$$

The algebraic equations (4.2.34) to (4.2.40) are solved by Mathematica which presents solutions as

Table 4.2.4: Temperatures along the major axis when $\mathrm{Ha} = 5.0$

$\mathrm{h}_1 = 0.000$	$\mathrm{h}_2 = 17.026$	$\mathrm{h}_3 = 33.045$	$\mathrm{h}_4 = 48.045$	$\mathrm{h}_5 = 62.021$
$\mathrm{h}_6 = 74.966$	$\mathrm{h}_7 = 86.878$	$\mathrm{h}_8 = 97.757$	$\mathrm{h}_9 = 107.600$	$\mathrm{h}_{10} = 116.408$
$\mathrm{h}_{11} = 124.181$	$\mathrm{h}_{12} = 130.918$	$\mathrm{h}_{13} = 136.619$	$\mathrm{h}_{14} = 141.284$	$\mathrm{h}_{15} = 144.913$
$\mathrm{h}_{16} = 147.506$	$\mathrm{h}_{17} = 149.063$	$\mathrm{h}_{18} = 149.585$	$\mathrm{h}_{19} = 149.070$	$\mathrm{h}_{20} = 147.520$
$\mathrm{h}_{21} = 144.933$	$\mathrm{h}_{22} = 141.311$	$\mathrm{h}_{23} = 136.652$	$\mathrm{h}_{24} = 130.958$	$\mathrm{h}_{25} = 124.228$
$\mathrm{h}_{26} = 116.462$	$\mathrm{h}_{27} = 107.660$	$\mathrm{h}_{28} = 97.822$	$\mathrm{h}_{29} = 86.948$	$\mathrm{h}_{30} = 75.039$
$\mathrm{h}_{31} = 62.094$	$\mathrm{h}_{32} = 48.114$	$\mathrm{h}_{33} = 33.101$	$\mathrm{h}_{34} = 17.060$	$\mathrm{h}_{35} = 0.000$

(ii) $\mathbf{Ha = 20.0, J^e = 0.0001, Pr = 1.0, Ec = 1.0, a = 0.0034, V_c = 1.895}$

Upon putting the above mentioned values of Pr and J^{e} in equation (3.7.73), it will be the same as equation (4.2.31) since constants are the same. Using equation (4.2.31), global stiffness matrix I becomes the same as equation (4..2.32). On considering 35 nodes, substituting parameters $\mathrm{Ha}, \mathrm{Ec}, \mathrm{f_i}$ (table 4.1.1) and equation (4.2.32) in equation (3.7.61), leads to

$$\begin{bmatrix} & & & & \\ 9.018 & -4.509 & 0 & 0 & \dots \\ -4.509 & 9.018 & -4.509 & 0 & \dots \\ 0 & -4.509 & 9.018 & -4.509 & \ddots \\ 0 & 0 & -4.509 & 9.018 & \ddots \\ \vdots & \vdots & \ddots & \ddots & \ddots \end{bmatrix} \begin{bmatrix} \mathrm{h}_2 \\ \mathrm{h}_3 \\ \mathrm{h}_4 \\ \vdots \\ \mathrm{h}_{33} \\ \mathrm{h}_{34} \end{bmatrix} = \begin{bmatrix} 5.054 \\ 5.804 \\ 6.342 \\ \vdots \\ 6.509 \\ 5.609 \end{bmatrix} \tag{4.2.41}$$

Collection of equations formed from equation (4.2.41) are

$$9.018h_2 - 4.509h_3 = 5.054 \tag{4.2.42}$$

$$-4.509h_2 + 9.018h_3 - 4.509h_4 = 5.804 \tag{4.2.43}$$

$$-4.509h_3 + 9.018h_4 - 4.509h_5 = 6.342 \tag{4.2.44}$$

$$\vdots \tag{4.2.45}$$

$$-4.509h_{31} + 9.018h_{32} - 4.509h_{33} = 6.885 \tag{4.2.46}$$

$$-4.509h_{32} + 9.018h_{33} - 4.509h_{34} = 6.509 \tag{4.2.47}$$

$$-4.509h_{33} + 9.018h_{34} = 5.609 \tag{4.2.48}$$

Equations (4.2.42) to (4.2.48) are solved by Mathematica which procure solutions of h_j's as

Table 4.2.5: Temperatures along the major axis when $Ha = 20.0$

$h_1 = 0.000$	$h_2 = 24.911$	$h_3 = 48.701$	$h_4 = 71.204$	$h_5 = 92.301$
$h_6 = 111.917$	$h_7 = 130.012$	$h_8 = 146.560$	$h_9 = 161.550$	$h_{10} = 174.973$
$h_{11} = 186.827$	$h_{12} = 197.109$	$h_{13} = 205.818$	$h_{14} = 212.954$	$h_{15} = 218.516$
$h_{16} = 222.503$	$h_{17} = 224.917$	$h_{18} = 225.757$	$h_{19} = 225.022$	$h_{20} = 222.713$
$h_{21} = 218.829$	$h_{22} = 213.371$	$h_{23} = 206.338$	$h_{24} = 197.731$	$h_{25} = 187.550$
$h_{26} = 175.794$	$h_{27} = 162.464$	$h_{28} = 147.560$	$h_{29} = 131.082$	$h_{30} = 113.032$
$h_{31} = 93.414$	$h_{32} = 72.239$	$h_{33} = 49.536$	$h_{34} = 25.390$	$h_{35} = 0.000$

(iii) $\mathbf{Ha = 40.0, h^e = 0.002, J^e = 0.001, Pr = 1.0, Ec = 1.0, a = 0.0034, V_c = 1.895}$

Settling the aforementioned values of Pr and J^e in equation (3.7.73), it will be the same as equation (4.2.31) since criterion is the same. Using equation (4.2.31), global stiffness matrix I becomes the same as equation (4.2.32). On considering 35 nodes, substituting parameters

$\mathrm{Ha}, \mathrm{Ec}, \mathrm{f_i}$ (table 4.1.1) and equation (4.2.32) in equation (3.7.61), leads to

$$\begin{bmatrix} & & & & \\ 9.018 & -4.509 & 0 & 0 & \dots \\ -4.509 & 9.018 & -4.509 & 0 & \dots \\ 0 & -4.509 & 9.018 & -4.509 & \ddots \\ 0 & 0 & -4.509 & 9.018 & \ddots \\ \vdots & \vdots & \ddots & \ddots & \ddots \end{bmatrix} \begin{bmatrix} \mathrm{h_2} \\ \mathrm{h_3} \\ \mathrm{h_4} \\ \vdots \\ \mathrm{h_{33}} \\ \mathrm{h_{34}} \end{bmatrix} = \begin{bmatrix} 6.688 \\ 9.690 \\ 11.841 \\ \vdots \\ 12.509 \\ 8.910 \end{bmatrix} \tag{4.2.49}$$

The set of equations formed from equation (4.2.49) are

$$9.018\mathrm{h_2} - 4.509\mathrm{h_3} = 6.688 \tag{4.2.50}$$

$$-4.509\mathrm{h_2} + 9.018\mathrm{h_3} - 4.509\mathrm{h_4} = 9.690 \tag{4.2.51}$$

$$-4.509\mathrm{h_3} + 9.018\mathrm{h_4} - 4.509\mathrm{h_5} = 11.841 \tag{4.2.52}$$

$$\vdots \tag{4.2.53}$$

$$-4.509\mathrm{h_{31}} + 9.018\mathrm{h_{32}} - 4.509\mathrm{h_{33}} = 14.014 \tag{4.2.54}$$

$$-4.509\mathrm{h_{32}} + 9.018\mathrm{h_{33}} - 4.509\mathrm{h_{34}} = 12.509 \tag{4.2.55}$$

$$-4.509\mathrm{h_{33}} + 9.018\mathrm{h_{34}} = 8.910 \tag{4.2.56}$$

Equations (4.2.50) to (4.2.56) are solved by Mathematica which furnishes solutions as

Table 4.2.6: Temperatures along the major axis when $\mathrm{Ha} = 40$

$h_1 = 0.000$	$h_2 = 50.146$	$h_3 = 98.909$	$h_4 = 145.322$	$h_5 = 189.210$
$h_6 = 230.178$	$h_7 = 268.058$	$h_8 = 302.751$	$h_9 = 334.211$	$h_{10} = 362.406$
$h_{11} = 387.323$	$h_{12} = 408.951$	$h_{13} = 427.951$	$h_{14} = 442.333$	$h_{15} = 454.082$
$h_{16} = 462.535$	$h_{17} = 467.693$	$h_{18} = 469.552$	$h_{19} = 468.113$	$h_{20} = 463.377$
$h_{21} = 455.342$	$h_{22} = 444.009$	$h_{23} = 429.378$	$h_{24} = 411.449$	$h_{25} = 390.222$
$h_{26} = 365.697$	$h_{27} = 337.874$	$h_{28} = 306.755$	$h_{29} = 272.343$	$h_{30} = 234.642$
$h_{31} = 193.668$	$h_{32} = 149.463$	$h_{33} = 102.150$	$h_{34} = 52.063$	$h_{35} = 0.000$

Blending temperatures in tables 4.2.4, 4.2.5 and 4.2.6 leads to outlines shown in figure 4.2.2.

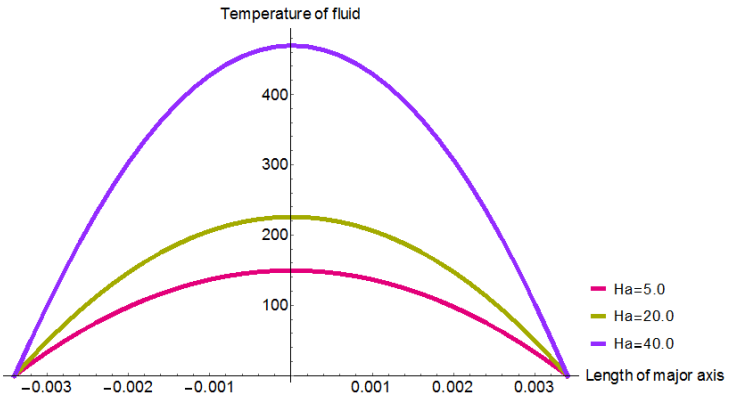

Figure 4.2.2: Fused temperature distributions for $\mathrm{Ha} = 5.0, \mathrm{Ha} = 20.0$ and $\mathrm{Ha} = 40.0$

Hartmann number determines the temperature distribution for the flow. As the value of Hartmann number is increased, temperature increases. The effect of the electromagnetic force is more prominent at the point of peak value as shown in figure 4.2.2 i.e the peak value increases with increase in magnetic field. The presence of magnetic field in an electrically conducting fluid introduces Lorentz force which acts against the flow. This force slows down the fluid velocity. The heat transfer mode in the fluid gradually changes towards conduction from convection. When Hartmann number is doubled from 20.0 to 40.0, core temperature increases 2.08 times. Dipjyoti *et.al* [15] declared also in their results that when Hartmann number is increased, fluid temperature increases.

4.2.3 Altering Eckert number while maintaining Prandtl number, Hartmann number, distance of major axis, velocity of fluid and length of elements

$$(\mathbf{I}) \quad \mathbf{Ha = 1.0, J^e = 0.0001, Pr = 1.0, Ec = 5.0, a = 0.0034, V_c = 1.895}$$

Bringing the above stated values of Pr and $\mathrm{J^e}$ in equation (3.7.73), it will be the same as equation (4.2.31) since specifications are similar. Employing equation (4.2.31), global stiffness matrix I becomes the same as equation (4.2.32). Taking into account 35 nodes, substituting parameters $\mathrm{Ha, Ec, f_i}$ (table 4.1.1) and equation (4.2.32) in equation (3.7.61), it converts to

$$\begin{bmatrix} 9.018 & -4.509 & 0 & 0 & \dots \\ -4.509 & 9.018 & -4.509 & 0 & \dots \\ 0 & -4.509 & 9.018 & -4.509 & \ddots \\ 0 & 0 & -4.509 & 9.018 & \ddots \\ \vdots & \vdots & \ddots & \ddots & \ddots \end{bmatrix} \begin{bmatrix} \mathrm{h_2} \\ \mathrm{h_3} \\ \mathrm{h_4} \\ \vdots \\ \mathrm{h_{33}} \\ \mathrm{h_{34}} \end{bmatrix} = \begin{bmatrix} 4.516 \\ 4.525 \\ 4.532 \\ \vdots \\ 4.534 \\ 4.523 \end{bmatrix} \tag{4.2.57}$$

Algebraic equations formed from equation (4.2.57) are

$$9.018h_2 - 4.509h_3 = 4.516 \tag{4.2.58}$$

$$-4.509h_2 + 9.018h_3 - 4.509h_4 = 4.525 \tag{4.2.59}$$

$$-4.509h_3 + 9.018h_4 - 4.509h_5 = 4.532 \tag{4.2.60}$$

$$\vdots \tag{4.2.61}$$

$$-4.509h_{31} + 9.018h_{32} - 4.509h_{33} = 4.539 \tag{4.2.62}$$

$$-4.509h_{32} + 9.018h_{33} - 4.509h_{34} = 4.534 \tag{4.2.63}$$

$$-4.509h_{33} + 9.018h_{34} = 4.523 \tag{4.2.64}$$

Mathematica is used to solve equations (4.2.58) to (4.2.64) and dispenses solutions of h_j's as

Table 4.2.7: Temperatures along the major axis with $Ec = 5.0$

$h_1 = 0.000$	$h_2 = 16.604$	$h_3 = 32.207$	$h_4 = 46.807$	$h_5 = 60.401$
$h_6 = 72.989$	$h_7 = 84.571$	$h_8 = 95.146$	$h_9 = 104.714$	$h_{10} = 113.274$
$h_{11} = 120.828$	$h_{12} = 127.375$	$h_{13} = 132.915$	$h_{14} = 137.447$	$h_{15} = 140.973$
$h_{16} = 143.491$	$h_{17} = 145.002$	$h_{18} = 145.506$	$h_{19} = 145.003$	$h_{20} = 143.493$
$h_{21} = 140.976$	$h_{22} = 137.452$	$h_{23} = 132.920$	$h_{24} = 127.382$	$h_{25} = 120.836$
$h_{26} = 113.284$	$h_{27} = 104.724$	$h_{28} = 95.157$	$h_{29} = 84.583$	$h_{30} = 73.002$
$h_{31} = 60.414$	$h_{32} = 46.819$	$h_{33} = 32.216$	$h_{34} = 16.610$	$h_{35} = 0.000$

(II) $\mathbf{Ha = 1.0, J^e = 0.0001, Pr = 1.0, Ec = 20.0, a = 0.0034, V_c = 1.895}$

Inserting the above mentioned values of Pr and J^e in equation (3.7.73), it will be the same as equation (4.2.31) since constants are equal. Utilizing equation (4.2.31), global stiffness matrix I becomes the same as equation (4.2.32). Considering 35 nodes, substituting values Ha, Ec, f_i

(table 4.1.1) and equation (4.2.32) in equation (3.7.61), it converts to

$$\begin{bmatrix} 9.018 & -4.509 & 0 & 0 & \dots \\ -4.509 & 9.018 & -4.509 & 0 & \dots \\ 0 & -4.509 & 9.018 & -4.509 & \ddots \\ 0 & 0 & -4.509 & 9.018 & \ddots \\ \vdots & \vdots & \ddots & \ddots & \ddots \end{bmatrix} \begin{bmatrix} h_2 \\ h_3 \\ h_4 \\ \vdots \\ h_{33} \\ h_{34} \end{bmatrix} = \begin{bmatrix} 4.536 \\ 4.574 \\ 4.601 \\ \vdots \\ 4.609 \\ 4.564 \end{bmatrix} \tag{4.2.65}$$

Equations formed from equation (4.2.65) are

$$9.018h_2 - 4.509h_3 = 4.536 \tag{4.2.66}$$

$$-4.509h_2 + 9.018h_3 - 4.509h_4 = 4.574 \tag{4.2.67}$$

$$-4.509h_3 + 9.018h_4 - 4.509h_5 = 4.601 \tag{4.2.68}$$

$$\vdots \tag{4.2.69}$$

$$-4.509h_{31} + 9.018h_{32} - 4.509h_{33} = 4.628 \tag{4.2.70}$$

$$-4.509h_{32} + 9.018h_{33} - 4.509h_{34} = 4.609 \tag{4.2.71}$$

$$-4.509h_{33} + 9.018h_{34} = 4.564 \tag{4.2.72}$$

On solving equations (4.2.66) to (4.2.72) by engaging Mathematica, solutions are presented as

Table 4.2.8: Temperatures along the major axis with $\mathrm{Ec} = 20.0$

$\mathrm{h}_1 = 0.000$	$\mathrm{h}_2 = 16.921$	$\mathrm{h}_3 = 32.836$	$\mathrm{h}_4 = 47.736$	$\mathrm{h}_5 = 61.616$
$\mathrm{h}_6 = 74.472$	$\mathrm{h}_7 = 86.302$	$\mathrm{h}_8 = 97.105$	$\mathrm{h}_9 = 106.879$	$\mathrm{h}_{10} = 115.626$
$\mathrm{h}_{11} = 123.344$	$\mathrm{h}_{12} = 130.033$	$\mathrm{h}_{13} = 135.694$	$\mathrm{h}_{14} = 140.326$	$\mathrm{h}_{15} = 143.929$
$\mathrm{h}_{16} = 146.504$	$\mathrm{h}_{17} = 148.050$	$\mathrm{h}_{18} = 148.568$	$\mathrm{h}_{19} = 148.056$	$\mathrm{h}_{20} = 146.516$
$\mathrm{h}_{21} = 143.947$	$\mathrm{h}_{22} = 140.349$	$\mathrm{h}_{23} = 135.722$	$\mathrm{h}_{24} = 130.067$	$\mathrm{h}_{25} = 123.382$
$\mathrm{h}_{26} = 115.669$	$\mathrm{h}_{27} = 106.927$	$\mathrm{h}_{28} = 97.156$	$\mathrm{h}_{29} = 86.357$	$\mathrm{h}_{30} = 74.529$
$\mathrm{h}_{31} = 61.673$	$\mathrm{h}_{32} = 47.788$	$\mathrm{h}_{33} = 32.878$	$\mathrm{h}_{34} = 16.945$	$\mathrm{h}_{35} = 0.000$

$(\mathbf{III}) \quad \mathbf{Ha = 1.0, J^e = 0.0001, Pr = 1.0, Ec = 40.0, a = 0.0034, V_c = 1.895}$

Putting the above stated values of Pr and J^{e} in equation (3.7.73), it will be the same as equation (4.2.31) since parameters are the same. Manipulating equation (4.2.31), global stiffness matrix I becomes the same as equation (4.2.32). Considering 35 nodes, substituting quantities $\mathrm{Ha}, \mathrm{Ec}, \mathrm{f_i}$ (table 4.1.1) and equation (4.2.32) in equation (3.7.61), it delivers

$$\begin{bmatrix} & & & & \\ 9.018 & -4.509 & 0 & 0 & \dots \\ -4.509 & 9.018 & -4.509 & 0 & \dots \\ 0 & -4.509 & 9.018 & -4.509 & \ddots \\ 0 & 0 & -4.509 & 9.018 & \ddots \\ \vdots & \vdots & \ddots & \ddots & \ddots \end{bmatrix} \begin{bmatrix} \mathrm{h}_2 \\ \mathrm{h}_3 \\ \mathrm{h}_4 \\ \vdots \\ \mathrm{h}_{33} \\ \mathrm{h}_{34} \end{bmatrix} = \begin{bmatrix} 4.563 \\ 4.639 \\ 4.692 \\ \vdots \\ 4.709 \\ 4.619 \end{bmatrix} \tag{4.2.73}$$

Equations formed from equation (4.2.73) are

$$9.018h_2 - 4.509h_3 = 4.563 \tag{4.2.74}$$

$$-4.509h_2 + 9.018h_3 - 4.509h_4 = 4.639 \tag{4.2.75}$$

$$-4.509h_3 + 9.018h_4 - 4.509h_5 = 4.692 \tag{4.2.76}$$

$$\vdots \tag{4.2.77}$$

$$-4.509h_{31} + 9.018h_{32} - 4.509h_{33} = 4.747 \tag{4.2.78}$$

$$-4.509h_{32} + 9.018h_{33} - 4.509h_{34} = 4.709 \tag{4.2.79}$$

$$-4.509h_{33} + 9.018h_{34} = 4.619 \tag{4.2.80}$$

Mathematica is used to solve the system of equations (4.2.74) to (4.2.80) and furnishes solutions of h_j's as

Table 4.2.9: Temperatures along the major axis with $Ec = 40.0$

$h_1 = 0.000$	$h_2 = 17.341$	$h_3 = 33.670$	$h_4 = 48.971$	$h_5 = 63.231$
$h_6 = 76.442$	$h_7 = 88.602$	$h_8 = 99.707$	$h_9 = 109.756$	$h_{10} = 118.748$
$h_{11} = 126.684$	$h_{12} = 133.562$	$h_{13} = 139.383$	$h_{14} = 144.147$	$h_{15} = 147.853$
$h_{16} = 150.502$	$h_{17} = 152.093$	$h_{18} = 152.627$	$h_{19} = 152.104$	$h_{20} = 150.523$
$h_{21} = 147.884$	$h_{22} = 144.188$	$h_{23} = 139.435$	$h_{24} = 133.624$	$h_{25} = 126.756$
$h_{26} = 118.831$	$h_{27} = 109.848$	$h_{28} = 99.807$	$h_{29} = 88.709$	$h_{30} = 76.554$
$h_{31} = 63.342$	$h_{32} = 49.074$	$h_{33} = 33.754$	$h_{34} = 17.389$	$h_{35} = 0.000$

Incorporating temperatures in tables 4.2.7, 4.2.8 and 4.2.9 presents profiles in figure 4.2.3.

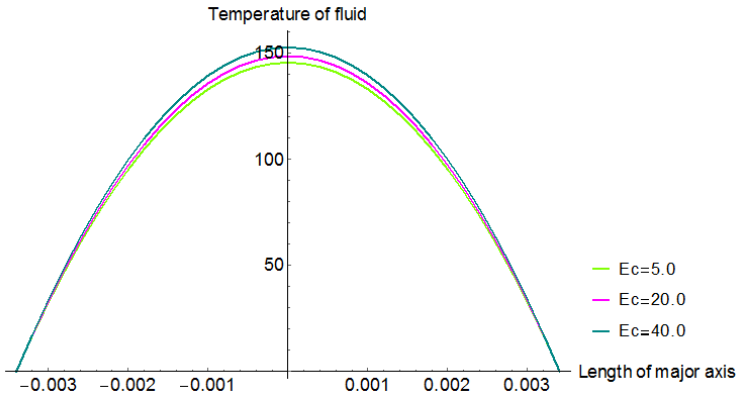

Figure 4.2.3: Mixed temperature profiles for $\mathrm{Ec} = 5.0, \mathrm{Ec} = 20.0$ and $\mathrm{Ec} = 40.0$

Increase in Eckert number, a dimensionless quantity, the ratio of the kinetic energy to the enthalpy, increases temperature distribution as shown in figure 4.2.3. At high velocities of fluid flow, there are effects of heat dissipation due to internal friction of the fluid. This leads to self heating which changes temperature distribution. On doubling Eckert number from 20 to 40, peak temperature increases by 2.7%. Utilizing different formation, results obtained by Liaquat [18] exposed also that rise in Eckert number led to rise in temperature.

Comparing temperature distribution when Hartmann number and Eckert number are the same eg $\mathrm{Ha} = \mathrm{Ec} = 20.0$, core temperature for Ha is 225.757 while that for Ec is 148.568 i.e Hartmann number's value is 1.52 times greater than that of Eckert number's value. This is because heat transmission by conduction is greater than that of effects of heat dissipation due to internal friction of the fluid. Ha is squared in the formulation while Ec is to power 1 in the formulation, equation (3.7.61).

4.2.4 Varying velocity of fluid while preserving Hartmann number, Eckert number, Prandtl number, distance of major axis and length of elements

In the investigation of velocity profile, subsection 4.1, velocity of fluid vary with change in Reynolds number, Re. This data is utilized in this subsector by embracing values in tables 4.1.7, 4.1.8 and 4.1.9

$$(\mathbf{A}) \quad \mathbf{Ha = 1.0, J^e = 0.0001, Pr = 1.0, Ec = 1.0, a = 0.0034, V_c = 3.789}$$

Fluid velocity obtained when $\mathrm{Re} = 2.0$ is as shown in table 4.1.7. Core velocity, for this table being $\mathrm{V_c} = 3.789$. Laying the above stated values of Pr and $\mathrm{J^e}$ in equation (3.7.73), it will be the same as equation (4.2.31) since constants are equal. Adopting equation (4.2.31), global stiffness matrix I becomes the same as equation (4.2.32). Considering 35 nodes, substituting parameters $\mathrm{Ha}, \mathrm{Ec}, \mathrm{f_i}$ (table 4.1.7) and equation (4.2.32) in equation (3.7.61), it turns out to

$$\begin{bmatrix} 9.018 & -4.509 & 0 & 0 & \dots \\ -4.509 & 9.018 & -4.509 & 0 & \dots \\ 0 & -4.509 & 9.018 & -4.509 & \ddots \\ 0 & 0 & -4.509 & 9.018 & \ddots \\ \vdots & \vdots & \ddots & \ddots & \ddots \end{bmatrix} \begin{bmatrix} \mathrm{h_2} \\ \mathrm{h_3} \\ \mathrm{h_4} \\ \vdots \\ \mathrm{h_{33}} \\ \mathrm{h_{34}} \end{bmatrix} = \begin{bmatrix} 4.514 \\ 4.522 \\ 4.527 \\ \vdots \\ 4.529 \\ 4.520 \end{bmatrix} \tag{4.2.81}$$

Algebraic equations formed from equation (4.2.81) are

$$9.018h_2 - 4.509h_3 = 4.514 \tag{4.2.82}$$

$$-4.509h_2 + 9.018h_3 - 4.509h_4 = 4.522 \tag{4.2.83}$$

$$-4.509h_3 + 9.018h_4 - 4.509h_5 = 4.527 \tag{4.2.84}$$

$$\vdots \tag{4.2.85}$$

$$-4.509h_{31} + 9.018h_{32} - 4.509h_{33} = 4.533 \tag{4.2.86}$$

$$-4.509h_{32} + 9.018h_{33} - 4.509h_{34} = 4.529 \tag{4.2.87}$$

$$-4.509h_{33} + 9.018h_{34} = 4.520 \tag{4.2.88}$$

Mathematica is used to solve equations (4.2.82) to (4.2.88) and dispenses solutions of h_j's as

Table 4.2.10: Temperatures along the major axis for $V_c = 3.789$

$h_1 = 0.000$	$h_2 = 16.585$	$h_3 = 32.168$	$h_4 = 46.749$	$h_5 = 60.326$
$h_6 = 72.898$	$h_7 = 84.464$	$h_8 = 95.025$	$h_9 = 104.580$	$h_{10} = 113.130$
$h_{11} = 120.673$	$h_{12} = 127.211$	$h_{13} = 132.743$	$h_{14} = 137.270$	$h_{15} = 140.790$
$h_{16} = 143.305$	$h_{17} = 144.814$	$h_{18} = 145.318$	$h_{19} = 144.815$	$h_{20} = 143.307$
$h_{21} = 140.793$	$h_{22} = 137.273$	$h_{23} = 132.748$	$h_{24} = 127.216$	$h_{25} = 120.679$
$h_{26} = 113.137$	$h_{27} = 104.588$	$h_{28} = 95.034$	$h_{29} = 84.474$	$h_{30} = 72.908$
$h_{31} = 60.336$	$h_{32} = 46.759$	$h_{33} = 32.176$	$h_{34} = 16.589$	$h_{35} = 0.000$

(B) $\mathbf{Ha = 1.0, J^e = 0.0001, Pr = 1.0, Ec = 1.0, a = 0.0034, V_c = 7.578}$

When $Re = 4.0$, fluid velocity is as shown in table 4.1.8. Putting the aforementioned values of Pr and J^e in equation (3.7.73), it will be the same as equation (4.2.31) since criterion is the same. Manipulating equation (4.2.31), global stiffness matrix I becomes the same as equation (4.2.32). Upon considering 35 nodes, substituting values Ha, Ec, f_i (table 4.1.8) and equation (4.2.32) in

equation (3.7.61), it metamorphoses to

$$\begin{bmatrix} 9.018 & -4.509 & 0 & 0 & \dots \\ -4.509 & 9.018 & -4.509 & 0 & \dots \\ 0 & -4.509 & 9.018 & -4.509 & \ddots \\ 0 & 0 & -4.509 & 9.018 & \ddots \\ \vdots & \vdots & \ddots & \ddots & \ddots \end{bmatrix} \begin{bmatrix} h_2 \\ h_3 \\ h_4 \\ \vdots \\ h_{33} \\ h_{34} \end{bmatrix} = \begin{bmatrix} 4.531 \\ 4.561 \\ 4.582 \\ \vdots \\ 4.589 \\ 4.553 \end{bmatrix} \tag{4.2.89}$$

Algebraic equations formed from equation (4.2.89) are

$$9.018h_2 - 4.509h_3 = 4.531 \tag{4.2.90}$$

$$-4.509h_2 + 9.018h_3 - 4.509h_4 = 4.561 \tag{4.2.91}$$

$$-4.509h_3 + 9.018h_4 - 4.509h_5 = 4.582 \tag{4.2.92}$$

$$\vdots \tag{4.2.93}$$

$$-4.509h_{31} + 9.018h_{32} - 4.509h_{33} = 4.604 \tag{4.2.94}$$

$$-4.509h_{32} + 9.018h_{33} - 4.509h_{34} = 4.589 \tag{4.2.95}$$

$$-4.509h_{33} + 9.018h_{34} = 4.553 \tag{4.2.96}$$

Mathematica is used to solve equations (4.2.90) to (4.2.96) and procures solutions of h_j's as

Table 4.2.11: Temperatures along the major axis for $\mathrm{V_c} = 7.578$

$\mathrm{h_1} = 0.000$	$\mathrm{h_2} = 16.837$	$\mathrm{h_3} = 32.669$	$\mathrm{h_4} = 47.490$	$\mathrm{h_5} = 61.294$
$\mathrm{h_6} = 74.079$	$\mathrm{h_7} = 85.843$	$\mathrm{h_8} = 96.586$	$\mathrm{h_9} = 106.306$	$\mathrm{h_{10}} = 115.003$
$\mathrm{h_{11}} = 122.678$	$\mathrm{h_{12}} = 129.329$	$\mathrm{h_{13}} = 134.958$	$\mathrm{h_{14}} = 139.564$	$\mathrm{h_{15}} = 143.147$
$\mathrm{h_{16}} = 145.707$	$\mathrm{h_{17}} = 147.244$	$\mathrm{h_{18}} = 147.758$	$\mathrm{h_{19}} = 147.249$	$\mathrm{h_{20}} = 145.716$
$\mathrm{h_{21}} = 143.161$	$\mathrm{h_{22}} = 139.582$	$\mathrm{h_{23}} = 134.981$	$\mathrm{h_{24}} = 129.356$	$\mathrm{h_{25}} = 122.709$
$\mathrm{h_{26}} = 115.038$	$\mathrm{h_{27}} = 106.344$	$\mathrm{h_{28}} = 96.627$	$\mathrm{h_{29}} = 85.888$	$\mathrm{h_{30}} = 74.125$
$\mathrm{h_{31}} = 61.340$	$\mathrm{h_{32}} = 47.532$	$\mathrm{h_{33}} = 32.703$	$\mathrm{h_{34}} = 16.856$	$\mathrm{h_{35}} = 0.000$

$(\mathbf{C}) \quad \mathbf{Ha = 1.0, J^e = 0.0001, Pr = 1.0, Ec = 1.0, a = 0.0034, V_c = 15.157}$

Table 4.1.9 shows velocity of fluid when $\mathrm{Re} = 8.0$. Setting the above stated values of Pr and $\mathrm{J^e}$ in equation (3.7.73), it will be the same as equation (4.2.31) since constants are equal. Utilizing equation (4.2.31), global stiffness matrix I becomes the same as equation (4.2.32). Taking into account 35 nodes, substituting values $\mathrm{Ha}, \mathrm{Ec}, \mathrm{f_i}$ (table 4.1.9) and equation (4.2.32) in equation (3.7.61), it hands out

$$\begin{bmatrix} & & & & \\ 9.018 & -4.509 & 0 & 0 & \dots \\ -4.509 & 9.018 & -4.509 & 0 & \dots \\ 0 & -4.509 & 9.018 & -4.509 & \ddots \\ 0 & 0 & -4.509 & 9.018 & \ddots \\ \vdots & \vdots & \ddots & \ddots & \ddots \end{bmatrix} \begin{bmatrix} \mathrm{h_2} \\ \mathrm{h_3} \\ \mathrm{h_4} \\ \vdots \\ \mathrm{h_{33}} \\ \mathrm{h_{34}} \end{bmatrix} = \begin{bmatrix} 4.596 \\ 4.716 \\ 4.802 \\ \vdots \\ 4.829 \\ 4.685 \end{bmatrix} \tag{4.2.97}$$

Set of equations formed from equation (4.2.97) are

$$9.018h_2 - 4.509h_3 = 4.596 \tag{4.2.98}$$

$$-4.509h_2 + 9.018h_3 - 4.509h_4 = 4.716 \tag{4.2.99}$$

$$-4.509h_3 + 9.018h_4 - 4.509h_5 = 4.802 \tag{4.2.100}$$

$$\vdots \tag{4.2.101}$$

$$-4.509h_{31} + 9.018h_{32} - 4.509h_{33} = 4.889 \tag{4.2.102}$$

$$-4.509h_{32} + 9.018h_{33} - 4.509h_{34} = 4.829 \tag{4.2.103}$$

$$-4.509h_{33} + 9.018h_{34} = 4.685 \tag{4.2.104}$$

Mathematica is used to solve equations (4.2.98) to (4.2.104) and delivers solutions of h_j's as

Table 4.2.12: Temperatures along the major axis for $V_c = 15.157$

$h_1 = 0.000$	$h_2 = 17.845$	$h_3 = 34.672$	$h_4 = 50.452$	$h_5 = 65.167$
$h_6 = 78.807$	$h_7 = 91.361$	$h_8 = 102.828$	$h_9 = 113.206$	$h_{10} = 122.494$
$h_{11} = 130.690$	$h_{12} = 137.795$	$h_{13} = 143.808$	$h_{14} = 148.729$	$h_{15} = 152.558$
$h_{16} = 155.296$	$h_{17} = 156.942$	$h_{18} = 157.496$	$h_{19} = 156.958$	$h_{20} = 155.329$
$h_{21} = 152.607$	$h_{22} = 148.794$	$h_{23} = 143.889$	$h_{24} = 137.892$	$h_{25} = 130.803$
$h_{26} = 122.623$	$h_{27} = 113.350$	$h_{28} = 102.986$	$h_{29} = 91.530$	$h_{30} = 78.983$
$h_{31} = 65.344$	$h_{32} = 50.617$	$h_{33} = 34.805$	$h_{34} = 17.922$	$h_{35} = 0.000$

Linking temperatures in tables 4.2.10, 4.2.11 and 4.2.12 presents contours in figure 4.2.4.

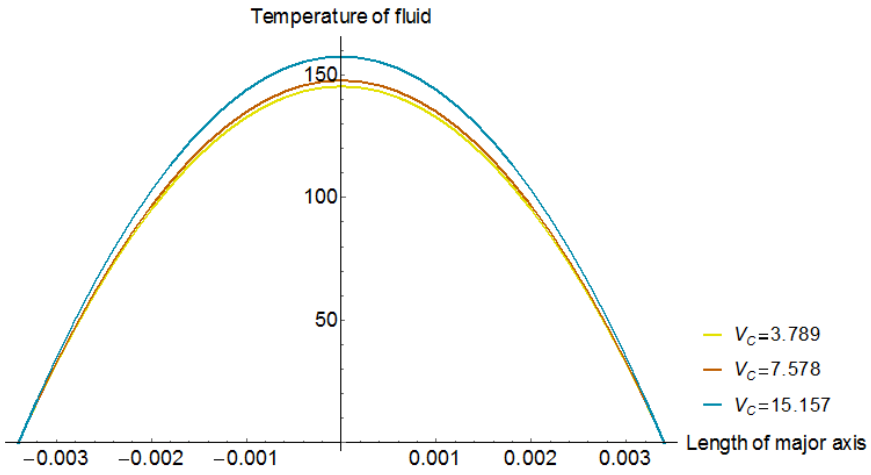

Figure 4.2.4: Coupled temperature outlines for $\mathrm{V_c} = 3.789, \mathrm{V_c} = 7.578$ and $\mathrm{V_c} = 15.157$

When core velocity of fluid is doubled from 7.578 to 15.157, figure 4.2.4, core temperature increases by 6.6%. Increase in velocity lead to increase in temperature.

4.2.5 Modifying distance of major axis while preserving Hartmann number, Eckert number, Prandtl number, velocity of fluid and length of elements

Distance of major axis is varied by increasing the number of nodes. When the number of nodes is increased, velocity at the nodes will also vary as found in the research on velocity profile. This means that values of velocity in tables 4.1.11, 4.1.12 and 4.1.13 will be adopted in this subsection.

$$(i) \quad \mathbf{Ha = 1.0, J^e = 0.0001, Pr = 1.0, Ec = 1.0, a = 0.002, V_c = 47.263}$$

The values of velocity for $\mathrm{a} = 0.002$ are shown in table 4.1.11. Settling the above stated values of Pr and $\mathrm{J^e}$ in equation (3.7.73), it will be the same as equation (4.2.31) since specifications are the same. Embracing equation (4.2.31), global stiffness matrix I becomes the same as equation

(4.2.32). Considering 21 nodes, substituting values $\mathrm{Ha}, \mathrm{Ec}, \mathrm{f_i}$ (table 4.1.11) and equation (4.2.32) in equation (3.7.61), it accords

$$\begin{bmatrix} 9.018 & -4.509 & 0 & 0 & \dots \\ -4.509 & 9.018 & -4.509 & 0 & \dots \\ 0 & -4.509 & 9.018 & -4.509 & \ddots \\ 0 & 0 & -4.509 & 9.018 & \ddots \\ \vdots & \vdots & \ddots & \ddots & \ddots \end{bmatrix} \begin{bmatrix} \mathrm{h_2} \\ \mathrm{h_3} \\ \mathrm{h_4} \\ \vdots \\ \mathrm{h_{19}} \\ \mathrm{h_{20}} \end{bmatrix} = \begin{bmatrix} 5.360 \\ 6.532 \\ 7.374 \\ \vdots \\ 7.635 \\ 6.229 \end{bmatrix} \tag{4.2.105}$$

Equations formed from equation (4.2.105) are

$$9.018\mathrm{h_2} - 4.509\mathrm{h_3} = 5.360 \tag{4.2.106}$$

$$-4.509\mathrm{h_2} + 9.018\mathrm{h_3} - 4.509\mathrm{h_4} = 6.532 \tag{4.2.107}$$

$$-4.509\mathrm{h_3} + 9.018\mathrm{h_4} - 4.509\mathrm{h_5} = 7.374 \tag{4.2.108}$$

$$\vdots \tag{4.2.109}$$

$$-4.509\mathrm{h_{17}} + 9.018\mathrm{h_{18}} - 4.509\mathrm{h_{19}} = 7.901 \tag{4.2.110}$$

$$-4.509\mathrm{h_{18}} + 9.018\mathrm{h_{19}} - 4.509\mathrm{h_{20}} = 7.635 \tag{4.2.111}$$

$$-4.509\mathrm{h_{19}} + 9.018\mathrm{h_{20}} = 6.229 \tag{4.2.112}$$

Mathematica is used to solve equations (4.2.106) to (4.2.112) and procures solutions of $\mathrm{h_j}$'s as

Table 4.2.13: Temperatures along the major axis when $\mathrm{a} = 0.002$

$\mathrm{h}_1 = 0.000$	$\mathrm{h}_2 = 16.407$	$\mathrm{h}_3 = 31.624$	$\mathrm{h}_4 = 45.393$	$\mathrm{h}_5 = 57.527$
$\mathrm{h}_6 = 67.911$	$\mathrm{h}_7 = 76.479$	$\mathrm{h}_8 = 83.194$	$\mathrm{h}_9 = 88.036$	$\mathrm{h}_{10} = 90.994$
$\mathrm{h}_{11} = 92.062$	$\mathrm{h}_{12} = 91.236$	$\mathrm{h}_{13} = 88.515$	$\mathrm{h}_{14} = 83.898$	$\mathrm{h}_{15} = 77.386$
$\mathrm{h}_{16} = 68.980$	$\mathrm{h}_{17} = 58.686$	$\mathrm{h}_{18} = 46.521$	$\mathrm{h}_{19} = 32.603$	$\mathrm{h}_{20} = 16.992$
$\mathrm{h}_{21} = 0.000$	–	–	–	–

$$(ii) \quad \mathbf{Ha = 1.0, J^e = 0.0001, Pr = 1.0, Ec = 1.0, a = 0.0028, V_c = 47.358}$$

Table 4.1.12 provides the values of velocity for $\mathrm{a} = 0.0028$. Putting the aforementioned values of Pr and J^{e} in equation (3.7.73), it will be the same as equation (4.2.31) since constants are the same. Manipulating equation (4.2.31), global stiffness matrix I becomes the same as equation (4.2.32). Upon considering 29 nodes, substituting parameters $\mathrm{Ha}, \mathrm{Ec}, \mathrm{f_i}$ (table 4.1.12) and equation (4.2.32) in equation (3.7.61), it hands out

$$\begin{bmatrix} 9.018 & -4.509 & 0 & 0 & \dots \\ -4.509 & 9.018 & -4.509 & 0 & \dots \\ 0 & -4.509 & 9.018 & -4.509 & \ddots \\ 0 & 0 & -4.509 & 9.018 & \ddots \\ \vdots & \vdots & \ddots & \ddots & \ddots \end{bmatrix} \begin{bmatrix} \mathrm{h}_2 \\ \mathrm{h}_3 \\ \mathrm{h}_4 \\ \vdots \\ \mathrm{h}_{27} \\ \mathrm{h}_{28} \end{bmatrix} = \begin{bmatrix} 5.360 \\ 6.532 \\ 7.374 \\ \vdots \\ 7.631 \\ 6.228 \end{bmatrix} \tag{4.2.113}$$

Set of equations formed from equation (4.2.113) are

$$9.018h_2 - 4.509h_3 = 5.360 \tag{4.2.114}$$

$$-4.509h_2 + 9.018h_3 - 4.509h_4 = 6.532 \tag{4.2.115}$$

$$-4.509h_3 + 9.018h_4 - 4.509h_5 = 7.374 \tag{4.2.116}$$

$$\vdots \tag{4.2.117}$$

$$-4.509h_{25} + 9.018h_{26} - 4.509h_{27} = 8.212 \tag{4.2.118}$$

$$-4.509h_{26} + 9.018h_{27} - 4.509h_{28} = 7.631 \tag{4.2.119}$$

$$-4.509h_{27} + 9.018h_{28} = 6.228 \tag{4.2.120}$$

Equations (4.2.114) to (4.2.120) are solved by Mathematica which grants solutions of h_j's as

Table 4.2.14: Temperatures along the major axis when $a = 0.0028$

$h_1 = 0.000$	$h_2 = 23.967$	$h_3 = 46.746$	$h_4 = 68.076$	$h_5 = 87.771$
$h_6 = 105.715$	$h_7 = 121.844$	$h_8 = 136.120$	$h_9 = 148.523$	$h_{10} = 159.042$
$h_{11} = 167.671$	$h_{12} = 174.406$	$h_{13} = 179.245$	$h_{14} = 182.189$	$h_{15} = 183.236$
$h_{16} = 182.385$	$h_{17} = 179.638$	$h_{18} = 174.993$	$h_{19} = 168.451$	$h_{20} = 160.011$
$h_{21} = 149.674$	$h_{22} = 137.44$	$h_{23} = 123.310$	$h_{24} = 107.285$	$h_{25} = 89.373$
$h_{26} = 69.589$	$h_{27} = 47.982$	$h_{28} = 24.682$	$h_{29} = 0.000$	–

(*iii*) $\mathbf{Ha = 1.0, J^e = 0.0001, Pr = 1.0, Ec = 1.0, a = 0.0032, V_c = 47.364}$

Values of velocity for $a = 0.0032$ are given by table 4.1.13. Inserting the above stated values of Pr and J^e in equation (3.7.73), it will be the same as equation (4.2.31) since specifications are the same. Using equation (4.2.31), global stiffness matrix I becomes the same as equation (4.2.32). Taking into account 33 nodes, substituting parameters Ha, Ec, f_i (table 4.1.13) and

equation (4.2.32) in equation (3.7.61), it converts to

$$\begin{bmatrix} 9.018 & -4.509 & 0 & 0 & \dots \\ -4.509 & 9.018 & -4.509 & 0 & \dots \\ 0 & -4.509 & 9.018 & -4.509 & \ddots \\ 0 & 0 & -4.509 & 9.018 & \ddots \\ \vdots & \vdots & \ddots & \ddots & \ddots \end{bmatrix} \begin{bmatrix} h_2 \\ h_3 \\ h_4 \\ \vdots \\ h_{31} \\ h_{32} \end{bmatrix} = \begin{bmatrix} 5.360 \\ 6.532 \\ 7.374 \\ \vdots \\ 7.635 \\ 6.229 \end{bmatrix} \tag{4.2.121}$$

Collection of equations formed from equation (4.2.121) are

$$9.018h_2 - 4.509h_3 = 5.360 \tag{4.2.122}$$

$$-4.509h_2 + 9.018h_3 - 4.509h_4 = 6.532 \tag{4.2.123}$$

$$-4.509h_3 + 9.018h_4 - 4.509h_5 = 7.374 \tag{4.2.124}$$

$$\vdots \tag{4.2.125}$$

$$-4.509h_{29} + 9.018h_{30} - 4.509h_{31} = 8.221 \tag{4.2.126}$$

$$-4.509h_{30} + 9.018h_{31} - 4.509h_{32} = 7.635 \tag{4.2.127}$$

$$-4.509h_{31} + 9.018h_{32} = 6.229 \tag{4.2.128}$$

Algebraic equations (4.2.122) to (4.2.128) are solved by Mathematica which yields solutions of h_j's as

Table 4.2.15: Temperatures along the major axis when $a = 0.0032$

$h_1 = 0.000$	$h_2 = 27.750$	$h_3 = 54.310$	$h_4 = 79.423$	$h_5 = 102.899$
$h_6 = 124.626$	$h_7 = 144.537$	$h_8 = 162.596$	$h_9 = 178.781$	$h_{10} = 193.082$
$h_{11} = 205.492$	$h_{12} = 216.009$	$h_{13} = 224.631$	$h_{14} = 231.357$	$h_{15} = 236.186$
$h_{16} = 239.118$	$h_{17} = 240.152$	$h_{18} = 239.290$	$h_{19} = 236.530$	$h_{20} = 231.873$
$h_{21} = 225.318$	$h_{22} = 216.867$	$h_{23} = 206.517$	$h_{24} = 194.271$	$h_{25} = 180.127$
$h_{26} = 164.087$	$h_{27} = 146.150$	$h_{28} = 126.313$	$h_{29} = 104.599$	$h_{30} = 81.009$
$h_{31} = 55.595$	$h_{32} = 28.488$	$h_{33} = 0.000$	–	–

Incorporating temperatures in tables 4.2.13, 4.2.14 and 4.2.15 gives form in figure 4.2.5.

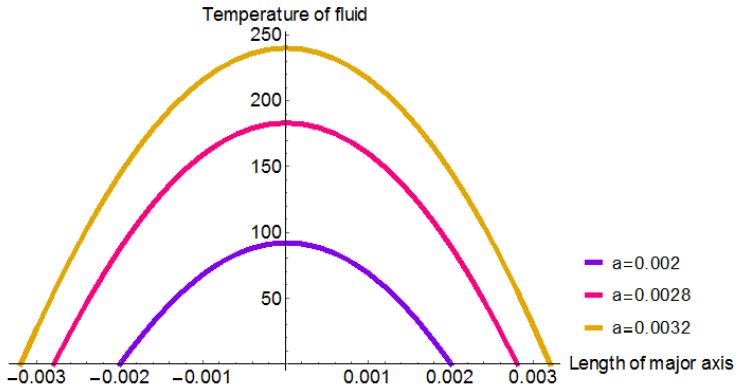

Figure 4.2.5: Merged temperature contours for $a = 0.002, a = 0.0028$ and $a = 0.0032$

Increasing half major axis from 0.0028 to 0.0032 i.e increasing aspect ratio, increases the core temperature 1.31 times as shown in figure 4.2.5. More fluid conducting particles are involved resulting in increase in Lorentz force that increases temperature. Employing a different set up, Naikoti and Balla [30] also averred that increase in aspect ratio increases temperature and velocity.

CHAPTER FIVE

CONCLUSION AND RECOMMENDATIONS

5.1 Conclusion

In this research, velocity profile and temperature distribution for MHD flow in a straight horizontal pipe of elliptical cross section has been described. The governing equations (pdes) have been formulated in terms of cylindrical coordinates, non-dimensionalised, expressed in terms of stream function, converted into odes and solved numerically using FEM. The solutions have been represented in terms of 28 tables and 11 graphs and disclose that: Increase in Hartmann number increases temperature but retards velocity. Rise in Reynolds number and aspect ratio leads to rise in both velocity and temperature. An upsurge in gravitational force results in an upsurge of velocity. Temperature increases when Eckert number increases but decreases when Prandtl number is raised. All the four objectives have been achieved. From these findings, increase in aspect ratio leads to increase in temperature and velocity which are among the main components of MHD. A pipe of elliptical cross section would be more productive in MHD processes than a circular one because it provides greater capacity than a circular one of the same depth. Secondly, elliptical pipe provides greater torque to the fluid which results in increase in fluid velocity which in turn increases fluid temperature, Moffatt [8].

5.2 Recommendations

A number of assumptions were considered in this research. A steady state investigation can also be carried out when the quantities are factored in. Also, there is still room to research on the unsteady state. The governing equations can again be solved by FEM.

REFERENCES

[1] Alam, S. and Khan, H., (2015), *Analysis of Magneto-hydrodynamics Jeffery-Hamet Flow with Nanoparticles by Hermite-Padé Approximation*. International Journal of Engineering, Vol. 28, No. 4, pp. 599-607.

[2] Kramer, D., (2011), *DOE looks again at Inertial Fusion as Clean-Energy Source*. Physics Today, Vol. 64, No. 3, pp. 26-28.

[3] Saman, R., Javad, A. and Mahla M., (2017), *Applications of Magnetohydrodynamics in Biological Systems-A Review on the Numerical Studies*. Journal of Magnetism and Magnetic Materials, Vol. 439, pp. 358-372.

[4] Cuevas S., (2021) Principles of Magnetohydrodynamics and Scope of Applications. Renewable Energy Institute. National Autonomous University of Mexico.

[5] Graebel, W., (2007), Advanced Fluid Mechanics, Academic Press. London.

[6] Darrell, W. and Juon, C., (2017), The Finite Element Method, Third Edition, CRC Press, Boca Raton.

[7] Al-Khawaja, M. and Selmi, M., (2010), *Finite Difference Solution of MFM Square Duct Flow with Heat Transfer Using Matlab Program*. Matlab-Modelling Programming and Simulations, pp. 365-388.

[8] Moffatt, K., (1978), *Rotation of a Liquid Metal under the Action of a Rotating Magnetic Field*. Proceedings of the Second BAT-SHEVA International Seminar. Israel Universities Press, pp. 45-62.

[9] Attia, A.H., (2011), *Transient Circular Pipe MHD Flow of a Dusty Fluid Considering the Hall Effect*. Kragujevac. J. Sci, Vol. 33, pp. 15-23.

[10] Gedik, E., Kurt, H. and Zecebli, Z., (2013), *CFD Simulation of Magnetohydrodynamic Flow of a Liquid-Metal Galistan Fluid in Circular Pipes*, FDMP, Vol. 9, No. 1, pp. 23-33.

[11] İbrahim, Ç., (2012), *Solution of Magnetohdrodynamic Flow in a Rectangular Duct by Chebyshev Polynomial Method*. Applied Mathematics, Vol. 2, No. 3, pp. 58-65.

[12] Altintas, A. and Ozkol, I. (2015), *Magnetohydrodynamic Flow of Liquid-Metal in Circular Pipes for Externally and Non-Heated Cases*, Journal of Applied Fluid Mechanics. Vol. 8, No. 3, pp. 507-514.

[13] Verma, K.V., (2014), *Analytical Solution of Magnetohydrodynamic Flow with Varying Viscosity in an Annular Channel.* Advances in Theoritical and Applied Mathematics, Vol. 9, pp. 105-122.

[14] Shahmardan, M., Norouzi, M. and Sedaghat, H., (2017), *An Exact Analytical Solution for Convective Heat Transfer in Elliptical Pipes*, AUT Journal of Mechanical Engineering. Vol. 1, No. 2, pp. 131-138.

[15] Dipjyoti, S., Deka, P.N. and Kakaty, S.C., (2014), *Numerical Study of Liquid Metal Magnetohydrodynamic Flow Through a Square Duct*. Asian Journal of Current Engineering and Mathematics, Vol. 2, pp. 15-19.

[16] Usman, M., Olayiwola, M. and Sikiru, B., (2018), *Steady Flow of Reactive MHD Fluid Through a Permeable Pipe Under Optically Thick Limit Radiation*, Anale. Seria Informatica, Vol. XVI fasc. pp. 121-129.

[17] Prasanna, M. and Ganesh, S., (2019), *Magnetohydrodynamic Flow Through Ducts with Different Cross Section*, International Journal of Recent Technology and Engineering, Vol. 8, Issue 3S2, pp. 853-859.

[18] Liaquat, A., Omar, Z., Khan, I., Raza, J., Sherif, M. and Seikh, A., (2020) *Magnetohydrodynamic Flow of Micropolarfluid with Effects of Viscous Dissipation and Joule Heating over an Exponential Shrinking Sheet :Triple Solutions and Stability Analysis*, MDPI Symmetry. Vol. 12, No. 1, pp 1-16.

[19] Mohammad, H., Morteza, A. and Mehran K., (2019), *Development Length of Laminar Magnetohydrodynamics Pipe Flows*, Journal of Computational and Applied Research in Mechanical Engineering, Vol. 9, No. 2, pp. 397-407.

[20] Okechi, F. N., Saleem, A. and Dawda, C., (2020), *Magnetohydrodynamic Flow Through a Wavy Curved Channel*, AIP Advances 035114, Vol. 10, pp. 1-13.

[21] Josef, K., (2012), Dimensionless Physical quantities in Science and Engineering. Elsevier, London.

[22] Nikolaos, K., (2019), Free-Surface flow-Environmental Fluid Mechanics. Butterworth-Heinemann, London.

[23] Abbott, D., Tsung-Yen and Arthur, H., (1967), *Similarity Analyses of Partial Differential Equations*, ORA project. The University of Michigan. pp 1-130.

[24] Reddy, J. N., (2019), Introduction to the Finite Element Method, McGraw-Hill Education. New York.

[25] Ioannis, K., (2018), Fundamentals of Finite Element Analysis: Linear Element Analysis. John Wiley. New York.

[26] Timothy, S., (2018), Numerical Analysis, 3^{rd} Edition. Pearson. London.

[27] Nazibuddin, A. and Dutta, M., (2015), *Heat Transfer in an Unsteady MHD Flow Through an Infinite Annulus with Radiation.* Aspringer Open Journal. pp. 1-17.

[28] Kiema, D., Manyonge, A. and Bitok, J., (2015), *On the Steady MHD Poiseuille fluid Flow Between Two Infinite Parallel Porous Plates*, International Journal of Scientific Research and Innovative Technology. Vol. 2, No. 2, pp. 100-108.

[29] Anwar, T., Kumam, P. and Watthayu, W., (2021), *Unsteady MHD natural convection flow of casson fluid incorporating thermal radiative flux and heat injection/ suction mechanism under variable wall conditions*, Sci Rep 11, https://doi.org/10.1038/s41598-021-83691-2.

[30] Naikoti, K. and Balla, C., (2015), *Finite Element Analysis of Fully Developed Unsteady MHD Convection Flow in a Vertical Rectangular Duct with Viscous Dissipation and Heat Source/Sink*. Journal of Applied Science and Engineering, Vol. 18, No. 2, pp. 143-152.

APPENDICES

Appendix A

Mathematica syntax for solving algebraic equations

Mathematica is manipulated to solve algebraic equations and the following syntax was used to solve equations (4.2.122) to (4.2.128):

Solve[$9.018h_2 - 4.509h_3 == 5.360 \&\& -4.509h_2 + 9.018h_3 - 4.509h_4 == 6.532 \&\& -4.509h_3 + 9.018h_4 - 4.509h_5 == 7.374 \&\& -4.509h_4 + 9.018h_5 - 4.509h_6 == 7.890 \&\& -4.509h_5 + 9.018h_6 - 4.509h_7 == 8.188 \&\& -4.509h_6 + 9.018h_7 - 4.509h_8 == 8.354 \&\& -4.509h_7 + 9.018h_8 - 4.509h_9 == 8.446 \&\& -4.509h_8 + 9.018h_9 - 4.509h_{10} == 8.496 \&\& -4.509h_9 + 9.018h_{10} - 4.509h_{11} == 8.523 \&\& -4.509h_{10} + 9.018h_{11} - 4.509h_{12} == 8.538 \&\& -4.509h_{11} + 9.018h_{12} - 4.509h_{13} == 8.546 \&\& -4.509h_{12} + 9.018h_{13} - 4.509h_{14} == 8.550 \&\& -4.509h_{13} + 9.018h_{14} - 4.509h_{15} == 8.552 \&\& -4.509h_{14} + 9.018h_{15} - 4.509h_{16} == 8.554 \&\& -4.509h_{15} + 9.018h_{16} - 4.509h_{17} == 8.554 \&\& -4.509h_{16} + 9.018h_{17} - 4.509h_{18} == 8.555 \&\& -4.509h_{17} + 9.018h_{18} - 4.509h_{19} == 8.555 \&\& -4.509h_{18} + 9.018h_{19} - 4.509h_{20} == 8.555 \&\& -4.509h_{19} + 9.018h_{20} - 4.509h_{21} == 8.555 \&\& -4.509h_{20} + 9.018h_{21} - 4.509h_{22} == 8.555 \&\& -4.509h_{21} + 9.018h_{22} - 4.509h_{23} == 8.555 \&\& -4.509h_{22} + 9.018h_{23} - 4.509h_{24} == 8.555 \&\& -4.509h_{23} + 9.018h_{24} - 4.509h_{25} == 8.555 \&\& -4.509h_{24} + 9.018h_{25} - 4.509h_{26} == 8.553 \&\& -4.509h_{25} + 9.018h_{26} - 4.509h_{27} == 8.550 \&\& -4.509h_{26} + 9.018h_{27} - 4.509h_{28} == 8.541 \&\& -4.509h_{27} + 9.018h_{28} - 4.509h_{29} == 8.514 \&\& -4.509h_{28} + 9.018h_{29} - 4.509h_{30} == 8.437 \&\& -4.509h_{29} + 9.018h_{30} - 4.509h_{31} == 8.221 \&\& -4.509h_{30} + 9.018h_{31} - 4.509h_{32} == 7.635 \&\& -4.509h_{31} + 9.018h_{32} == 6.229,$

$\{h_2, h_3, h_4, h_5, h_6, h_7, h_8, h_9, h_{10}, h_{11}, h_{12}, h_{13}, h_{14}, h_{15}, h_{16}, h_{17}, h_{18}, h_{19}, h_{20}, h_{21}, h_{22}, h_{23}, h_{24}, h_{25}, h_{26}, h_{27}, h_{28}, h_{29}, h_{30}, h_{31}, h_{32}\}$]

Appendix B

Mathematica syntax for constructing, colouring and labeling graphs

Figure 4.37 is procured by Mathematica 12.0 syntax written as: ListLinePlot[{{{-0.002, 0}, {-0.0018, 16.406520292748}, {-0.0016, 31.624306941672}, {-0.0014, 45.393435351519}, {-0.0012, 57.527167886449}, {-0.001, 67.911066755378}, {-0.0008, 76.479041916167}, {-0.0006, 83.194278110445}, {-0.0004, 88.036371701042}, {-0.0002, 90.994233754713}, {0, 92.061876247505}, {0.0002, 91.235972499445}, {0.0004, 88.514970059880}, {0.0006, 83.898203592814}, {0.0008, 77.385894876912}, {0.001, 68.979818141495}, {0.0012, 58.685739631847}, {0.0014, 46.520514526503}, {0.0016, 32.603016189842}, {0.0018, 16.992237746729}, {0.002, 0}}, {{-0.0028, 0}, {-0.0026, 23.9673985362616}, {-0.0024, 46.746063428698}, {-0.0022, 68.076070082058}, {-0.002, 87.770680860501}, {-0.0018, 105.715457972943}, {-0.0016, 121.844311377245}, {-0.0014, 136.120425815037}, {-0.0012, 148.523397649146}, {-0.001, 159.042137946329}, {-0.0008, 167.670658682634}, {-0.0006, 174.405633178088}, {-0.0004, 179.245287203370}, {-0.0002, 182.188733643823}, {0, 183.235528942115}, {0.0002, 182.385229540918}, {0.0004, 179.637835440230}, {0.0006, 174.993124861388}, {0.0008, 168.451097804391}, {0.001, 160.011088933244}, {0.0012, 149.673985362608}, {0.0014, 137.440008871147}, {0.0016, 123.309824794855}, {0.0018, 107.285429141717}, {0.002, 89.372809935684}, {0.0022, 69.589044133954}, {0.0024, 47.982035928144}, {0.0026, 24.681747615879}, {0.0028, 0}}, {{-0.0032, 0}, {-0.003, 27.749563373253}, {-0.0028, 54.310393102684}, {-0.0026, 79.422564593036}, {-0.0024, 102.899340208472}, {-0.0022, 124.626282157906}, {-0.002, 144.537300399202}, {-0.0018, 162.595579673985}, {-0.0016, 178.780716345087}, {-0.0014, 193.081621479263}, {-0.0012, 205.492307052561}, {-0.001, 216.009446385008},

{-0.0008, 224.631265247283}, {-0.0006, 231.356876524728}, {-0.0004, 236.185836660013}, {-0.0002, 239.117702095808}, {0, 240.152472832113}, {0.0002, 239.289927090264}, {0.0004, 236.530064870259}, {0.0006, 231.872886172100}, {0.0008, 225.318390995786}, {0.001, 216.866579341317}, {0.0012, 206.517451208695}, {0.0014, 194.271006597915}, {0.0016, 180.12724550898}, {0.0018, 164.086611499228}, {0.002, 146.149769904635}, {0.0022, 126.318716733200}, {0.0024, 104.599440008871}, {0.0026, 81.009016688845}, {0.0028, 55.595350964737}, {0.003, 28.488405134176}, {0.0032, 0}}}, PlotLegends -> {"a=0.002", "a=0.0028", "a=0.0032"}, PlotStyle -> {{RGBColor[0.51, 0., 0.93], AbsoluteThickness[6], Solid}, {RGBColor[0.99, 0., 0.49], AbsoluteThickness[6], Solid}, {RGBColor[0.89, 0.66, 0.], AbsoluteThickness[6], Solid}}, AxesStyle -> Black, AxesLabel -> {HoldForm[Length of major axis], HoldForm[Temperature of fluid]}, PlotLabel -> None, LabelStyle -> 20, GrayLevel[0], ImageSize -> Full].